University of Leeds
Faculty of Engineering
School of Electronic and Electrical Engineering

Energy Efficient IP over WDM Networks Using Network Coding

Mohamed Osman Ibrahim Musa

Submitted in accordance with the requirements for the degree of
Doctor of Philosophy,September 2016

The candidate confirms that the work submitted is his/her own, except where work which has formed part of jointly authored publications has been included. The contribution of the candidate and the other authors to this work has been explicitly indicated below. The candidate confirms that appropriate credit has been given within the thesis where reference has been made to the work of others.

Chapter 3 is based on the work from:
M. Musa, T. El-Gorashi, and J. Elmirghani, "Energy Efficient Core Networks Using Network Coding," in Transparent Optical Networks (ICTON), 2015 17th International Conference on, July 2015.

And:

M. Musa, T. El-Gorashi, and J. Elmirghani, "Network Coding for Energy Efficiency in Bypass IP/WDM Networks" in Transparent Optical Networks (ICTON), 2016 18th International Conference on, July 2016.

And:

M. Musa, T. El-Gorashi, and J. Elmirghani, "Network Coding for Energy Efficiency in Core Networks " Lightwave Technology, Journal of,2016, Submitted for publication.

These papers have been published jointly with my PhD supervisors Prof. Jaafar Elmirghani and Dr. Taisir Elgorashi.

Chapter 4 is based on the work from:

M. Musa, T. El-Gorashi, and J. Elmirghani, "Bounds on Energy Efficient Network Coding in Core Networks" IEEE Transactions on Communications, 2016, Submitted for publication.

This paper have been published jointly with my PhD supervisors Prof. Jaafar Elmirghani and Dr. Taisir Elgorashi.

Chapter 5 is based on the work from:

M. Musa, T. El-Gorashi, and J. Elmirghani, "Energy Efficient Survivable IP over WDM networks with network coding" Optical Communications and Networking, Journal of, 2016.

This paper have been published jointly with my PhD supervisors Prof. Jaafar Elmirghani and Dr. Taisir Elgorashi.

Chapter 6 is based on the work from:

M. Musa, T. El-Gorashi, and J. Elmirghani, "Bounds On Energy Efficient Survivable Optical Networks With And Without Network Coding" IEEE/ACM Transactions on Networking, 2016, Submitted for publication.

This paper have been published jointly with my PhD supervisors Prof. Jaafar Elmirghani and Dr. Taisir Elgorashi.

To my father and my mother, this thesis is dedicated to you.

Acknowledgements

Foremost, all praise is due to Allah, for life, good health and all the blessings I have. I would like to express my sincere gratitude to my supervisor Prof. Jaafar Elmirghani for the support during my Ph.D, for his patience, guidance and sharing of his immense knowledge. His guidance helped me during the time of research and writing of this thesis.

I would like to thank my second supervisor Dr. Taisir Elgorashi for the continuous support, encouragement, insightful comments, and useful discussions I had with her during my PhD.

I thank my fellow colleagues in the Communication Systems and Networking group for the stimulating discussions, for all the help and support they provided me, and for all the good times we have had in the last four years.

Finally, I would like to dedicate this thesis to my parents; to my father, Osman Ibrahim Musa and my mother, Amal Mohamed Hamdeen. I have been extremely fortunate in my life to have parents who have shown me unconditional love and support. They have played an important role in the development of my identity and shaping who I am today. I am very grateful for their sacrifices, their dedication, for instilling into me the desire for success, and for supporting me spiritually throughout my life. Many thanks also to my beloved brothers and sisters for making my life enjoyable and full of fun.

Abstract

In this thesis we propose the use of network coding to improve the energy efficiency in core networks, by reducing the resources required to process traffic flows at intermediate nodes. We study the energy efficiency of the proposed scheme through three approaches: (i) developing a mixed integer linear programme (MILP) to optimise the use of network resources. (ii) developing a heuristic based on minimum hop routing. (iii) deriving an analytical bounds and closed form expressions. The results of the MILP model show that implementing network coding over typical networks can introduce savings up to 33% compared to the conventional architectures. The results of the heuristic show that the energy efficient minimum hop routing in network coding enabled networks achieves power savings approaching those of the MILP model. The analytically calculated power savings also confirm the savings achieved by the model. Furthermore, we study the impact of network topology on the savings obtained by implementing network coding. The results show that the savings increase as the hop count of the network topology increases. Using the derived expressions, we calculated the maximum power savings for regular topologies as the number of nodes grows. The power savings asymptotically approach 45% and 23% for the ring (and line) and star topology, respectively.

We also investigate the use of network coding in 1+1 survivable IP over WDM networks. We study the energy efficiency of this scheme through MILP, a heuristic with five operating options, and analytical bounds. We evaluate the MILP and the heuristics on typical and regular network topologies. Implementing network coding can produce savings up to 37% on the ring topology and 23% considering typical topologies. We also study the impact of varying the demand volumes on the network coding performance. We also develop analytical bounds for the conventional 1+1 protection and the 1+1 with network coding to verify the results of the MILP and

the heuristics and study the impact of topology, focusing on the full mesh and ring topologies, providing a detailed analysis considering the impact of the network size.

Contents

List of Figures

List of Tables

Nomenclature

AMPL	A Mathematical Programming Language
ATM	Asynchronous transfer mode
CBC	Coin-or branch and cu
CCN	Content Centric Networking
CRS	Cisco Carrier Routing System
CWDM	Coarse Wavelength Division Multiplexing
dB	Decibel
DeMUX	De Multiplexer
DWDM	Dense Wavelength Division Multiplexing
EDFA	Erbium Doped Fibre Amplifier
EPON	Ethernet Passive Optical Network
FDM	Frequency Division Multiplexing
FiWi	Fibre Wireless
GaAs	Galium Arsenide

GB	Giga Bytes
Gbps	Giga Bits Per Seconds
GeSI	Global e-Sustainability Initiative
GHG	Green House Gases
GNU	GNU Not Unix
IBM	International Business Machines
ICT	Information and Communication Technologies
InGaAsP	Indium gallium arsenide phosphide
IP	Internet Protocol
KIT	Karlsruhe Institute of Technology
km	Kilo Meters
Mbps	Mega Bits Per Seconds
MILP	Mixed Integer Linear Program
MPλS	MultiProtocol Lambda Switching
MPLS	MultiProtocol Label Switching
MUX	Multiplexer
NC	Network Coding
NEC	Nippon Electric Company
NetFPGA	Network Field Programmable Gate Array

NG-PON	Next Generation Passive Optical Network
NP	Nondeterministic Polynomial time
NRZ	Non Return to Zero
NSFNET	National Science Foundation Network
NTT	Nippon Telegraph and Telephone
OC	Optical Carrier
OEO	Optical Electrical Optical
OLT	Optical Line Terminal
ONU	Optical Network Unit
OOK	On Off Keying
OXC	Optical Cross Connects
PON	Passive Optical Network
PPP	Point to Point Protocol
QoS	Quality Of Service
RAM	Random Access Memory
SDH	Synchronous digital hierarchy
SMF	Single Mode Fibre
SONET	Synchronous Optical Networking
STM	Synchronous Transport Module

Tbps	Tera Bits Per Seconds
TDM	Time Division Multiplexing
US	The United States
USA	The United States of America
USNET	United States Network
WDM	Wavelength Division Multiplexing
XOR	Exclusive OR

Chapter 1

Introduction

There is no denying that the recent years have experienced an explosion in data usage accompanied by a shift of trends in data generation, consumption and storage. This change has brought about a unique and improved set of new uses and applications and expanded the horizons, but required a considerable evolution to the underlying infrastructure to support its operation. One of the main challenges experienced in ICT is its energy efficiency, and evolving the ICT infrastructure to be energy efficient sustaining the ever increasing demands has been one of the main themes of ICT research in the last few years.

The GeSI SMARTer 2020 report [3] estimates the total emission of ICT in 2011 to be 1.9% of the global emissions, comparable to the aviation industry, and expected to rise to 2.3% by the year 2020. Economically, as an example, European telecoms are expected to cost over 4 Billion US dollars for energy operational expenses [4]. What adds to the problem is that traffic continues to grow exponentially. The total Internet traffic is expected to double every year, which is more than 1000x in 20 years [1]. The energy saving growth, on the other hand, is growing slowly at a rate

of 10-15% every year. The gap between traffic growth and energy consumption will continue to expand if the current systems are left as they are.

Several proposals have been put forward to make networks energy efficient, including improved networking equipment, improved network design and architecture, improving operational techniques to maximise consolidation of resources, improving traffic routing, and many more. Several organisations and standards have been setup to define energy efficient systems. The work is still on-going and this research aims at contributing to the solution of the problem.

One of the ideas that has enjoyed a great reception from the networking research community is network coding, introduced in 2000, promising to improve the capacity of the network leading to a considerable improvement in throughput by performing coding operations on top of conventional routing [5]. Of all the sectors, wireless networks received most of the efforts due to the suitability of implementation to network coding requirements, as wireless terminals and access points are multicast mediums in nature. Optical networks, however, received almost no attention from the network coding research community, leaving a big gap in the literature, and potential to improve network performance.

A key question relates to the suitability of network coding in optical networks. If suitable, how significant it is and under what conditions, and most importantly how to devise systems and techniques to maximise these improvements. These are the headline questions that this thesis investigates, with particular emphasis on improving network energy efficiency.

1.1 Motivation and Objectives

The main objective is to build an energy efficient IP over WDM network by using network coding and investigate the potential energy savings possible, optimise the network operations to maximise energy efficiency, as well as open doors for research in optical networks using network coding. In order to perform this, the following objectives are set:

- Evaluate the use of network coding in optical networks and the potential savings in typical networks using common traffic. From there the main factors affecting network coding performance are to be studied and optimised using a Mixed Integer Linear Programming (MILP) model. In addition, develop heuristics that provide savings closer to the MILP model performance, and study the impact of varying the traffic demands as well as the network topology.

- Produce analytical closed-form expressions and bounds to validate the MILP and the heuristic and use them as a tool to study scenarios that are too complex to be studied using the MILP model, and provide an upper limit to the achievable energy efficiency which aids in deciding how much more effort needs to be dedicated to reach the maximum energy efficiency.

- Evaluate the use of network coding in survivable optical networks using 1+1 protection schemes, and study its behaviour, optimise it using MILP, develop heuristics that can be used in large network sizes, and develop analytical bounds to understands the limits of performance and to validate the MILP and heuristics as well as study network situations like big network sizes, that are harder to solve using the MILP.

1.2 Original Contributions

- We were the first to introduce network coding in IP over WDM networks by designing a new type of router port that employs the simplest of the network codes, i.e. the XOR code, to improve energy efficiency of IP over WDM networks. We developed a MILP model and a heuristic and quantified the savings using the NSFNET and USNET topologies. We designed two architectures considering the potential imbalance between the two encoded flows, one zero pads the smaller flow and the other partitions the bigger flow. We investigated network coding in both non-bypass and bypass variants of IP over WDM networks.

- We developed analytical bounds and closed form expressions to the power consumption for the network coded approach as well as the conventional approach and used them to validate the MILP model. In addition to that, we studied the behaviour of networks with a high number of nodes.

- We investigated the use of network coding in survivable optical networks with 1+1 protection to approach the efficiency of 1:1 protection with the reliability of the 1+1 protection by encoding one of the link disjoint paths of a demand with another. We developed a MILP model and a heuristic with five operating options and studied the behaviour in common networks as well as regular topologies, and studied the impact of traffic on the savings.

- We derived analytical bounds for the performance of 1+1 survivable optical networks and studied the impact of topology, focusing on the special full mesh and ring topology providing a detailed analysis considering the impact of the network size.

1.3 Publications

The following Journal and conference papers have been published and submitted for publications:

1. M. Musa, T. El-Gorashi, and J. Elmirghani, "Energy Efficient Core Networks Using Network Coding," in Transparent Optical Networks (ICTON), 2015 17th International Conference on, July 2015.

2. M. Musa, T. El-Gorashi, and J. Elmirghani, "Network Coding for Energy Efficiency in Bypass IP/WDM Networks" in Transparent Optical Networks (ICTON), 2016 18th International Conference on, July 2016.

3. M. Musa, T. El-Gorashi, and J. Elmirghani, "Network Coding for Energy Efficiency in Core Networks" Lightwave Technology, Journal of,2016, Submitted for publication.

4. M. Musa, T. El-Gorashi, and J. Elmirghani, "Bounds on Energy Efficient Network Coding in Core Networks" IEEE Transactions on Communications, 2016, Submitted for publication.

5. M. Musa, T. El-Gorashi, and J. Elmirghani, "Energy Efficient Survivable IP over WDM networks with network coding" Optical Communications and Networking, Journal of, 2016, Submitted for publication.

6. M. Musa, T. El-Gorashi, and J. Elmirghani, "Bounds On Energy Efficient Survivable Optical Networks with And Without Network Coding" IEEE/ACM Transactions on Networking, 2016, Submitted for publication.

1.4 Thesis Outline

Following this chapter, this thesis is organized as follows:

Chapter 2 presents a review of the core network and its components, network coding as well as a brief overview of the efforts underway to improve the energy efficiency in optical networks.

Chapter 3 presents the new optical network architecture that exploits network coding. A thorough study of the energy efficiency benefits of the approach with evaluation using an MILP model and a heuristic is provided.

Chapter 4 provides closed form expressions and analytical lower and upper bounds for network coding supported IP over WDM networks presented in Chapter 3.

Chapter 5 provides a study on the use of network coding to provide energy efficient 1+1 protection in optical networks, by evaluating it through a MILP and a heuristic and studying the traffic and topological impact of the network.

Chapter 6 provides analytical bounds on the survivable network coded 1+1 optical networks provided in Chapter 5, as a verification an extension to very large network sizes.

Chapter 7 summarises the thesis contributions and provides a set of possible future directions of work.

Chapter 2

Review of Optical Networks and Network Coding

2.1 Introduction

In this chapter an overview of the components of this thesis is presented. An examination of the IP over WDM networks architecture and components followed by an overview of energy efficiency with a focus on core networks, presenting the current situation, efforts and potential research areas. We follow that by an introduction to network coding, followed by a review on the work done in using network coding for optical networks. We also give a brief introduction to the mixed integer linear programming approach used to provide one of the models of networks in this thesis.

2.2 Optical networks

IP over WDM is a networking scheme where IP data units are transported over optical networks employing wavelength division multiplexing (WDM). The combination of these two systems came about after a long phase of improvements to the previously used architectures. In this section we give a brief introduction to existing optical network architectures, and then we focus on IP over WDM networks and their elements

2.2.1 A brief history

In 1966, Charles Kao and George Hockam [6], in the middle of an era that used copper wire as a main mean of communication, proposed using light guided inside a long tube of glass for transporting information. Although the idea was revolutionary, it was not practical enough due to the inability to manufacture optical cables with very low attenuation as the attenuation factor was 1000 dB/km compared to 5-10 dB/km for coaxial cables at that time. However, these high losses were not inherent but rather due to contaminants which, if removed, would lead to extremely low losses [6]. Improvements followed over the years in optical fibre manufacturing and light sources such as lasers. In 1975, a fibre with 45 Mbps rate using GaAs semiconductor laser, operating at 0.8 µm was commercialised. This system however, required the presence of repeaters every 7 km [7].

In the 1980s, the central wavelength moved to the low losses window around 1.33 µm and a major leap was the introduction of the single mode fibre (core diameter of 8-10 microns compared to 50-100 microns of the multimode fibre). The single mode fibre (SMF) improved the performance by many folds. However another type of

laser had to be used compatible with the SMF, so InGaAsP semiconductor lasers were used. The bit rates reached 1.7 Gbps and the spacing between repeaters was 50 km [8]. The next move was centring the transmission on the 1.55 µm window, in which the fibre has the lowest attenuation; 0.2 dB/km. The dispersion, however, was high in this region, but with the help of dispersion shifted fibres and using a limited spectrum laser, 8 Gbps transmission was achieved with doubled repeater spacing to 68km [9].

In the early 1990's two major achievements paved the way to huge data rates systems; the invention of the optical fibre amplifier [10] and wavelength division multiplexing [11] for capacity improvement. A WDM system capable of transmitting 8 channels each carrying 10 Gbps was demonstrated [12]. Improvements followed each other; data rates passed the Tbps barrier in the mid 1990's [13]. Alcatel-Lucent in 2009 achieved 15 Tbps using 155 channels of 100Gbps each. In 2010 NTT achieved a 69.1 Tbps over a large span of 240 km, using 432 wavelengths each carrying 171 Gbps [14]. KIT managed in 2011 to transmit 26 Tbps per wavelength, for a distance of 50 km [15]. In 2011, NEC managed to transmit a 101 Tbps over a long distance of 165 km, using 370 channels of 273 Gbps each [16]. Another breakthrough came at the end of 2012, where NEC and Corning managed to break the petabit/s level by using a 12 core fibre over a distance 52.4 km [17].

In a recent paper, the authors in [18] experimentally demonstrated WDM data transmission at propagation speed 99.7% of the speed of light, by improving upon photonic band-gap fibres that have a hollow-core. This propagation speed is a significant improvement over the silica glass fibres, in which light propagates 31% slower than vacuum. The rate they managed to transmit is 73.7 Tbps.

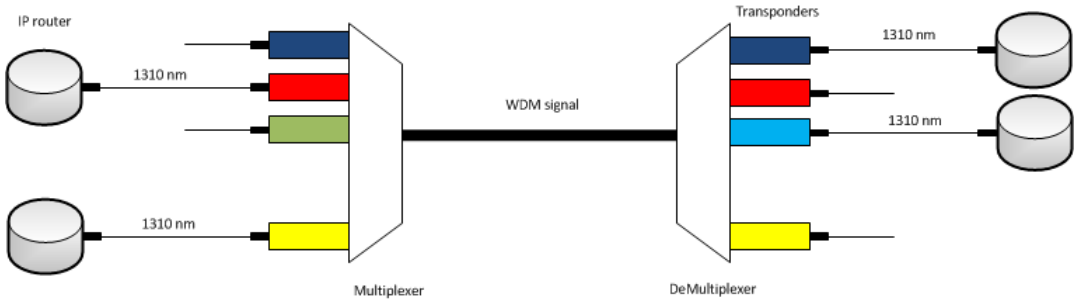

Figure 2.1: Simple configuration of the WDM network

2.2.2 Optical networks

The fast rise in optical fibre capacities, with the electronic limitations on the devices speed signalled the need for multiplexing techniques where low rate signals are combined into a higher rate transmission. The first way to perform this multiplexing is by the use of time division multiplexing, and it can be done electronically or optically. The famous SONET/SDH standards use electronic TDM and the highest transmission available today is the OC-768/STM-256 40Gbps which multiplexes 4 10Gbps OC-192/STM-64. The hierarchy goes up in multiples of four in data rates from to the basic OC-3/STM-1 rate of 155 Mb/s. Optical TDM is faster, although commercially not yet available, experiments demonstrated multiplexing 10 Gbps streams into a 250 Gbps stream [19].

Wavelength division multiplexing (WDM), shown in Figure 2.1 is a multiplexing scheme that is analogous to FDM in radio system. The optical bandwidth is divided into slower narrowband bandwidth components, referred to as wavelengths. Signals from the client side are transformed into a compatible wavelength configuration through the use of transponders and multiplexed using wavelength multiplexers and are carried over the optical fibre. At the receiver side, the composite WDM signal is demultiplexed into its individual wavelengths to be consumed by received clients.

The total available bandwidth is divided in the WDM scheme into two standards: Coarse WDM (CWDM) [20] and Dense WDM (DWDM) [21]. The CWDM uses multiple transmission windows and provide 16 channels. The DWDM standard, uses the C-band region (1530 nm-1560 nm) and can provide two schemes, the first provides 40 channels at 100GHz wavelength separation and the second provides 80 channels at 50GHz separation.

The first use of WDM was for expanding the bandwidth of point to point optical communications systems. The bandwidth expansion turned into bandwidth management with the creation of more wavelength sensitive equipment such as switching and routing and with advent of active elements, this added wavelength as another degree of freedom in addition to time and space.

There are two approaches of routing wavelengths in WDM networks; wavelength routing and broadcast and select. In wavelength routing networks, switching is done based on the knowledge of the wavelength and the port of entry. For an NxN network, there is a way of wavelength assignment where only N wavelengths are needed instead of N^2, however, N^2 fibres are needed [22]. The other option is broadcast and select; here a broadcasting star couples all inputs and broadcasts them to every output, the receiver then selects the desired channel/transmitter based on its current pass frequency. If the lasers and detectors are tunable, several configurations can be realised such as the multicast functionality [11].

2.2.3 IP over WDM

The Internet Protocol (IP) came as a natural progressive choice to carry the variety of service forms (voice, data, and media content such as video) by encapsulating them into the packets format provided by the IP protocol. This is the result of the

popularity of the Internet and the rapid advances in broadband technologies. WDM as the direct provider of capacity is the logical choice to carry the IP payload and hence the selection of the current layered combination as IP over WDM [23] [24]. This combination was a result of multiple protocol stack changes as technologies were being displaced for a better alternatives.

In the early 1990's IP was carried over ATM, a protocol that proved itself in terms of integrating multiple services and providing QoS. This is fed to another layer that multiplexes many ATM low rate flows into a higher rate flow using the TDM based SONET/SDH protocol, which is finally handed to the WDM layer where the latter is carried over fibre. This stack required four major devices, IP routers, ATM switches, SONET Add drop multiplexer and WDM equipment. It lacked efficiency, there was overlap in functionality, and the protocols overhead was large. SONET and IP both perform aggregation, each layer has its own restoration functionality, and all layers perform routing, while the MPλS performs QoS. Having multiple layers with shared functionality decreased the reliability of the system.

In the late 1990's, MPλS (the optical equivalent to MPLS) [25], was introduced to the stack replacing the ATM. It was first carried over Point-to-Point Protocol (PPP) and was encapsulated in SONET frames. But later in 2000 the PPP was replaced by Ethernet. IP over WDM emerged as the winning combination [26]. IP routers are now capable of running at 10Gbps, 40Gbps and 100Gbps and the IP layer is used for traffic aggregation, protection and route calculation [27]. WDM layer is used for providing the routes, flow protection and network restoration. The protection and route assignment are coordinated between these layers [19], [28]. Figure 2.2 shows the components used in an IP over WDM network (3 nodes shown for simplicity). We describe them here briefly:

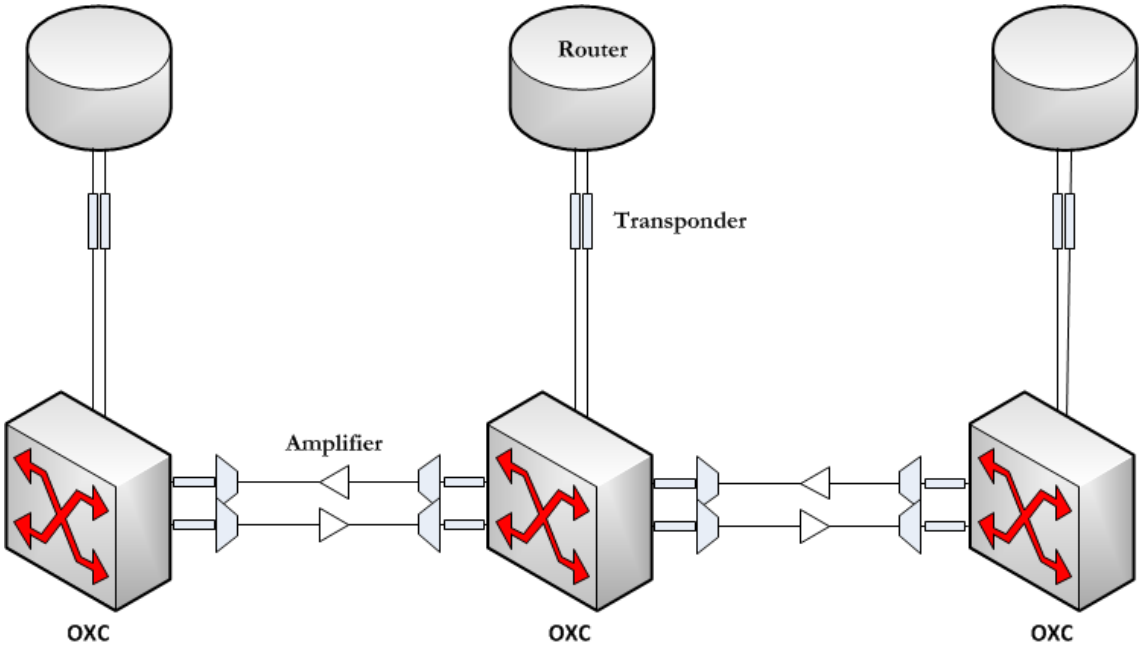

Figure 2.2: The architecture of IP over WDM networks

IP routers are the parts responsible for routing in the IP layers and represent the client side of the optical terminal. They receive the aggregated traffic from edge routers and interface the optical side of the network.

Optical Cross Connects (OXC) are essential elements in the WDM network as they provide switching of optical signals between input and output ports. They can provide light path instantiation and can close down paths dynamically. Additionally they can support switching light paths, management and protection functionality. They may also include wavelength conversion capabilities, multiplexing and grooming capabilities internally [29].

OXC have migrated from being opaque to transparent with the third option of being translucent [30] [31]. In the opaque OXC the switching fabric is either entirely electrical or a mixture of optical fabric with optical-electrical-optical conversion. In transparent OXC the signal is switched between the input and output ports without the need for an optical-electrical-conversion. The opaque OXC supports regenera-

tion, wavelength conversion and bit-level monitoring at the cost of the electrical conversion delay and power consumption. In translucent OXCs, the switching stage consists of both the electronic module and optical module offering both options for switching signals. While the optical switching module is preferred, the electronic module comes in handy when the optical switching module is occupied or the functionality of regeneration is needed, therefore providing a compromise between full transparency and the choice of regeneration.

Transponders are used when the format of the optical signal needs to be adapted to another format. The client side of the transponder receives the signal from the IP router, which is generally carried on an optical fibre operating at the 1310nm wavelength. The transponder converts the client side signal into an electronic signal which is back converted to the required WDM wavelength. The reverse is done on the receiving side of the network. Although this functionality is carried out using Optical-Electrical-Optical conversion, it is expected to change to all optical with the maturing of the all optical technology. Transponders can also have network management functionality and monitoring by adding an overhead and they have the ability to add Forward error correction.

Optical amplifiers amplify optical signals directly without converting them to electrical signals. Erbium doped fibre amplifiers (EDFAs) have revolutionised optical communications in WDM networks, because they provide high gains in the 1.55 µm window in the order of 25dB and are independent of the signal shape and bit rate. They can be used as in-line amplifiers where the links are attenuation limited. Here they are placed at regular link intervals (80-120 km) to compensate for the 0.2 dB/km attenuation of the fibre. They are used also as post amplifiers to increase the power of the transmitter, or as preamplifiers to improve receiver sensitivity. EDFAs can also be used as booster amplifiers when couplers are used to compensate

for the losses [32], [33].

2.2.3.1 Multiplexers/Demultiplexers

Multiplexers are used to combine and separate the multiple wavelengths carried in the fibre. Currently the standards for multiplexing are the coarse and dense WDM multiplexing (CWDM and DWDM) differing by the channel separation; 20nm for the CWDM and 0.8 nm for the DWDM [20], [21].

2.3 Energy Efficiency in Core Networks

According to GeSI SMARTer 2020 report [3], the ICT sector contributes about 2.6% of the total greenhouse gas (GHG) emission, an alarming amount comparable in magnitude to the aviation industry. Telecom infrastructure contributes about 22% of the total ICT power consumption while data centres' share is 19%, with the 59% of the ICT power consumption contribution coming from end user equipment. This however is expected to change by the year 2020, where The power consumption from end user equipment will drop to 53%, while data centres will experience a growth in power consumption to 24%, and the telecom networks will remain close to 23%. While ICT itself is used to mitigate the GHG emission, it is not energy efficient. This continuous expansion in ICT calls for new approaches to cut the power consumption of ICT to its lowest possible levels.

Figure 2.3 shows the traffic trends for the different services [1]. It shows that the IP traffic exhibits a 22 percent compound annual growth rate from 2015 to 2020, exceeding 2.3 ZetaBytes per year by 2020. The figure also shows the different services and their contributions, with Internet video and IP video on demand reaching over

80 percent of the total traffic. The escalation of demands as shown in Figure 2.3 will lead to continued increase in energy consumption in the network, unless measures are taken to reduce power consumption.

Figure 2.3: Cisco Global IP Traffic Forecast for different services [1]

The roadmap toward achieving energy efficiency goals is first to estimate the current energy efficiency trends and then assess possible solutions. Possible research areas are to be identified and major challenges need to be addressed. These areas are integrated in a holistic and consolidated way, so all the savings are combined together. Finally measurements and benchmarking should take place to determine where along the way the current savings are.

The work on energy consumption of the Internet was pioneered by the work of [34] and [35] by showing the necessity to improve the power consumption of the Internet. Greentouch is a consortium [36] formed in 2010 with the aim of increasing network energy efficiency by 1000x compared to the level of 2010 by delivering efficient architectures, roadmaps and specifications by fostering collaboration between academics, ICT industry experts and non-governmental research experts from the entire world.

2.3.1 Approaches

There has been a growing amount of effort to improve energy efficiency in ICT. The work spans all the ICT domains, including terminal equipment, networks and data centres. Here we focus on the network side, and among the 3 network variants, core, metro or access, we focus on the core network where the energy density is highest and where the group has contributed to GreenTouch [37].

The first effort on improving the Internet energy efficiency was carried out by [34], where the authors showed that selectively putting network elements to sleep improves energy efficiency, but requires changes to the current system. Here we group energy efficiency approaches in core networks into 4 main approaches: components, data, network and energy source. Each category has its own subcategories, and all of them can be applied in a holistic approach, combining the benefits of each in a coherent manner.

2.3.1.1 Energy efficient components

In the components level, the approach is to take each element of the network and improve its energy efficiency by engineering efficient electronics and reducing the level of complexity. First, all components can migrate to include power efficient electronics and optical devices can use power efficient photonics as well as power efficient integration. For instance, improving optical fibres properties and mitigating impairments reduces the need for amplifiers and regenerators, and hence reduces energy consumption.

Migration to all optical architectures eliminates the need for using optical to electrical conversion, hence using less equipment to route traffic. The authors in [38]

discussed how optics can improve energy efficiency of networking components. The authors in [39] have examined the benefits of using photonic switching in terms of energy efficiency improvement. They analysed the contribution of buffers and OXCs to the total energy consumption. They have shown that these elements vary slowly with access rate and their contribution in energy consumption is low. So even if photonic switching is used, the reduction in power consumption is not significant. One may argue that this result only considers the components savings alone. Migration into all optical switches has an impact on higher layer on the higher layers of the network, and future work has the potential to coordinate transmissions through optical band switching, optical flow switching, and the use of large optical packets which can reduce the use of routers and improve energy efficiency [40].

Cisco [41] has introduced a new router/OXC platform that changes the interaction between the IP and DWDM layers. Based on the fact that 70-80% of the overall traffic handled by the router is a pass through traffic, but OEO conversion occurs anyway, resulting in additional cost in terms of operational power, cooling power and space cost where many racks are needed [41]. This approach keeps traffic as much as possible in the optical domain, and transponders are shifted to the router line cards instead of OXC ports. CRS-1 is an example of a router that uses this feature.

In the IP layer, routers are the most power consuming elements of the network. A significant portion of this power is dedicated to cooling, and it's shared for the whole chassis. It was shown in [42] that the full chassis consumes less power per transferred bit the less full it is. Also they showed that a chassis with high speed line cards supported, is more energy efficient. The authors in [43] addressed the issue of mixed line rates and its effect on energy efficiency. They show that using mixed line rates is better than a single line rate network.

2.3.1.2 Power Adaptive Components

Network components possess a power profile which dictates the power consumption given a certain utilisation. This offers opportunities in allowing the component to adapt to the current load by introducing sleep modes in the general case or selectively switching on and off components resulting in a considerable amount of power savings. The authors in [44] developed multiple traffic models from traffic observations showing the potential for power savings if these traffic changes were followed by the operating equipment. In [45], it was shown that shutting down idle line cards and chassis of IP routers can save energy. A similar approach was presented in [46] by shutting down line cards when the traffic load is low. Putting network elements to sleep has been shown in [47] to save up to half of the core network power consumption by reconfiguring nodes and links to follow traffic variation.

The authors in [48] divided the level of turning off various elements into three levels: the instruction level where elements inside the CPU can be turned off, this scale is the sub microseconds scale. The seconds is between the microseconds and milliseconds, where the CPU can be put to sleep, situations in this level are like inter-packet communication. Between flows, scales from seconds to hours, is the third case where the entire system can be turned off. This approach can be implemented by shaping the traffic pattern, grouping information to add more sleeping opportunities.

2.3.1.3 Data Distribution

Packet size has been shown in [49] to be a significant parameter in reducing the power consumption of router ports as the smaller the packet size is, the more power is consumed in the router. Therefore carefully engineering packet sizes has the

potential to save power at the possible cost of increased delay. Data presentation includes protocols encapsulation and coding. The information can be compressed to its minimum possible value. Compression can be at the network level. There can be cross layer compression and inter-flow coding. Reliability of the transmission can be increased by channel coding, which reduces the need for regenerators along the way, saving energy. This approach is the least used approach in achieving energy efficiency, while having a great potential. The authors in [50] provide a discussion of the data compression benefits in energy efficiency in optical networks and the authors in [51] investigated the savings in power consumption by compressing data in IP over WDM networks through MILP modelling and heuristics using fixed and mixed line rates and different compression rates for different data types.

The authors in [49] showed that the packet size can be optimised to save energy, the larger the packet size the more is the energy efficiency achieved, with impact on delay, hence there exists an energy efficiency delay trade-off.

End to end grooming is shown by [52] to be more efficient than link by link grooming. Grooming is an essential function of IP over WDM network, and by increasing utilisation of link power efficiency is increased.

Data centres constitute a huge section of savings. In [53], the authors considered the impact of the number of data centres, their locations and the upload and download rates on the energy efficiency. They also studied the effect of replicating content with different popularity in the network and minimising the overall routing cost. With the availability of renewable energy, they found that it is better to move data centres to the location of renewable energy sources than to transmit renewable energy to data centres. To minimise access overhead to the limited number of data centres, caches are used. The impact of using caches on energy efficiency has been

addressed by [54]. They show the savings offered using different content popularity distributions.

In [55], the authors evaluated the savings achieved by using content delivery networks with dynamic optical bypass. They show that this configuration achieves better savings when high download rates are used to access very large files. The same authors in another paper [56] compare the dynamic optical bypass savings with content centric networking (CCN). They show that CCN is more efficient with popular content, while the other is more efficient with less popular content.

The advantage of using bit torrent peer-to-peer content distribution over the client server has been studied in [57] where the authors showed that having random peers selection is not different from the client server model energy-wise, but using a power minimised approach leads to savings of up to 30%.

2.3.1.4 Network Design

At the network level, switching traffic from source to destination is affected by the network topology and architecture and the route traffic takes. By carefully managing network topology by allowing the traffic flow to consume the lowest power possible, and hence switching off network equipment, a considerable amount of savings can be achieved. The authors in [58] provide a good survey of this approach.

The work in [59], considered designing an energy efficient IP over WDM core network. They quantified the effect of using bypass where traffic is routed only in the optical layer, and they found it to be significantly higher in efficiency that the non-bypass case.

Architecture on demand offers a great tool to change the topology and architecture

dynamically based on the requirements. The design of the topology for energy efficiency takes the traffic demand as a parameter. The fact that the demands are dynamic, and the topology is static introduces inefficiency and under-utilisation to the system. Architecture on demand tries to bridge this dynamism seamlessly. The study in [60] proposed an architecture on demand which can be interconnected in 20 ms to build flexible OXC architectures that follow traffic needs.

In [61] the authors investigated the application of virtual network embedding in core networks where the network is virtualised to multiple virtual networks, and by consolidating networking resources, energy efficiency can be achieved.

2.3.1.5 Energy source

Here, the energy sources are divided to renewable and non-renewable sources. It is desirable to migrate to a full renewable energy source operated network, potentially saving energy running costs and having reduced carbon footprint. However, there are many challenges to provision of renewable energy sources.

The work in [62] considered the problem of using a limited number of renewable energy sources in the IP over WDM network. They investigated the impact of the number of sources and their location on the energy efficiency and carbon footprint minimisation problems. The results show that it is more efficient to place renewable energy sources at the centre of the network.

2.4 Network Coding

2.4.1 What is Network Coding?

Communication is about transmitting a piece of information from one point to another. In a network, this transmission is assisted by intermediate nodes that relay the information until it reaches its destination. While the source can encode the information which is later decoded by the receiver, intermediate nodes simply receive and forward it without any coding. Information in this regard is considered a commodity, and the essence of network design is flow conservation (what goes in, comes out).

While the commodity flow paradigm has kept the network in operation since its first days, it has not utilised its potential to the limit; intermediate nodes are essential to data transmission and hence should be utilised to improve overall performance. This is what Ahlswede et al. proposed in their pioneering paper [5].

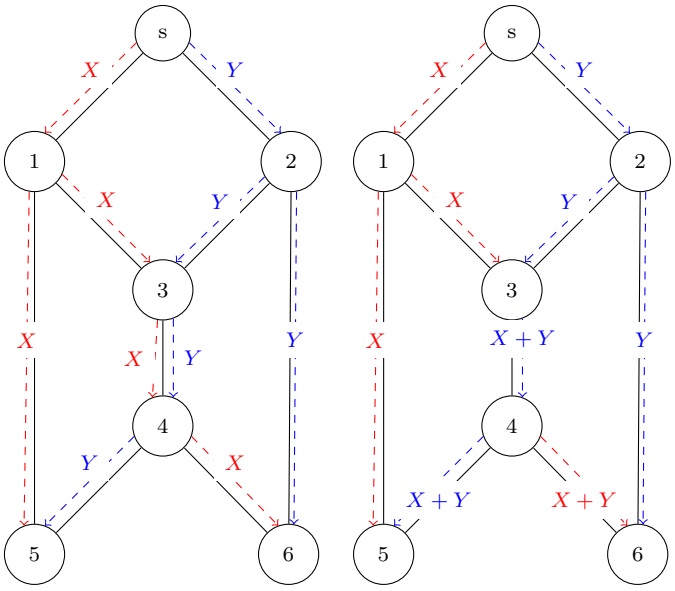

Figure 2.4: The butterfly network with network coding

To simply represent network coding, we use the famous butterfly network shown in Figure 2.4. Starting with the conventional routing approach (left), assume source s is to multicast two pieces of information (X and Y) of a unit rate each using the butterfly network with edges of a unit capacity each, to the two receivers $d1$ and $d2$. It is only possible if the min cut max flow theorem holds for each of the transmissions separately. The min-cut max-flow theorem [63], [64] states that the value of the minimum cut that separates the source from the receiver is the maximum amount of information that can be sent; the cut is the collection of edges that if removed, the source and destination get disconnected. In this case, the middle link $(3, 4)$ will be a bottleneck. And so the multicast will not be admissible with the rate intended. In contrast, if we allow node 3 to perform an XOR operation on the two pieces (addition in the binary field), and later at the destination nodes the xor is performed again on the two packets received, this bottleneck is avoided and the intended rate is achieved. This achievable rate is the multicast capacity of the network. Network coding is a generalisation of this case, for arbitrary topologies, arbitrary traffic and demands scenarios and arbitrary codes.

The work of Ahlswede et al. was followed by the significant work of [65] which described an approach to achieve optimal solution for multicast over directed acyclic graphs by applying linear codes and proving they are sufficient to achieve the multicast capacity. The work of [66] provided an Algebraic framework for network coding, which later drove the development of random linear network codes [67], [68] where the coding coefficients at different nodes in the network are selected randomly.

Following its discovered potential, researchers expanded the study and implementation in different dimensions. An information theoretical framework was developed in [69–71]. The use of network coding in undirected networks was started by [72], and [73]. It showed that the previous work that assumed acyclic networks can be

extended to cyclic scenarios. Another significant extension of network coding was made by [74] and [75] where they showed that the network coding problem represents a generalisation of the classical problem of error correcting codes, by providing redundancy in the extra space dimension in addition to the time domain.

Complexity and algorithms for optimal codes are currently among the main branches of network coding theory. Different factors were studied, such as the size of the alphabet and the number of destination nodes and their distribution [76], while [77–79] provided low complexity polynomial time algorithms for multicast network coding.

2.4.2 Benefits of Network Coding

2.4.2.1 Throughput

Network coding makes better use of shared links in the network. Many information flows are combined together over a finite field, the result is a flow several times smaller than the flows combined in the normal routing scheme. This throughput gain depends on the network architecture and traffic demands. There is no specific figure to quantise throughput, but given a certain topology and traffic demands one can quantify the possible gain region over these circumstances.

2.4.2.2 Resources

Resource savings can be achieved by the introduction of network coding. The fact that we need fewer resources to satisfy the same demands of the classical non-network coding approach minimises the cost of the employment of these resources; the cost

can mean expenses or energy footprint. In certain circumstances, network coding can reduce transmission time as compared to the classical approach (3 transmissions instead of 4 [80]). This minimises the delay greatly.

2.4.2.3 Security

The free added security by implementing coding at nodes and the multipath diversity that occurs as a result of network coding constitutes a significant security enhancement. However, it's a double edged sword; it is also a challenge, as we will see later.

2.4.3 Challenges of Network Coding

2.4.3.1 Complexity

While implementing network coding improves performance, it comes at the expense of complexity of the functionality implemented in nodes. The level of complexity and its corresponding performance gain is a major question. Achieving high performance with the minimum possible complexity is a goal everybody is looking to achieve. Complexity should also be considered at the network level. The number of nodes with coding ability, their location given a certain topology and the level of complexity of each are few examples of the issues. The complexity problem is in itself a complex problem.

2.4.3.2 Delay

Delay can be a consequence of complexity, but we rather think of it as a separate matter. Even with the simplest codes, the node may be waiting for information flow from other nodes to perform an operation. Also the benefits of network coding are impeded by the delay generated by the process. The delay is mentioned also in the benefits section, which makes it also an interesting property. The net benefit of the delay issue must be significant when implementing network coding.

2.4.3.3 Synchronisation

Nodes that may take more than one information flow should acquire extra information for synchronisation, especially for real time applications (e.g voice, video streaming). It is worth noting that in a specific class of networks where synchronisation is an inherent property of their design and implementation, network coding becomes a viable possibility.

2.4.3.4 Scalability

Two features have to be considered, the first is the migration of existing infrastructure to support network coding, and the second is the change of network coding scheme as the network expands and requirements change. The goal in solving such a problem will be to minimise the differential coding requirement as the network changes, ultimately to zero.

2.4.3.5 Security

Introducing intermediate entities that can perform operations on the data can result in serious preaches to the security, contrary to the scheme where the only involved parties in communication (source, destination) are allowed to perform coding and decoding. This requires investment in increasing security measures of the implemented system.

2.4.4 Network Coding in Optical Networks

The use of network coding in optical networks has received little attention. Most of its use was the direct and apparent exploitation of the areas where there are multicast scenarios, such as passive optical networks, or the case of multiple paths as in protection, here we review all the work carried out so far.

2.4.4.1 Protection

The first application of network coding in optical networks started in 2006, by [81] where the authors considered the problem of protection in mesh optical networks. They built on the 1+N p-cycles protection approach and introduced network coding. They showed that the outage time in a failure scenario is no longer than the delay over the cycle. The authors in [82] used network coding with reduced link capacities to provide protection over single link failures by providing backup protection paths which carry coded data from all sources, instead of using dedicated protection paths. They also provide implementation aspects of their two proposed protection schemes NPS-1 and NPS-2.

The work in [81] was extended in [83] by implementing the network coding protection scheme on an overlay layer which makes the deployment simple, scalable and does not require the synchronisation required by the original scheme. They also compared the cost of the proposed scheme with the 1+1 scheme and included multiple link failures, by sharing of the protection circuit by a number of paths.

2.4.4.2 Passive Optical Network

It has been shown in [84] that through the use of network coding for multicast in the PON, a reduction in the total packet delay and the packet loss ratio is achieved. The simulation was done for intra-ONU traffic using 1Gbps EPON. Improvements on the throughput of the downlink by 50% in [85] were achieved without imposing any hardware changes. The approach carried out to quantify the gains is analytical and by simulation. The results showed the outcome of this approach in the queuing delays, gains in throughput, and the variability of traffic. The implementation for PON was taken to the NG-PONs by the work in [85] which showed that using NC in NG-PONs has a great potential in improving throughput, reliability in bad conditions and delay. Their work, in contrast to the previous two, focused in more detail on the impact on performance. They also showed that applying NC for FiWi networks has additional benefits.

The only work, to our knowledge, that addressed the energy efficiency of network coding was done by [86], applied to NG-PONs. They used NetFPGAs to emulate the use of NC in EPON (IEEE 802.3ah). They combined NC with sleep cycles in the downstream, which resulted in better energy efficiency. The work in [87] and [88] introduced network coding in optical networks by finding multicast scenarios in optical networks, which is similar to what have been done in wireless. The authors

exploit multicast OXCs and solves the problem by dividing it into two stages, the first is finding sub graphs of the topology to code over and then finding suitable codes.

2.4.4.3 Physical Layer Network Coding (All Optical)

An optical layer network coding approach was presented in [89] though it is more of a polarisation multiplexing scheme where two streams are combined through a polarisation beam combiner. At the receiving end, with delay differences from the two streams a preamble for the first stream and a postamble from the second stream can be detected where useful information about each of them can be detected and an estimate of each stream can be received. The work demonstrated a practical prototype as a proof of concept with 10Gbps NRZ OOK optical frames.

2.5 Mixed Integer Linear programming (MILP)

Mathematical programming is an optimisation technique where an optimum solution to a function referred to as the objective function is found satisfying a set of bounds and constraints [90]. The programme consists of four main elements:

- The objective function: this is maximised or minimised during the optimisation process and whose value represents the outcome of the programme.
- Optimisation variables: these are the variables that are varied adhering to constraints to optimise the objective function.
- Constraints: which are a set of mathematical inequalities that define the feasibility region of the solution

- Bounds of variables: determine the upper and lower bounds of each variable in the problem.

Mixed Integer Linear Programming is a mathematical optimisation programme in which all the bounds, constraints and the objective function are linear and the variables are a mixture of integer and non-integer values [91]. An important subclass is the binary mixed integer linear programmes where some of the variable have $0, 1$ values which are used to model decision variables. Integer programming is an NP-complete problem where the time to find a solution to the problem cannot be found in polynomial time. For this kind of problems, even for smaller instances of the problem is hard to have a polynomial time solution. Polynomial time solutions are fast, as the number of steps to calculate the solution is a polynomial function of the size of the input. The standard form is:
Objective function

$$f = c_1x_1 + c_2x_2 + ... + c_nx_n$$

Constraints:

$$a_{11}x_1 + a_{12}x_2 + ... + a_{1n}x_n \leq b_1$$

$$a_{21}x_1 + a_{22}x_2 + ... + a_{2n}x_n \leq b_2$$

$$a_{n1}x_1 + a_{n2}x_2 + ... + a_{nn}x_n \leq b_n$$

and non-negativity constraints:

$$x_1 \geq 0, x_2 \geq 0, ..., x_n \geq 0$$

Normally, the variables are continuous, making the problem solvable in polynomial time. If some or all of them, however, are constrained to integers, the problem is called mixed integer linear programming (MILP), and the problem turns into an NP hard problem for which no polynomial time algorithm has been discovered yet.

MILP problems are non-convex, therefore systematic approaches are used for their solution and the most common way is Branch and bound approach [92]. Branch and bound approach divides the problem solution into stages, the first is solving the relaxed problem with no integer constraints through the standard optimisation methods. In case the integer solution is found in this result, the optimisation stops. depending on the number of integer variables having non-integer relaxed solution, the algorithms selects one variable and branches by creating subproblems. The solution is repeated until the solution satisfies all the integral constraints.

Genetic algorithms [93] are also used to find a solution by performing successive iterations on randomly generated solutions and continuously optimising over generations. The algorithm randomly generates potential solutions satisfying the integer constraints which at the first stage are usually not optimal. These candidate solutions are transformed into more optimal solutions through mutations and crossovers and filtered by performing a fitness test after which only the best solutions survive. Although these methods provide near optimal solutions, generally they are not able to prove that the solution is optimal.

The network is based on sharing resources, most of the time there is no direct path between the source and destination. The traffic has to pass through intermediate nodes, passing several links. The set of links connecting the source and the desti-

nation is called a path. There may be many paths for a single demand, and each path carries a portion of the demand; the demand flow variables represent the traffic carried in each path. The link capacity is the amount of traffic the link can handle at low error rates, and the unit representing the demand volume should be the same as the link capacity unit, e.g. Gbps. The nodal degree of a node is the number of links that enter or leave that node, and so can be divided into the in-degree and an out-degree respectively.

The main approach adopted when using linear programming in network design involves representing the basic functionality of the network in terms of constraints, and a feasible region. The programme must search inside the feasible set and selects the optimum values of the variables that maximises (or minimises) a defined objective function. In networks, the objective function is the aim of the design represented by a function that is dependent on many design variables. Examples of objectives include Minimising Energy consumption, minimising routing cost, minimising congestion, minimising delay. . . etc.
Constraints define limitations on the set of feasible solutions. Three constraints are typically essential to every network design problem, as they represent the main and basic function of the network, these are:

- Capacity conservation: This simply states that, the total amount of flow passing through a given link cannot exceed its capacity.
- Flow conservation: This states that the traffic flowing into a node is the same traffic flowing out of a node, if the node is not a source or a destination. If it is a source, the traffic out of the node minus the traffic entering the node equals the demand originating in the node. If it is a destination, the traffic that enters it minus the traffic that leaves it equals the demand destined to it.

- Flow variables legitimacy constraint: These constraints that define the possible region over which flow variables can take values, and most of the time these are non-negativity constraints. Since each flow variable should have a positive value, if not zero.

The mathematical formulation is represented in computer systems in many ways, the most popular of which is the AMPL (A Mathematical Programming Language) [94]. This AMPL formulation is fed into MILP solvers of which there exist many options (CPLEX [95], GNU GLPK [96], CBC [97], lpsolve [98],...etc). The one commonly used and the one used in this work is the IBM ILP CPLEX optimisation suite [95]. This solver either ran on an i5, 3.3 GHz, 64GB of RAM machine, or in a High Performance Computing cluster with 16 cores and 256 GB RAM.

Chapter 3

Network Coding in Optical Networks

3.1 Introduction

In this chapter a change in node architecture to improve the energy efficiency of IP over WDM networks under unicast connections is proposed. This new architecture facilitates network coding for the unicast bidirectional flows between node pairs. The functionality of a node is upgraded from the mere store and forward to the store, code and forward functionality, where the coding is done with the flow from the opposite direction. This can be done at the IP layer (IP router) or the optical layer.

3.2 Concept Description

The concept of network coding is usually illustrated by the well-known butterfly network shown in Figure 3.1 (left). Here the sources k and n want to multicast two units of information, X, and Y, to two receivers, $d2$ and $d1$, respectively. Assuming all links have a unit capacity, tracing the flows will lead to a bottleneck in link (m, u). Instead of doubling the link capacity to resolve this bottleneck, the link capacity can be shared by the two flows by encoding the flows by an XOR operation in node m and multicasting the encoded flow to $d1$ and $d2$ from node u.

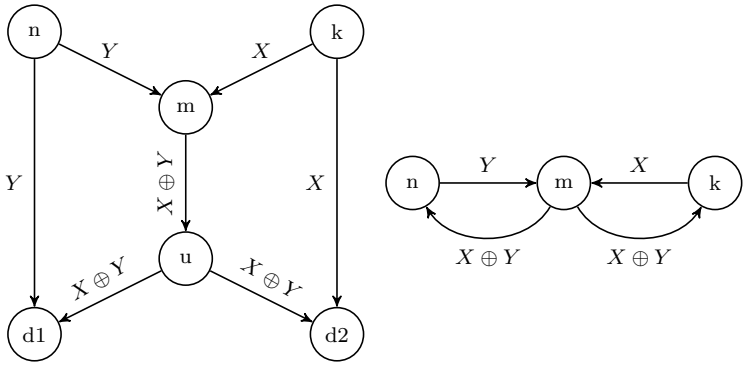

Figure 3.1: The butterfly network (a) and the three nodes network (b)

Figure 3.1 (b) shows a special case of the butterfly network where each of the nodes pairs $(n, d1)$, (m, u) and $(k, d2)$ are considered a single node, where the links connecting them are regarded as storage rather than communication links, this converts the butterfly network to a 3 node network n, m and k. This special butterfly can perform network coding in a unicast scenario. Suppose node k wants to transmit the information units X to node n, and node n wants to transmit Y to node k. Both flows will go through the intermediate node m, which can combine the flows using the XOR gate and multicast back the encoded flow to both end nodes. Each node retrieves the information unit intended to it by XOR coding the received unit

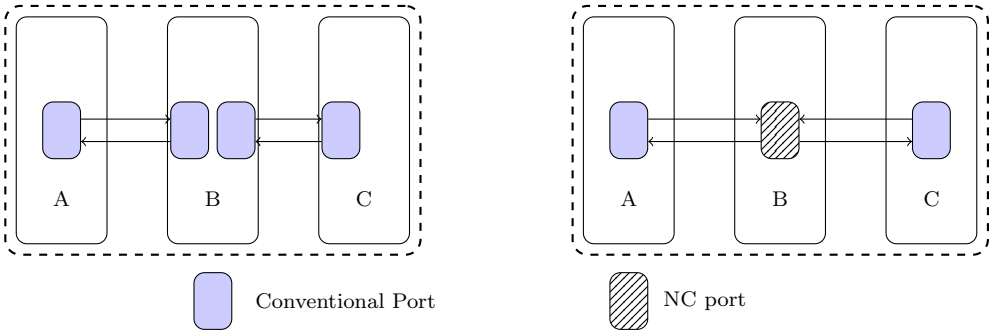

Figure 3.2: Conventional architecture (a), and Network coding architecture (b)

with the stored information unit. In the middle node where coding is performed, we encounter resource savings.

The new approach is described in Figure 3.2. At end nodes where flows originate or terminate, the same ports as the conventional routing approach will be used. At intermediate nodes, however, two conventional ports will be replaced by a single port that implements the coding functionality. During the course of this work, we will use the term conventional port (architecture) to refer to the current implementation, and the NC port (architecture) for the network coding enabled IP port. The coding functionality used here is the mere modulo-2 addition (XOR). For the three nodes example shown in Figure 3.2 the number of ports is reduced from 4 conventional ports to 1 NC port and 2 conventional ports. The amount of power savings will depend on the ratio of the power consumption of the two types of ports as well as how the network assign flows to routes.

The architecture of the network coding enabled IP over WDM node is illustrated in Figure 3.3. In addition to the transmitter and receiver found in conventional ports, an extra receiver is required to enable the port to receive the two flows to be encoded. Storage is needed to synchronise data before encoding. Note that, even if we perform the synchronisation in the IP layer, different data flows may not arrive at the intermediate node at the same time therefore, storage is essential here. The

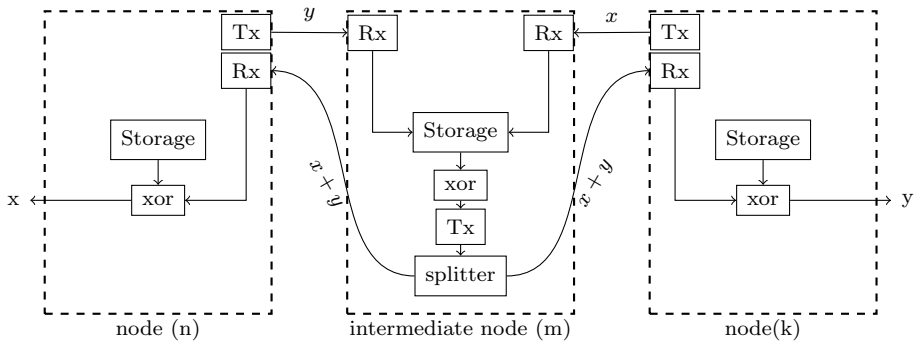

Figure 3.3: Network coding node architecture

XOR unit is used to encode the flows. The transmitter is connected to a coupler in the optical layer for multicasting, as well as an amplifier to compensate for the power loss due to splitting, and support long distance optical transmission. Note that the coding operation is done in the IP layer, and the new coding scheme will be implemented as an NC card that is plugged in the IP router chassis in addition to the conventional router cards. In the source and destination nodes, the storage unit is used to store the original data and the XOR is used to decode the received encoded flow. The fact that the coding is done in the IP layer makes the additional storage and the simple XOR code come at a low cost as the storage functionality is already in existence in conventional ports, and the XOR functionality can become part of the processing. Performing the coding operation in the optical layer is also a possible extension and can reduce the processing energy cost in the IP layer. However, all optical coding gates and controllable optical delay buffers are still in their infancy, which makes the IP implementation more favourable to support the overall approach.

Network coding can be performed at all intermediate nodes of bidirectional flows. Figure 3.4 illustrates how the network coding is performed in a bidirectional flow traversing two intermediate hops. We consider an example where node $n1$ needs to send packets 1, 2 and 3 to node $n4$ and node $n4$ needs to send packets A, B, and

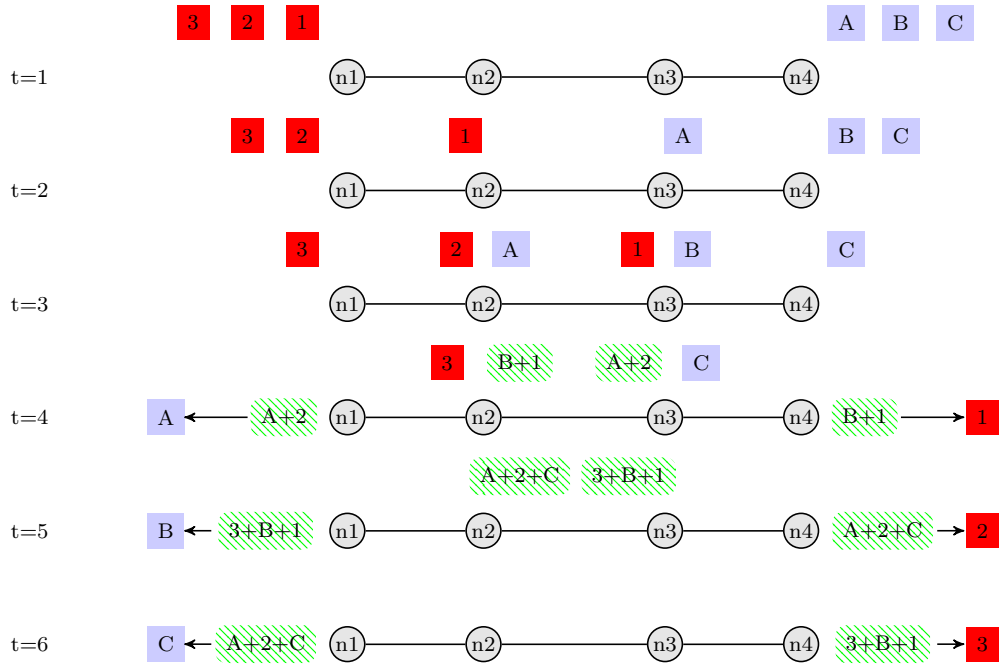

Figure 3.4: Network coding at two intermediate nodes

C to node $n1$. The packets being sent, received or processed by a node are shown above the node.

- At $t = 1$, packets (1) and (A) are being prepared for transmission by $(n1)$ and $(n4)$, respectively.
- At $t = 2$, packets (1) and (A) arrive at their neighbouring intermediate nodes, meanwhile packets (2) and (B) are being prepared by nodes $(n1)$ and $(n4)$, respectively. As intermediate nodes $(n2)$ and $(n3)$ receive only a single packet from one side no coding takes place and the packets are forwarded to the next node.
- At $t = 3$, packets (1) and (B) arrive at node $(n3)$ and packets (A) and (2) arrive at node $(n2)$. Nodes $(n2)$ and $(n3)$ encode their packets and produce $(2 + A)$ and $(1 + B)$ respectively. The encoded packets are multicast to the two neighbouring nodes (e.g. for node $(n2)$ it goes to nodes $(n1)$ and $(n3)$).

- At $t = 4$, end node $(n1)$ receives packet $(A + 2)$ and decodes it using the stored packet (2). The same applies to node $(n4)$ decoding packet $(B + 1)$ with the stored packet (B). Meanwhile, intermediate nodes $(n2)$ and $(n3)$ receive packets $(B + 1)$ and $(A + 2)$. First they decode them using the stored packets (1) and (A), to produce packets (B) and (2), $(n2)$ then encodes (B) with (3) to produce $(B+3)$, and $(n3)$ encodes (C) with (2) to produce $(C+2)$, which both are multicast to their two intended neighbours.

- At the remaining time slots, end nodes decode their received coded packets using their stored packets in a straightforward manner.

We assume that packets are fully synchronised at reception (buffering can be used to help the synchronisation process). Nodes decide which packets are encoded in a given packet from a metadata, which is carried in the header and presumably negligible compared to packet sizes. Another possibility is to do coding on established paths in a circuit switched network, where paths are decided, and hence encoding possibilities, will be decided beforehand. We also assume the control and management overhead is negligible since it can be performed as a result of a software upgrade to the system.

3.3 The MILP Model

In this section we develop an MILP model to minimise the total power consumption of a non-bypass IP over WDM network with the aforementioned network coding implementation by optimising the routes each demand takes, and optimising the number and location of conventional and NC ports, for a given network topology

and demands matrix. Below are lists of sets, parameters and variables defined in the MILP model:

Table 3.1: List of the sets used in the MILP model

Set	description
$\mathcal{N}$	Set of network nodes
$\mathcal{N}_m$	Set of neighbouring nodes to node m

Table 3.2: List of the parameters used in the MILP model

Parameter	Description
λ^{sd}	The volume of demand (s, d) in multiples of wavelengths
L^{mn}	The length of physical link (m, n)
B	The wavelength capacity in Gbps
W	Number of wavelengths per fibre
s, d	Denotes source and destination of a traffic demand
m, n	Denotes end points of a physical link
p_p	Power consumption of a conventional router port
p_x	Power consumption of a NC router port
p_t	Power consumption of a transponder
p_e	Power consumption of an EDFA
p_o	Power consumption of an optical switch
p_{md}	Power consumption of a multiplexer/demultiplexer
S	Distance between neighbouring EDFAs

Table 3.3: List of the variables used in the MILP model

variable	description
P_T	The total power consumption of the network (W)
$w_{m,n}^{sd}$	The traffic flow between node pair (s, d) that traverses physical link (m, n), in Gbps
$b_{m,n}^{sd}$	Binary equivalent of $w_{m,n}^{sd}$, $b_{m,n}^{sd} = 1$ if $w_{m,n}^{sd} > 0$, $b_{m,n}^{sd} = 0$ otherwise
c_{nmk}^{sd}	$c_{nmk}^{sd} = 1$ if demand (s, d) traverses links (n, m) and (m, k) (i.e. bidirectional traffic flows can be encoded in node m)
Y_m	Number of conventional ports at node m
X_m	Number of NC ports at node m
X_{nk}^{m}	Number of NC ports at node m catering for the traffic encoding between the node pair (n, k)
A_{mn}	The number of EDFAs on a physical link (m, n). Typically $A_{mn} = \lfloor L_{mn}/S - 1 \rfloor$, where S is the distance between two neighbouring EDFAs.
f_{mn}	The number of fibres on physical link (m, n)
w_{mn}	The total traffic flow carried on physical link (m, n)
w_{nk}^{m}	The total traffic flow carried between the node pair (n, k) passing through the intermediate node m
Npo_{mn}	The number of conventional router ports where the traffic starts at source node m and terminates in a node n
Npi_{mn}	The number of conventional router ports where the traffic terminates at destination node n and starts in a node m
Np_{mn}	The number of conventional router ports at node m interfacing node n

We assume that the network is fully synchronised, i.e. the information units to be XOR coded arrive at the same time, or are buffered before being coded. This requirement for buffering is a consequence of the randomness of the arrival process. This buffering process also absorbs the delay introduced by the XOR coding process. The consequence of this assumption is the introduction of a lower bound on power consumption. In reality, and under tight real time communication requirements, the coding process may be forced to encode the traffic alone with a stream of zeros, reducing the potential of network coding in terms of energy.

Objective: minimise the total power of the network:

$$P_T = \sum_{m \in \mathcal{N}} \left(P_p Y_m + P_x X_m + Po_m + Pmd_m + \sum_{n \in \mathcal{N}_m} (P_t w_{mn} + P_e A_{mn} f_{mn}) \right). \quad (3.1)$$

The total power consumption in 5.1 is the composed of the following contributions:

- The total power consumption of conventional router ports

$$\sum_{m \in \mathcal{N}} P_p Y_m. \quad (3.2)$$

- The total power consumption of NC router ports

$$\sum_{m \in \mathcal{N}} P_x X_m. \quad (3.3)$$

- The total power consumption of optical switches

$$\sum_{m \in \mathcal{N}} Po_m. \quad (3.4)$$

- The total power consumption contribution from multiplexers and demultiplexers

$$\sum_{m \in \mathcal{N}} Pmd_m. \tag{3.5}$$

- The total power consumption of transponders

$$\sum_{m \in \mathcal{N}} \sum_{n \in N_m} P_t w_{mn}.$$

- The power consumption of all the EDFAs

$$\sum_{m \in \mathcal{N}} \sum_{n \in N_m} P_e A_{mn} f_{mn}.$$

Subject to:

$$\sum_{n \in \mathcal{N}_m} b_{mn}^{sd} - \sum_{n \in \mathcal{N}_m} b_{nm}^{sd} = \begin{cases} 1 & : m = s \\ -1 & : m = d \\ 0 & : otherwise \end{cases} \tag{3.6}$$

$$\forall s, d, m \in \mathcal{N} \quad .$$

Constraint (3.6) represents the flow conservation constraint where the total incoming traffic equals the outgoing traffic for all nodes except the source and destination.

$$w_{mn}^{sd} = \lambda^{sd} b_{mn}^{sd}, \tag{3.7}$$

$$\forall s, d \in \mathcal{N}, \forall m \in \mathcal{N}, n \in \mathcal{N}_m \quad .$$

Constraint (3.7) calculates the flow of a traffic demand that traverses a link based

on the binary variable b_{mn}^{sd}.

$$w_{mn} = \sum_{s \in \mathcal{N}} \sum_{d \in \mathcal{N}: s \neq d} w_{mn}^{sd}, \tag{3.8}$$

$$\forall m \in \mathcal{N}, n \in \mathcal{N}_m \quad .$$

Constraint (3.8) calculates the total traffic on a given link which is represented by the total flow of all demands passing through that link.

$$\sum_{s \in \mathcal{N}} \sum_{\substack{d \in \mathcal{N} \\ s \neq d}} w_{mn}^{sd} \leq W B f_{mn}, \tag{3.9}$$

$$\forall s, d, m \in \mathcal{N}, n \in \mathcal{N}_m \quad .$$

The link capacity conservation constraint is ensured by constraint (3.9), where the total flow on a link must not exceed the total capacity of all fibres on that link.

$$Npo_{mn} = \sum_{s \in \mathcal{N}} \sum_{\substack{d \in \mathcal{N} \\ s \neq d \\ s = m}} \frac{w_{mn}^{sd}}{B}. \tag{3.10}$$

Equation (3.10), and (3.11) are used in the MILP implementation instead of the more accurate $\lceil \sum_{s \in \mathcal{N}} \sum_{\substack{d \in \mathcal{N} \\ s \neq d \\ s = m}} \frac{w_{mn}^{sd}}{B} \rceil$ and $\lceil \sum_{s \in \mathcal{N}} \sum_{\substack{d \in \mathcal{N} \\ s \neq d \\ d = m}} \frac{w_{mn}^{sd}}{B} \rceil$ respectively which select the next integer greater than a given real value. This is due to relaxation of the MILP model.

$$Npi_{mn} = \sum_{s \in \mathcal{N}} \sum_{\substack{d \in \mathcal{N} \\ s \neq d \\ d = m}} \frac{w_{mn}^{sd}}{B}. \tag{3.11}$$

Now that the number of ports leaving and entering a node are determined by equations (3.10) and (3.11) respectively, and noting that router ports have a pair (i.e. Tx and Rx components), then under the asymmetric traffic the larger of the outgoing and the incoming traffic at a node determines the number of router ports needed as

shown in Equation 3.12.

$$Np_{mn} = \max(Npo_{mn}, Npi_{mn}) \tag{3.12}$$

$$\forall m \in \mathcal{N}, n \in \mathcal{N}_m$$

The total number of conventional ports is then given by:

$$Y_m = \sum_{n \in N_m} Np_{mn}, \tag{3.13}$$

$$\forall m \in \mathcal{N} \quad .$$

$$c^{sd}_{nmk} \leq b^{sd}_{nm}, \tag{3.14}$$

$$c^{sd}_{nmk} \leq b^{sd}_{mk}, \tag{3.15}$$

$$c^{sd}_{nmk} \geq b^{sd}_{nm} + b^{sd}_{mk} - 1, \tag{3.16}$$

$$\forall s, d \in \mathcal{N}, \forall m, n, k \in \mathcal{N} : m \neq n \neq k \quad .$$

Constraints (3.14, 3.15, 3.16) calculate the variable c^{sd}_{nmk} for each node and different traffic flows, the three constraints are equivalent to the $c^{sd}_{nmk} = b^{sd}_{nm} b^{sd}_{mk}$, and they are used to maintain the linearity of the model that is otherwise lost due to the multiplication of variables.

$$X^m_{nk} = \sum_{s \in \mathcal{N}} \sum_{\substack{d \in \mathcal{N} \\ s \neq d}} max(\frac{c^{sd}_{nmk} \lambda^{sd}, c^{ds}_{nmk} \lambda^{ds}}{B}), \tag{3.17}$$

$$\forall m, n, k \in \mathcal{N} : m \neq n \neq k \quad .$$

Constraint 3.17 calculates the total number of coded ports at node m that encodes the bidirectional traffic between nodes pair (n, k). Note that the number of NC

ports at a given node is determined according to the maximum flow of the bidirectional traffic demand of which the node is intermediate. The presence of the $max()$ function in equation (3.17) makes the model nonlinear, hence we use instead the following six constraints collectively to maintain the linearity of the model.

$$w_{nk}^{m} = \sum_{s \in \mathcal{N}} \sum_{\substack{d \in \mathcal{N} \\ s \neq d}} c_{nmk}^{sd} \lambda^{sd}. \tag{3.18}$$

Constraint 3.18 calculates the traffic flow value from node n to node k passing through node m. To determine the maximum of the bidirectional flows (i.e. between w_{nk}^{m} and w_{kn}^{m}), the variables Δ_{nk}^{m+} and Δ_{nk}^{m+} are introduced as binary variables, used to tell if the difference of opposite flows is positive or negative. The variable Δ_{nk}^{m} calculates the difference of the bidirectional traffic between nodes n, k that passes through node m, calculated in Constraint (3.19).

$$\Delta_{nk}^{m} = w_{nk}^{m} - w_{kn}^{m}, \tag{3.19}$$

$$\forall m, n, k \in \mathcal{N} : m \neq n \neq k \quad .$$

$$\Delta_{nk}^{m} \leq M \Delta_{nk}^{m+}. \tag{3.20}$$

$$\Delta_{nk}^{m} \geq -M \Delta_{nk}^{m-}. \tag{3.21}$$

The binary indicator variables Δ_{nk}^{m+} and Δ_{nk}^{m-} are used to tell if the bidirectional flow difference variable (i.e. Δ_{nk}^{m}) is positive or negative. If Δ_{nk}^{m} is positive, then Δ_{nk}^{m+} is set to 1, and if Δ_{nk}^{m} is negative, then Δ_{nk}^{m-} is set to 1. The case of $\Delta_{nk}^{m} = 0$ means both Δ_{nk}^{m+} and Δ_{nk}^{m-} can take the value 0 or 1, and to resolve this ambiguity,

constraint (3.22) is used to ensure that they are not both set to 1.

$$\Delta_{nk}^{m+} + \Delta_{nk}^{m-} \leq 1. \tag{3.22}$$

$$X_{nk}^{m} = \begin{cases} \frac{w_{nk}^{m}}{B} & \text{if } \Delta_{nk}^{m+} = 1 \\ \frac{w_{kn}^{m}}{B} & \text{otherwise} \end{cases} \tag{3.23}$$

$$\forall m, s, d \in \mathcal{N}, n, k \in \mathcal{N}_m, n < k$$

.

$$X_m = \sum_{n \in \mathcal{N}_m} \sum_{\substack{k \in \mathcal{N}_m \\ n<k}} X_{nk}^{m} \tag{3.24}$$

Constraint (3.24) calculates the total number of NC ports at each node.

3.4 Network Performance Evaluation

We use regular and common network topologies in our analysis. For regular topologies we analyse the ring, line, star and full mesh and for real world core networks we consider the NSFNET and the USNET networks in the USA. The NSFNET, shown in figure 3.5 has 14 nodes and 21 links and an average hop count of 2.17, while the USNET, depicted in Figure 3.6, has 24 nodes and 43 links with an average hop count of 3.

We model traffic demands by using the average traffic demands of the network at different times of the day as shown in Figure 3.7 [53], following a uniform distribution with values ranging from 20 Gb/s to 120 Gb/s where the peak occurs at 22:00.

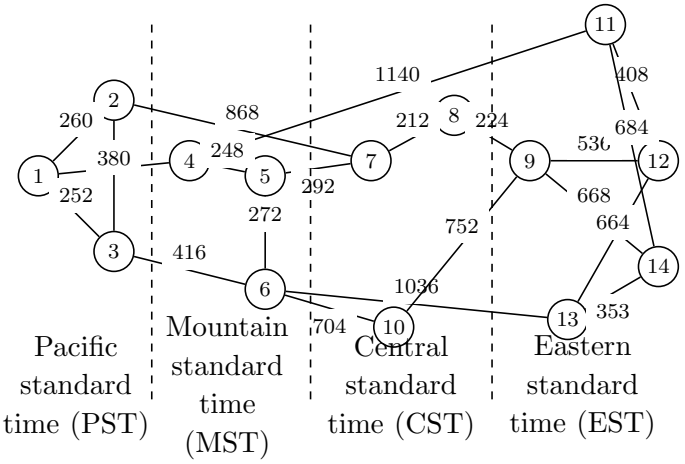

Figure 3.5: The NSFNET topology

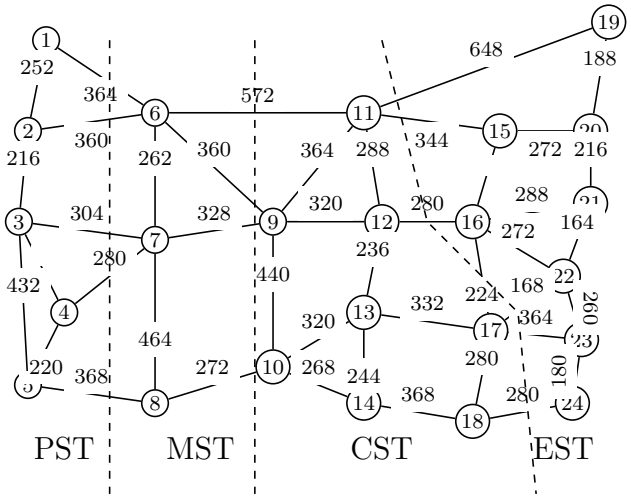

Figure 3.6: The USNET topology

This peak shifts according to the time zones by 1 hour. The actual traffic matrix is generated randomly and ensures that the average traffic at each time zone (including intra-zone traffic and inter-zone traffic) is that of Figure 3.7. This traffic model shows two kinds of variations, the first is the variation between different times of the day and the second between different nodes at a given time point. The traffic demands between node pairs takes values between 10 and 230 Gbps.

Other network parameters are shown in Table 3.4 , including the power consumption of different components. The power consumption of the network devices are derived

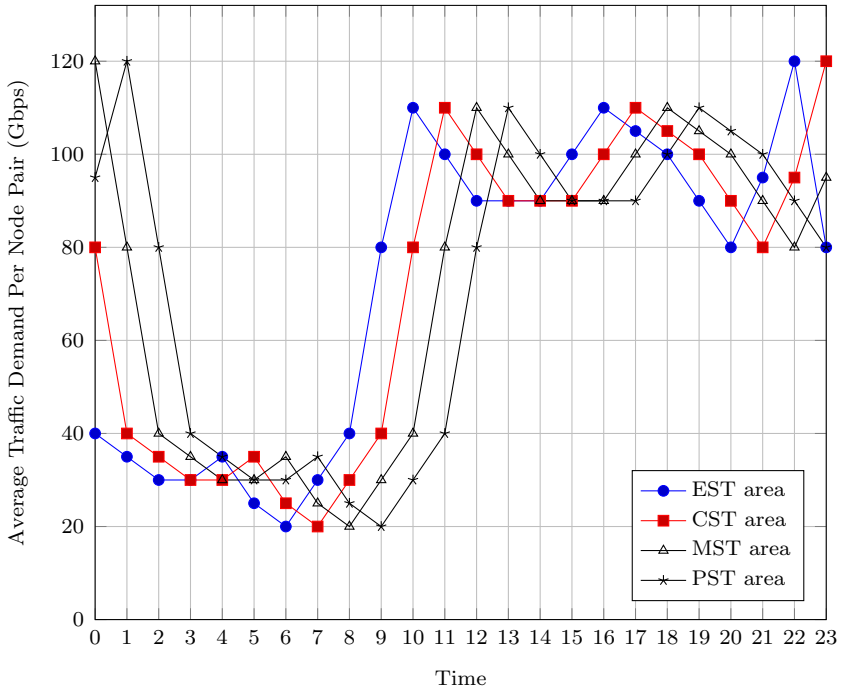

Figure 3.7: Average traffic demands at different times of the day[4]

from [99], [100], [101], [102], [103]. The 100 Watts increase in power consumption for the NC ports represents a good estimate of the power consumption of the processing of the XOR operation and the added transmitter and amplifier at the physical interface module of the port. The estimate is based on the architecture of Cisco Carrier Routing System [99] where the router is composed of multiple Line cards connected through switch fabric, and each line card consists of an interface module that performs layer 1 and layer 2 functionality of the network, and a modular service card that performs layer 3 processing and forwarding. This increased power consumption of the network coded port takes into account the fact that the majority of the router port will remain unchanged such as the switching fabric, packet's header processing and look-up tables reading. In the calculations, a partially used wavelength was assumed to consume part of a router port and a transponder proportional to traffic volume. This assumes either grooming or a proportional power profile for router ports and transponders and such a proportional power profile is desirable and is a

Parameter	Value
Distance between neighbouring EDFAs	80 km
Number of wavelengths in a fibre (W)	16
Capacity of each wavelength (B)	40 Gbps
Power consumption or a normal port(Pp) [99]	1 kW
Power consumption of a coded port (Px)	1.1 kW
Power consumption of a transponder (Pt) [100]	73 W
Power consumption of an Optical Switch (PO) [101]	85 W
Power consumption of a MUX/DeMUX [102]	16 W
EDFAs power consumption (Pe) [103]	8 W

Table 3.4: Network Parameters

goal of current equipment manufactures and grooming can be practically achieved. We performed the MILP optimisation using AMPL/CPLEX software running on a High Performance Computing cluster with 16 cores CPU and 256GB RAM.

The energy efficient routing heuristic used in our case can be simply described by routing all demands based on the minimum hop path between the source and destination, selecting the shortest path in case two alternative paths have the same minimum hops. Based on this flow allocation, network coding is performed at all intermediate nodes, then the total power consumption and the amount of conventional ports and NC ports are calculated.

3.4.1 Example Topologies

Figure 3.8 and Figure 3.9 show the power consumption of the NSFNET and USNET topologies, at different times of the day, respectively. Daily average power savings of 27% and 33% are obtained by introducing network coding to the NSFNET and USNET topologies, respectively. Note that the higher average hop count of the USNET topology has a limited effect in terms of increasing the power savings. Although a higher hop count means that more conventional ports will be replaced

by NC ports, however it also means more conventional ports are needed to establish flows between neighbouring nodes where the traffic flows cannot be encoded. The total power savings obtained by network coding depends on the ratio of the traffic between neighbouring nodes (cannot be coded) and the non-neighbouring nodes (can be coded). Higher savings can be obtained for networks of high hop counts as discussed below.

Figure 3.10 compares the distribution of conventional ports and NC ports across the NSFNET nodes. The conventional ports tend to be almost equally distributed among nodes, while NC ports are used more in the middle of the network at nodes with high nodal degree. This is because middle nodes are more likely to serve as intermediate nodes to traffic flows. Node 6 deploys the highest number of NC ports as it is located in the centre of the network with a nodal degree of 4. Nodes of lower hop count and/or not centrally located deploy lower number of NC ports.

The routes selected by the solution of the MILP model show no departure from the minimum hop routes selected by the conventional scenario. This fact can help facilitate the migration to the new architecture. Consequently, the amount of required coded ports at each node can be estimated at the time of design.

Figure 3.8 and 3.9 show that the average power savings achieved by the energy efficient routing heuristic in network coding enabled networks (19% and 22% considering the NSFNET and the USNET networks, respectively) approach those of the energy efficient network coding model.

We also analysed the performance of the energy efficient network coding scenario under a traffic profile based on the gravity model where the traffic production volume and attractiveness of each node is proportional to the population of that node. The traffic demands between node pairs were normalised to give averages corresponding

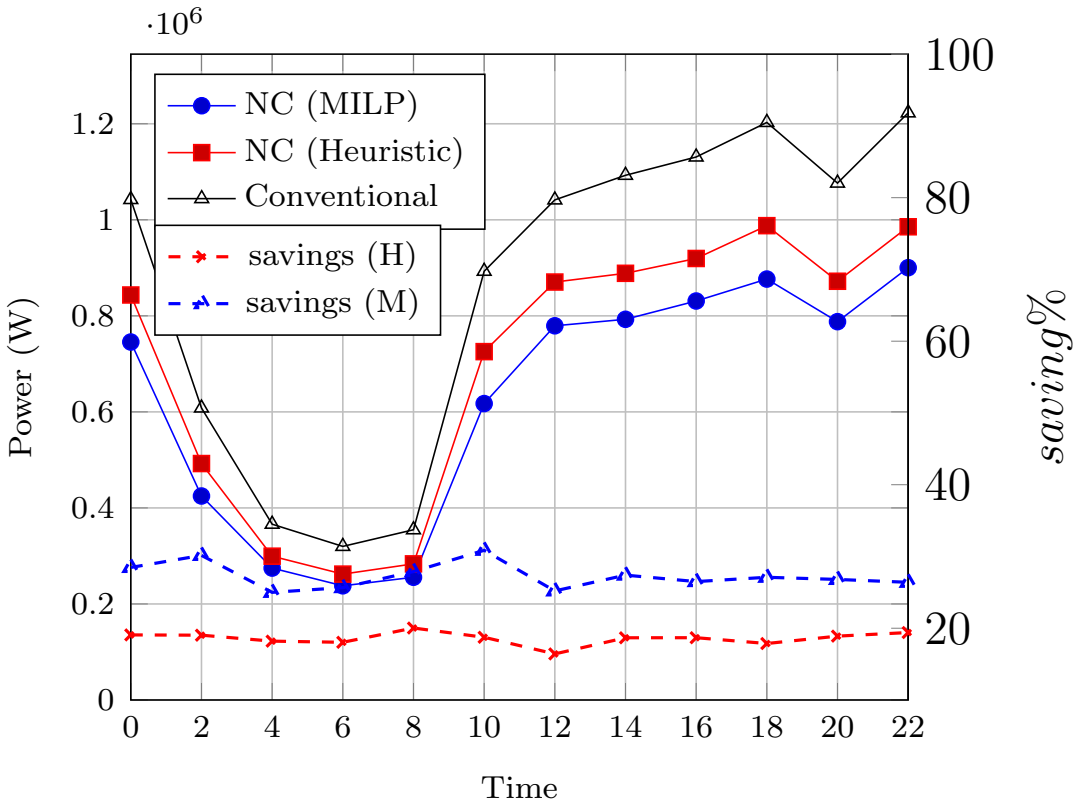

Figure 3.8: The power consumption of the NSFNET network with and without network coding

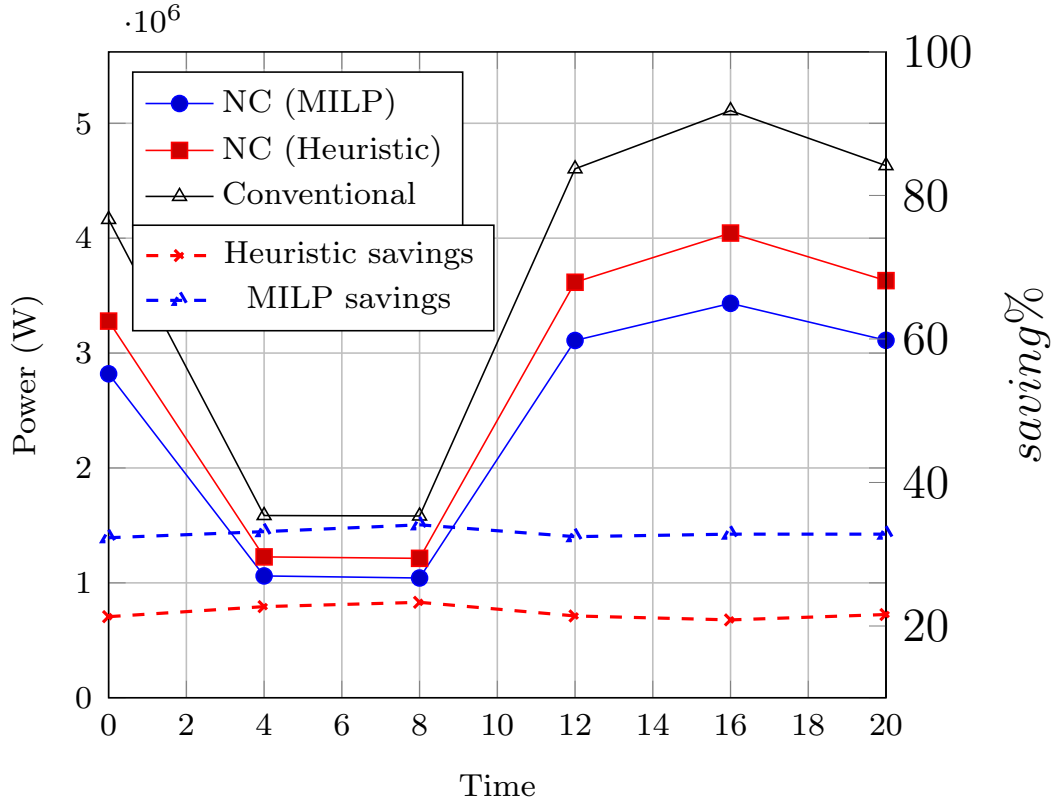

Figure 3.9: The power consumption of the USNET network with and without network coding

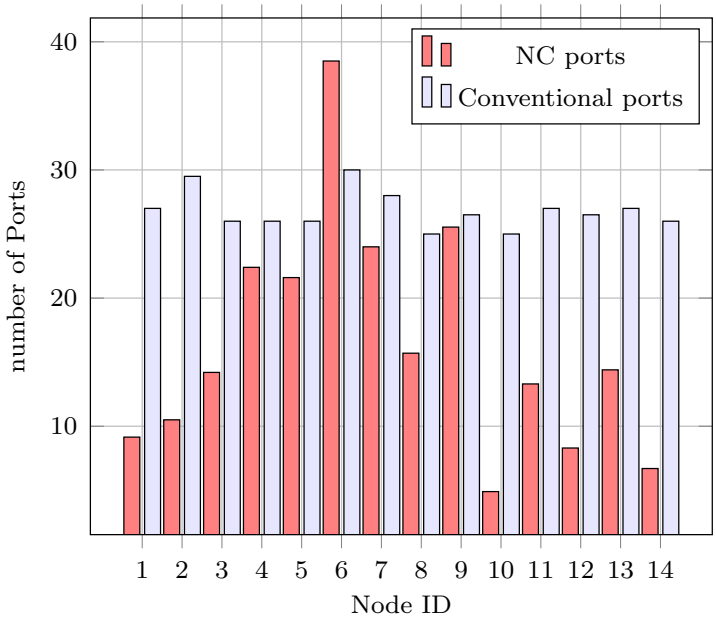

Figure 3.10: Comparison between the number of the two port types in the NSFNET nodes

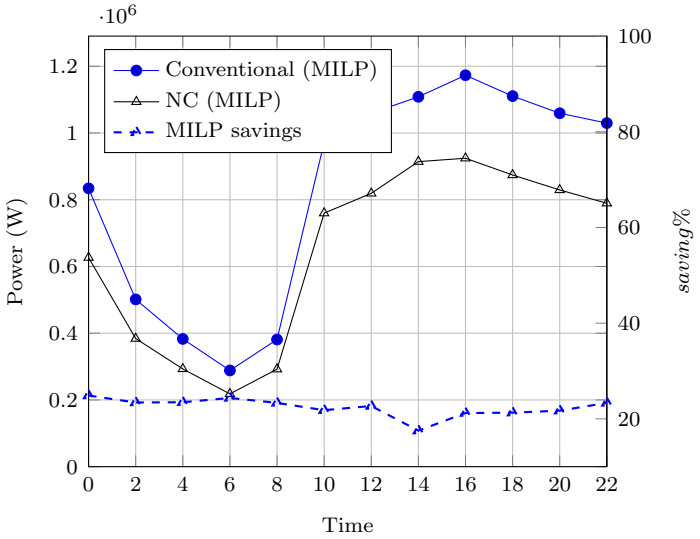

Figure 3.11: The power consumption of the NSFNET network with and without network coding using gravity model

to those provided in Figure 3.7. The results in Figure 3.11 show a pattern similar to the one obtained by the uniform traffic model. Daily average savings of 22% are obtained when applied on the NSFNET.

3.4.2 Regular Topologies

To investigate the impact of the topology, we reconfigured the NSFNET network into a bidirectional ring, and a star as seen in Figure 3.12, as well as a line (by removing link (12-14) from the ring), and a full mesh. Note that a star topology can result in practice if the traffic due to a large data centre dominates the network. The full mesh can be an attractive network topology if delay and power consumption are key metrics [104]. The ring and line topologies have high average hop counts and hence were considered. The distances (in km) shown on these links are estimates according to nodes locations. Network coding contributes the highest reduction in network power consumption (33% daily average saving) in the line topology. The high power

saving of the line topology is attributed to its high average hop count of 5, increasing the number of intermediate nodes, which increases the number conventional ports to be replaced by NC ports. On the other hand network coding adds no gain to the full mesh topology, as all the demands are routed through single hop routes. The savings obtained by the other topologies exist between these two extremes. Implementing network coding in a bidirectional ring topology (average hop count of 3.77) has saved 30% of the network power consumption while a star topology centred at node 5 with an average hop count of 1.85 has saved 16% of the network power consumption.

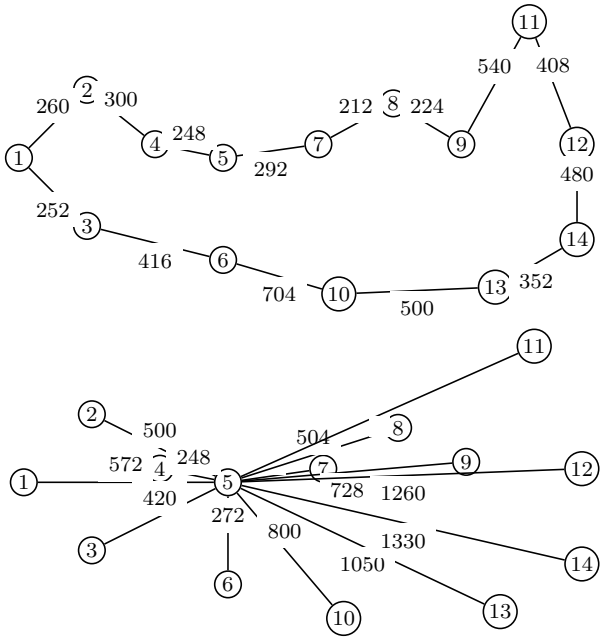

Figure 3.12: The NSFNET connected by ring and star topologies

The topologies we considered, vary from the full mesh topology having the maximum number of links, to the star topology, having the lowest number of links while maintaining connectivity.

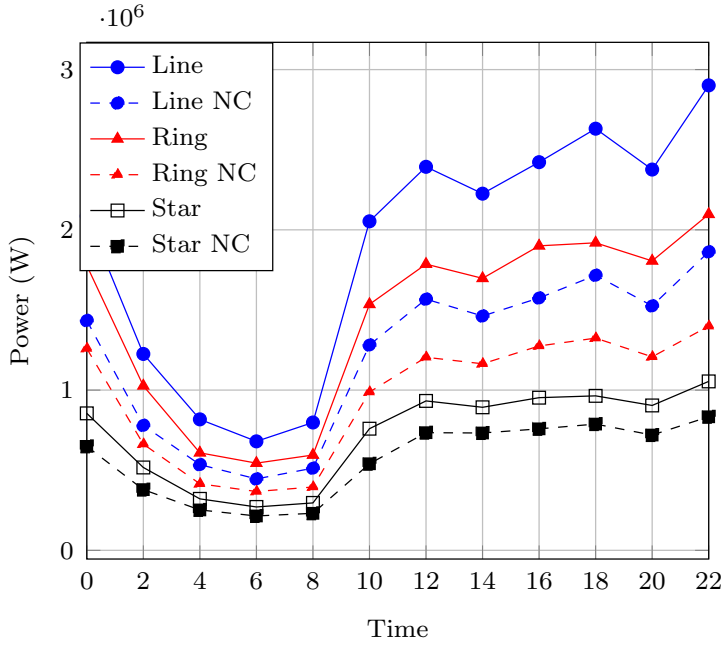

Figure 3.13: power consumption of the Ring and Star topologies with and without network coding (MILP results)

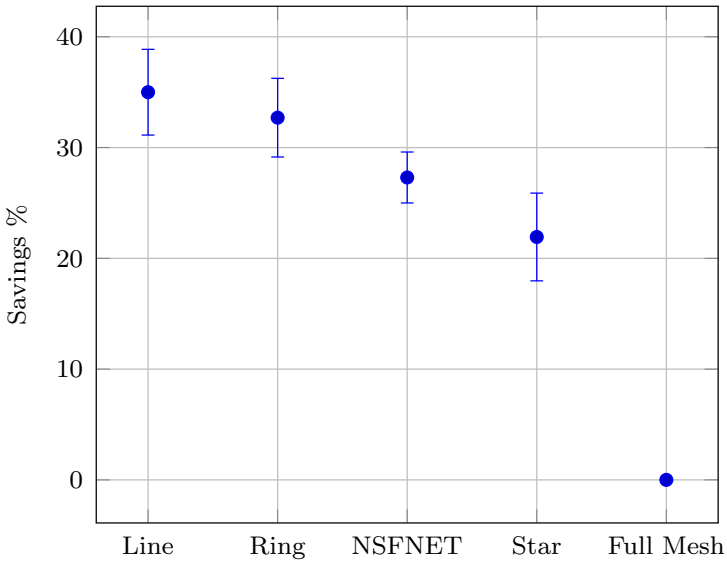

Figure 3.14: Maximum, minimum and average daily power savings in different network coded topologies

We extended the physical network topology MILP design model in [104] to perform network coding at intermediate nodes of bidirectional traffic flows. We carried

out extensive scenario evaluations. For example examined the optimum physical topology with a minimum nodal degree of 1, and 21 links (number of links in the NSFNET). The optimum topology considering network coding was in agreement with that obtained in [104].

3.5 Network coding With Partitioning

In the previous sections we assumed that the smaller of the two bidirectional flows (packets) is padded with zeros before encoding it with the other flow; hence the maximum of the two bidirectional flows is used to calculate the resources used. An alternative approach to prepare packets for network coding is to partition the bigger packet (flow) into two parts, the first part has the size of the smaller packet (flow) to be encoded, and the other part will be routed normally without encoding. Figure 3.15 (a) and (b) shows the zero padding approach (a) and the partitioning approach (b), respectively.

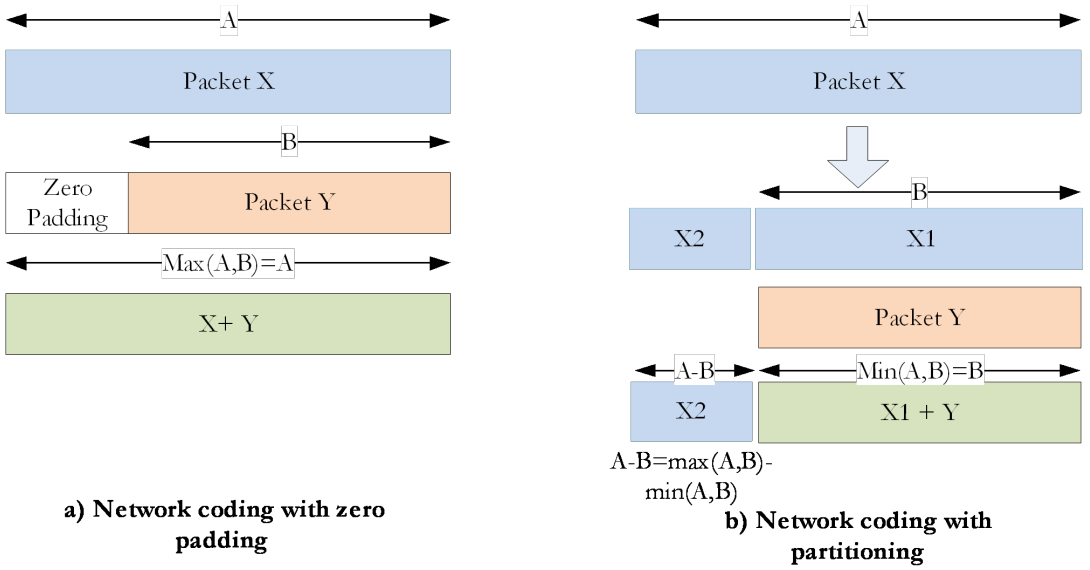

Figure 3.15: Approaches to ports calculation

The zero padding approach is the easier of the two, but less resource efficient. The partitioning approach, on the other hand, saves resources at the expense of adding control and management overheads to decide when and how to partition packets for the maximum benefit. We update the model in Section 3.3 to support the partitioning approach by changing the previous definition of the variable Y_{nk}^{m} to represent the difference between the two packet sizes calculated as

$$Y_{nk}^{m} = \frac{w_{nk}^{m} - w_{nk}^{m}}{B}, \tag{3.25}$$

and changing the variable X_{nk}^{m} to represent the minimum of the opposite flows, this will mean constraint (3.17) will change into

$$X_{nk}^{m} = \sum_{s \in \mathcal{N}} \sum_{\substack{d \in \mathcal{N} \\ s \neq d}} min(\frac{c_{nmk}^{sd} \lambda^{sd}, c_{nmk}^{ds} \lambda^{ds}}{B}). \tag{3.26}$$

and constraint (3.23) will be replaced by

$$X_{nk}^{m} = \begin{cases} \frac{w_{nk}^{m}}{B} & \text{if } \Delta_{nk}^{m-} = 1 \\ \frac{w_{kn}^{m}}{B} & \text{otherwise} \end{cases} . \tag{3.27}$$

The network coding with partitioning is subject to all the constraints in Section III except constraint (9) that calculates the total number of conventional ports which is replaced by

$$Y_m = \sum_{n \in \mathcal{N}_m} \sum_{s \in \mathcal{N}} \sum_{\substack{d \in \mathcal{N} \\ s \neq d}} \frac{w_{nm}^{sd}}{B} + \sum_{n \in \mathcal{N}_m} \sum_{\substack{k \in \mathcal{N}_m \\ k < n}} Y_{nk}^{m} \tag{3.28}$$

The first term of equation 3.28 is used to calculate the number of conventional ports in the zero padding case, where the zero padding case used the max() function in (3.12). The use of the max function was necessary as traffic was asymmetric. If source nodes, for instance, sum the traffic leaving plus entering and divide this sum by the wavelength rate, this will lead to an underestimation of the required number of ports. The correct number for the zero padding approach is dictated by the larger of the two traffic volumes leaving and entering the port, hence the max() function is needed in (3.12). In the partitioning case, however, the asymmetry is removed by the partitioning process and the residual traffic is handled using conventional network ports.

The first term of equation 3.28 accounts for the conventional ports at source and destination nodes, while the second term accounts for the residual flow from the partitioning process. For example, if the bidirectional flow is 80Gbps in one direction and 50Gbps in the other, then in intermediate nodes 50Gbps will use a coded port while the rest (i.e. 30Gbps) will be served using conventional ports. Figure 3.16 shows that the improvement obtained by implementing the partitioning approach

is limited compared to the zero padding approach under the uniform traffic profile. This is because the bidirectional flows of the traffic demands are comparable. The advantage of the portioning approach under an asymmetric traffic profile will be discussed later.

All the previous results are based on the estimation of the power consumption of the NC port given in Section 3.3. Figure 3.17 studies how the savings obtained by network coding are effected as r (the ratio of the power consumption of the network coding scheme (i.e. router ports and transponders) and the conventional scheme) grows. The savings achieved compared to the conventional case reduces as r increases. While the zero padding approach out performs the conventional approach up to $r = 1.6$, the benefit of partitioning approach can be observed up to $r = 2$.

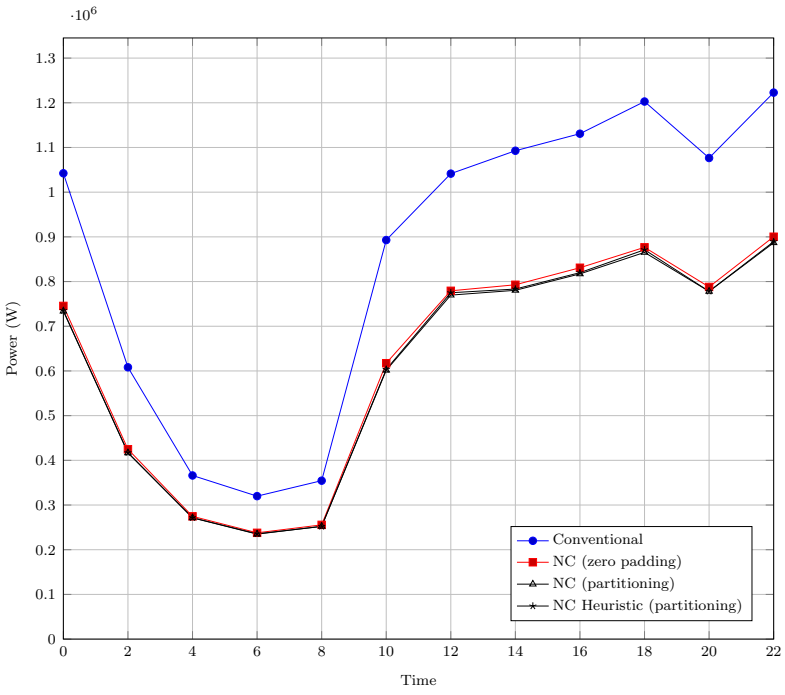

Figure 3.16: Power consumption of the NSFNET under NC with partitioning approach

Figure 3.17 shows the dependence of the power consumption in the network coding

case on the ports ratio $r = \frac{p_x+p_t}{p_p+p_t}$ for the conventional and the the network coding case with packet partitioning and zero padding under random traffic using the MILP model. It shows that the port ratio has an impact on the savings, which are better in the case of the packet partitioning. We observe savings as long as the the power consumption of the NC port (including the transponder) is less than twice that of the conventional port power consumption.

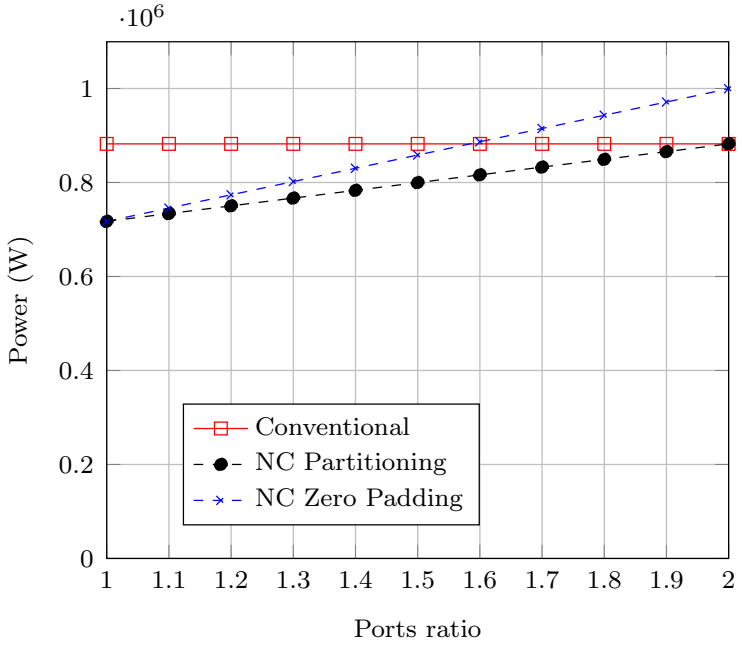

Figure 3.17: power consumption versus ports ratio using the MILP model

3.6 Network Coding in Bypass IP over WDM Networks

We showed that network coding can provide savings around 33% for common core networks compared to the conventional non-bypass architectures. In this section we evaluate this approach when it is applied to the bypass case, where flows bypass the IP layer of intermediate nodes and only undergo electro-optical conversion in the

intermediate translucent optical cross connects. In a bidirectional flow, source and destination nodes use non network coding transponders while intermediate nodes use network coding transponders. Flows between neighbouring nodes use standard non network coding transponders.

The existence of two physical layers, introduces two approaches for routing the flows from source to destination using either the lightpath non-bypass or bypass approaches. In the non-bypass approach traffic flows pass through the IP layer of each intermediate node while in the bypass approach the traffic only passes through the optical layer at intermediate nodes.

The model decides the optimum number and locations of encoding transponders, and the power consumption of the network for different coded ports power consumption. We compare the power consumption of the model with two other MILP models for the conventional bypass and non-bypass cases, both minimising the network power consumption satisfying the flow and capacity conservation constraints, as well as the bypass and non-bypass flow routing constraints respectively. We perform also a sensitivity analysis considering different values of the encoded ports to account for the possibility of higher power consumption for coded transponders as well as suggest the possible improved savings that can be attained by improving the coded transponders power consumption.

The power consumption of the network devices are shown in Table 3.5. The reason behind using the GreenTouch 2020 power consumption values [2] is that the power savings of network coding under the 2010 power consumption values are very small as router ports are the most significant power consumption equipment in the network, which reduces significantly the contribution of savings in transponders due to network coding. However, The GreenTouch consortium expects that in 2020,

Parameter	Value
Distance between neighbouring EDFAs	80 km
Number of wavelengths in a fibre (W)	32
Capacity of each wavelength (B)	400 Gbps
Power consumption or a normal port(Pp)	46.7 W
Power consumption of a coded transponder (Px)	360 W
Power consumption of a transponder (Pt)	332.6 W
Power consumption of an Optical Switch (PO)	8.5 W
EDFAs power consumption (Pe)	15.3 W

Table 3.5: Network Parameters for the bypass case [2]

transponders will consume more power than the router ports. Since the optical bypass significantly reduces the number of router port, this eventually makes network coding savings more significant. This GreenTouch prediction is based on the expected increase in the use of digital signal processing in transponders at higher data rates, while routers are expected to drop significantly in power consumption due to the use of optical interconnects and packet size adaptation techniques. We used wavelengths of capacity 400 Gbps matching the traffic increase in 2020, and assume the power consumption of the network coding results in network coding ports that consume 10% and 50% more than the conventional counterparts accounting for the extra components. We also show the results for the ratios of 0% up to 100% increase in power consumption values of transponders.

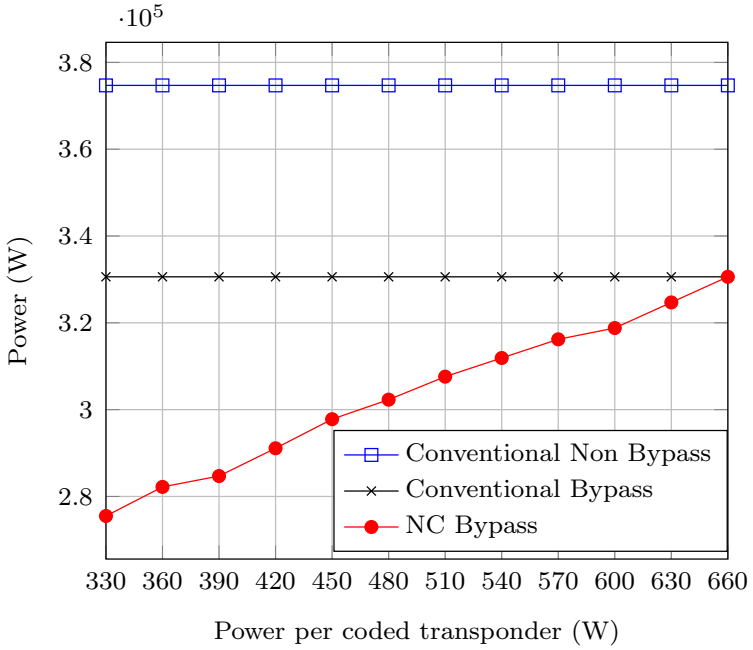

Figure 3.18: Power consumption of the network for different coded transponders' power values

In Figure 3.18, network power consumption is plotted for different network coding transponder power consumption values while the conventional transponders power consumption remains fixed to account for the uncertainty in the additional power consumption that is needed to implement the additional functions related to network coding. Such sensitivity analysis helps in determining the maximum allowed power consumption for the network coded transponder, where the network coding still produces a power saving compared to other schemes (bypass and non-bypass routing schemes).

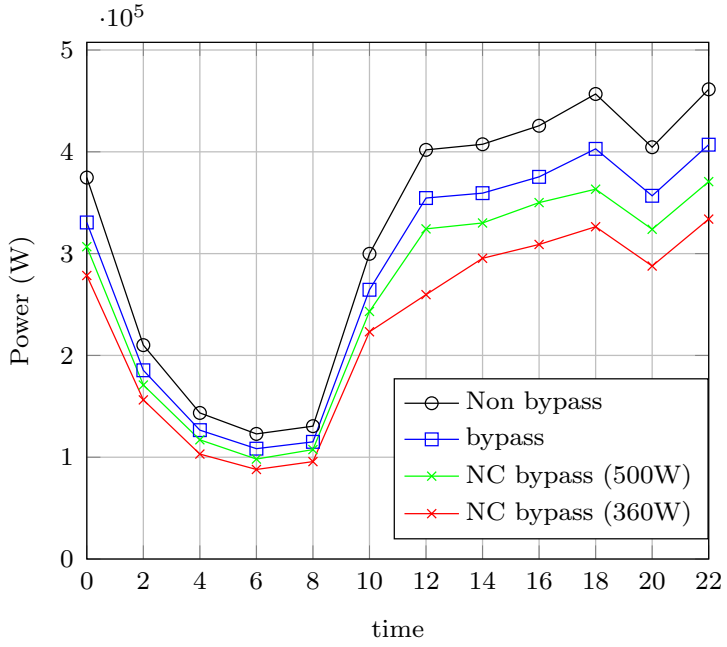

Figure 3.19: Power consumption of the NSFNET with bypass at different time of the day

Figure 3.19 shows an average power savings of 28% and 19% obtained by introducing network coding to the NSFNET topology under the bypass approach compared to the non-bypass approach considering 10% and 50% increase in coded transponders power consumption respectively. It also shows that network coding reduces the conventional bypass approach energy consumption by 18% and 9% respectively for the two investigated transponders consumption values. The results show that network coding produces power savings of 18% and 28% compared to bypass and non-bypass IP over WDM routing at our estimated network coding transponder power consumption of 330W at 400 Gb/s in 2020 and using the other 2020 GreenTouch projected values in Table 3.5 [2]. More importantly, the sensitivity results in Figure 3.18 show that our proposed network coding approach outperforms non-bypass and bypass IP over WDM networks even if the network coding transponder was to consume a high power of 660W in the bypass case (at 400 Gb/s) and even

higher in the non-bypass case showing the flexibility of our approach even in the face of variable circuit implementation options and power consumption per network coding transponder.

3.7 Summary

In this chapter we proposed the use of network coding to improve the energy efficiency of IP over WDM networks for both the non-bypass and bypass routing approaches. Considering a simple coding technique based on the xor operation in a unicast scenario, we have formulated the problem as a MILP optimisation to minimise the network power consumption by optimising the use of network resources. Daily average savings up to 27% and 33% are achieved through the use of network coding in the USNET and NSFNET topologies compared to the conventinoal architectures respectively. The impact of the topology on the savings was studied by replacing the NSFNET topology by line, ring and star topologies.

Chapter 4

Bounds on Energy Efficient Network Coding

4.1 Introduction

In this chapter we derive analytical bounds and closed form expressions for the power consumption of networks that implement network coding, and verify the results obtained by the MILP model. We develop the bounds for network coding with zero padding as well as with partitioning for the nonbypass case.

4.2 Conventional scenario

Let $G(\mathcal{N}, E)$ be a network composed of a collection of undirected edges, E, connecting a set of nodes, $\mathcal{N}$. We define the bidirectional traffic demand as the triple (s, d, λ^{sd}), where $s \in \mathcal{N}$ and $d \in \mathcal{N}$ are end nodes of the demand and λ^{sd} is the

data rate requirement of the demand. Assuming each demand follows a single path, i.e. no traffic bifurcation, the hop count traversed by a single traffic flow of the bidirectional demand is given by

$$h^{sd} = \sum_{m \in \mathcal{N}} \sum_{n \in \mathcal{N}_m} b_{mn}^{sd}, \tag{4.1}$$

where b_{mn}^{sd} is a binary variable, $b_{mn}^{sd} = 1$ if the flow between node pair (s, d) is routed through link (m, n), $b_{mn}^{sd} = 0$ otherwise. The average hop count for all flows in the network is given by

$$h = \frac{1}{N(N-1)} \sum_{s \in \mathcal{N}} \sum_{\substack{d \in \mathcal{N} \\ s \neq d}} h^{sd}. \tag{4.2}$$

The power consumption of a single traffic flow, (s, d), of the bidirectional demand in a conventional IP over WDM network under the non-bypass approach is given by

$$P_{sd} = (p_p + p_t) \sum_{m \in \mathcal{N}} \sum_{n \in \mathcal{N}_m} \frac{w_{mn}^{sd}}{B}. \tag{4.3}$$

Note that we considered only the most power consuming devices; router ports and transponders, for simplicity. Also, note that the use of traffic grooming results in efficient wavelength and router resources utilisation and improves the accuracy of (4.3). Assuming all demands of the network are equal, i.e. $\lambda^{sd} = \lambda, \forall s, d \in \mathcal{N}, s \neq d$,

$$\sum_{m \in \mathcal{N}} \sum_{n \in \mathcal{N}_m} w_{mn}^{sd} = \lambda \sum_{m \in \mathcal{N}} \sum_{n \in \mathcal{N}_m} b_{m,n}^{sd} = \lambda h^{sd}. \tag{4.4}$$

Therefore the power consumption of the single flow can be given as

$$P_{sd} = \left(\frac{P_t + P_p}{B} \right) \lambda h^{sd}. \tag{4.5}$$

The total network power consumption can be given as

$$P = \left(\frac{P_t + P_p}{B}\right) \lambda \sum_{s \in \mathcal{N}} \sum_{\substack{d \in \mathcal{N} \\ s \neq d}} h^{sd}. \tag{4.6}$$

Let $P_\lambda^{sd} = \left(\frac{P_t+P_p}{B}\right) \lambda^{sd}$ be the single hop power consumption and $P_\lambda^{sd} = P_\lambda, \forall s, d \in \mathcal{N}, s \neq d$; then the power consumption can be given as

$$P = P_\lambda \sum_{s \in \mathcal{N}} \sum_{\substack{d \in \mathcal{N} \\ s \neq d}} h^{sd}. \tag{4.7}$$

The hop count of a traffic demand in the network can be given as a function of the average hop count h as

$$\sum_{s \in \mathcal{N}} \sum_{\substack{d \in \mathcal{N} \\ s \neq d}} h^{sd} = N(N-1) \frac{\sum_s \sum_d h^{sd}}{N(N-1)} = N(N-1)h. \tag{4.8}$$

Therefore the power consumption of the IP over WDM network can be given as

$$P = P_\lambda h N(N-1). \tag{4.9}$$

4.3 Network Coding Scenario

For network coding enabled IP over WDM network, both flows of the bidirectional demand are routed through the same path so network coding is performed at intermediate nodes. In this case the power consumption of the two flows of the bidirec-

tional demand ((s,d) and (d,s)) is given as

$$\tilde{P^{sd}} = 2\left(\frac{P_t + P_p}{B}\right)\lambda^{sd} + \left(\frac{P_t + P_x}{B}\right)\lambda^{sd}(h^{sd} - 1), \tag{4.10}$$

$$\forall s, d, \in \mathcal{N}, s < d \quad .$$

The first term in Equation (4.10) gives the power consumption of end nodes where a conventional port is used to send and receive the flows at each end. Note that the XOR gate and storage at the end nodes have small power consumption and are not included here. The second term is attributed to intermediate nodes where coding is implemented. Equation (4.10) is evaluated for all values of $s < d$, as opposed to the $s \neq d$ used in the conventional case, because here we take flows in pairs, and hence $\tilde{P^{sd}}$ accounts for the total power consumed for the flow (s,d) and (d,s). The power consumption can be re arranged as

$$\tilde{P^{sd}} = 2\lambda^{sd}\frac{P_t + P_p}{B}\left(1 + \frac{p_t + p_x}{p_t + p_p}\left(\frac{h^{sd} - 1}{2}\right)\right). \tag{4.11}$$

Let $r = \frac{p_t + p_x}{p_t + p_p}$ represent the ratio of the power consumption of the network coding scheme (router ports and transponders) and the conventional scheme, then the power consumption of the bidirectional demand can be written as

$$\tilde{P^{sd}} = 2P_\lambda^{sd}\left(1 + r\frac{h^{sd} - 1}{2}\right). \tag{4.12}$$

The total power consumption of the network with network coding is

$$\tilde{P} = 2\sum_{s\in\mathcal{N}}\sum_{\substack{d\in\mathcal{N}\\ d<s}}\left(P_\lambda^{sd} + P_\lambda^{sd} r\frac{h^{sd} - 1}{2}\right), \tag{4.13}$$

giving

$$\tilde{P} = 2\left(\sum_{s\in\mathcal{N}}\sum_{\substack{d\in\mathcal{N}\\ d<s}} P_\lambda^{sd}\left(1-\frac{r}{2}\right) + \frac{r}{2}\sum_{s\in\mathcal{N}}\sum_{\substack{d\in\mathcal{N}\\ d<s}} P_\lambda^{sd}h^{sd}\right). \tag{4.14}$$

We start with the equal traffic demands case where all the demands in the network have the same value, i.e. $P_\lambda^{sd} = P_\lambda, \forall s,d \in \mathcal{N}$. The total power consumption becomes

$$\tilde{P} = 2P_\lambda\left(\left(1-\frac{r}{2}\right)\left(\frac{N(N-1)}{2}\right) + \frac{rN(N-1)h}{4}\right), \tag{4.15}$$

$$\tilde{P} = P_\lambda N(N-1)\left(1+\frac{r}{2}(h-1)\right). \tag{4.16}$$

The power savings ϕ is then given by

$$\phi = 1-\frac{\tilde{P}}{P} = 1-\left(\frac{P_\lambda N(N-1)\left(1+\frac{r(h-1)}{2}\right)}{P_\lambda hN(N-1)}\right), \tag{4.17}$$

which gives

$$\phi = \left(1-\frac{1+0.5r(h-1)}{h}\right). \tag{4.18}$$

Using the power consumption values of the conventional and NC ports given in Table 3.4, $r \approx 1.1$, reducing the savings expression to

$$\phi = \left(1-\frac{1+0.55(h-1)}{h}\right). \tag{4.19}$$

$$\phi = \left(0.45\frac{h-1}{h}\right). \tag{4.20}$$

The derived expression is used to calculate the maximum saving gained by implementing network coding in regular topologies (star, ring, line) as the number of nodes grows to infinity.

4.3.1 Star Topology

$$\phi = \left(0.45\frac{\frac{2(N-1)}{N} - 1}{\frac{2(N-1)}{N}}\right) = \left(0.45\frac{N-2}{2(N-1)}\right). \tag{4.21}$$

$$\lim_{n\to\infty} \phi = \lim_{n\to\infty} \left(0.45\frac{\frac{2(N-1)}{N} - 1}{\frac{2(N-1)}{N}}\right) = 0.225. \tag{4.22}$$

4.3.2 Ring Topology: Odd number of nodes

$$\phi = \left(0.45\frac{\frac{N+1}{4} - 1}{\frac{N+1}{4}}\right) = \left(0.45\frac{N-3}{N+1}\right). \tag{4.23}$$

$$\lim_{n\to\infty} \phi = \lim_{n\to\infty} \left(0.45\frac{N-3}{N+1}\right) = 0.45. \tag{4.24}$$

4.3.3 Ring Topology: Even number of nodes

$$\phi = \left(0.45\frac{\frac{N^2}{4(N-1)} - 1}{\frac{N^2}{4(N-1)}}\right) = \left(0.45(\frac{N-2}{N})^2\right). \tag{4.25}$$

$$\lim_{n\to\infty} \phi = \lim_{n\to\infty} \left(0.45(\frac{N-2}{N})^2\right) = 0.45. \tag{4.26}$$

4.3.4 Line Topology

$$\phi = \left(0.45\frac{\frac{N+1}{3} - 1}{\frac{N+1}{3}}\right) = \left(0.45\frac{N-2}{N+1}\right). \tag{4.27}$$

$$\lim_{n\to\infty} \phi = \lim_{n\to\infty} \left(0.45\frac{N-2}{N+1}\right) = 0.45. \tag{4.28}$$

The power savings asymptotically approach 45% and 22.5% for the ring (and line), and star topology respectively. With network coding ports as power efficient as conventional ports (i.e. $r = 1$), the savings increase to 50% and 25% respectively.

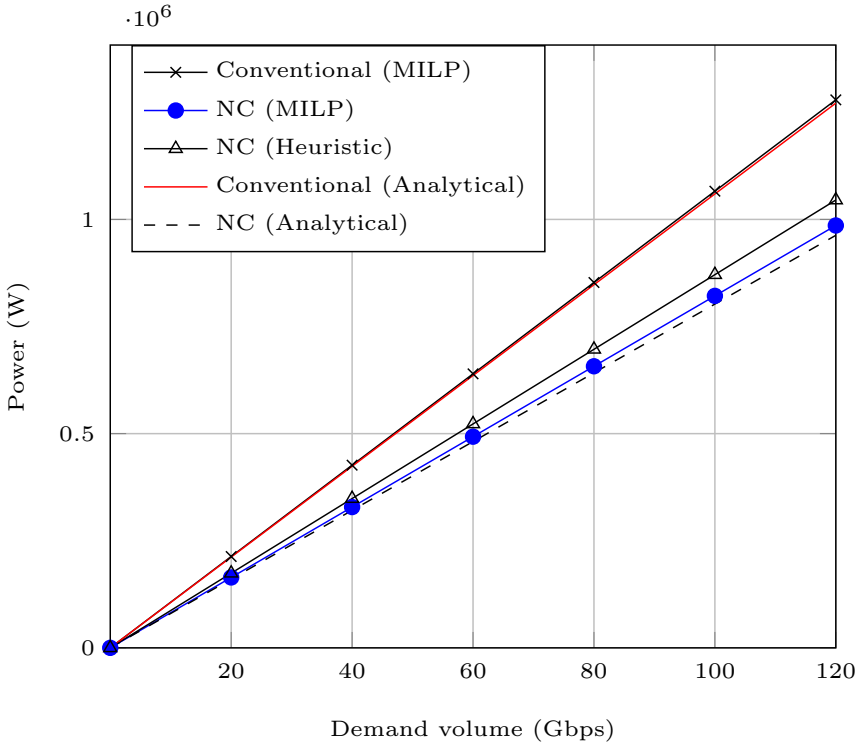

Figure 4.1: Power consumption of the analytical and MILP models for the NSFNET under the zero padding approach

Figure 4.1 shows a comparison between the MILP model, the analytical bounds derived and the heuristic for the case of equal traffic demands between all nodes for the zero padding approach. The small difference between the analytical model and the MILP model is attributed to the simplicity of the analytical formulae which takes into account only the routers and transponders.

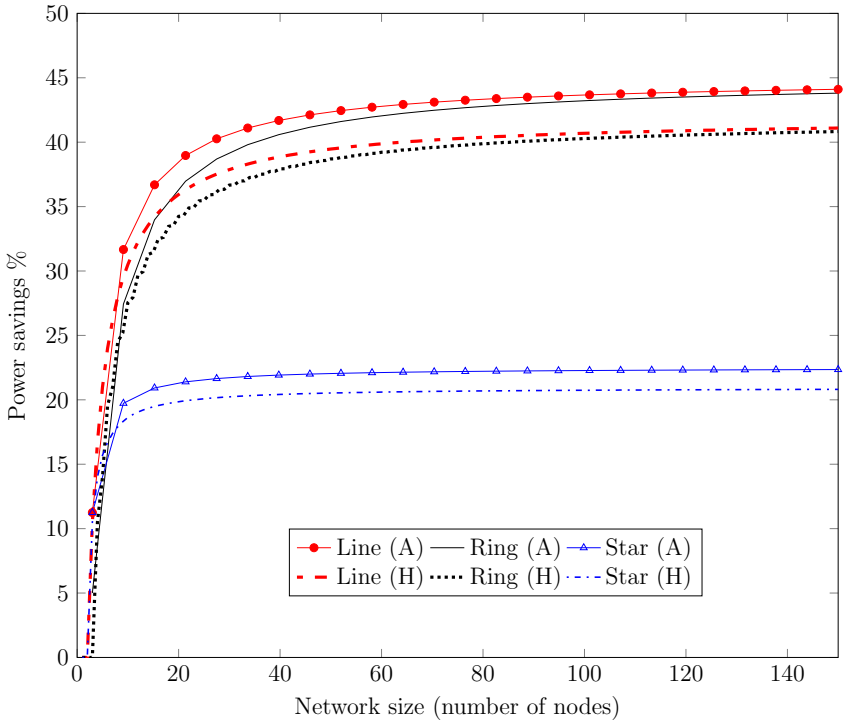

Figure 4.2: Effect of network coding on large network sizes (A:analytical and H:Heuristic)

Figure 4.2 shows the power savings as calculated by the analytical formulae for the line, ring and star topologies up to a network size of 150 nodes and compares these savings to the savings of the minimum hop routing heuristic for the network coding enabled networks for the zero padding approach. For each network size, the topologies are built with link distances equal to the average NSFNET link distance. The figure also provides results for the NSFNET and USNET to show an example of where common core networks are located. The analytically calculated power savings confirm those of the heuristic. The savings saturate just below 45% and 22.5% as the size increases. The figure shows that the ring topology converges to the maximum value faster than the line topology. Note that the power consumption of the analytical results does not take into account the power consumption of EDFAs, multiplexers and optical switches; therefore the power savings of the heuristic are

lower than the analytically calculated power savings.

For the general case when the bidirectional traffic demand volume is randomly distributed we prove first that the previous case of equal average traffic demands has better power efficiency compared to the random demands case. Considering the case of random traffic demands, equation (4.13) becomes

$$\tilde{P} = \sum_{s\in\mathcal{N}} \sum_{\substack{d\in\mathcal{N} \\ d<s}} \Big[2\max(P_\lambda^{sd}, P_\lambda^{ds}) + \max(P_\lambda^{sd}, P_\lambda^{ds}) r(h^{sd}-1) \Big]. \tag{4.29}$$

The first part of equation (4.29) accounts for the power consumption at end nodes which uses conventional ports, while the second part accounts for the power consumption at intermediate nodes which uses NC ports. We treat demands in pairs and hence the use of $(d < s)$ under the summation and the reason for the multiplication by 2.

The value of $\max(P_\lambda^{sd}, P_\lambda^{ds})$ can be written as

$$\max(P_\lambda^{sd}, P_\lambda^{ds}) = \left(\frac{p_t + p_x}{B}\right) \max(\lambda^{sd}, \lambda^{ds}). \tag{4.30}$$

$$\max(\lambda^{sd}, \lambda^{ds}) = \max(\lambda + \Delta^{sd}, \lambda + \Delta^{ds}) = \lambda + \max(\Delta^{sd}, \Delta^{ds}), \tag{4.31}$$

where λ is the average traffic of all the network. The total power of the NC case can be written as

$$\tilde{P} = 2\left(\frac{p_t + p_p}{B}\right) \sum_{s\in\mathcal{N}} \sum_{\substack{d\in\mathcal{N} \\ d<s}} \Big[\lambda + \max(\Delta^{sd}, \Delta^{ds})\Big] \left[1 + r\frac{h^{sd}-1}{2}\right], \tag{4.32}$$

which can be written as

$$\tilde{P} = P_\lambda N(N-1)\left[1 + r\frac{h-1}{2}\right] + 2\left(\frac{p_t + p_p}{B}\right)\sum_{s\in\mathcal{N}}\sum_{\substack{d\in\mathcal{N}\\ d<s}} \max(\Delta^{sd}, \Delta^{ds})\left[1 + r\frac{h^{sd}-1}{2}\right]. \quad (4.33)$$

The first two components of equation (4.33) are the power consumption of the network coded case, when the traffic demands are all equal to the average. We call it $\tilde{P^{(1)}}$ and we call the second part $\tilde{P^{(2)}}$. Therefore

$$\tilde{P^{(1)}} = P_\lambda N(N-1)\left(1 + r\frac{h-1}{2}\right). \quad (4.34)$$

$$\tilde{P^{(2)}} = 2\left(\frac{p_t + p_p}{B}\right)\sum_{s\in\mathcal{N}}\sum_{\substack{d\in\mathcal{N}\\ d<s}}\left(\max(\Delta^{sd}, \Delta^{ds})\left[1 + r\frac{h^{sd}-1}{2}\right]\right). \quad (4.35)$$

The value $\tilde{P^{(1)}}$ represents the power consumption of the network coding case when all demands are equal, the same as given by equation (4.16).

By dividing the set of all demands into subsets, each identified by the number of hops they take, i.e. H_k is the set of demands with minimum hop paths of k hops, then equation (4.35) can be written as

$$\tilde{P^{(2)}} = \frac{p_t + p_p}{B}\left[r\sum_{\substack{(s,d)\in H_2\\ d<s}}\max(\Delta^{sd}, \Delta^{ds}) + 2r\sum_{\substack{(s,d)\in H_3\\ d<s}}\max(\Delta^{sd}, \Delta^{ds}) + ... + (k-1)r\sum_{\substack{(s,d)\in H_k\\ d<s}}\max(\Delta^{sd}, \Delta^{ds})\right] + 2\frac{p_t + p_p}{B}\sum_{s\in N}\sum_{\substack{d\in\mathcal{N}\\ d<s}}\max(\Delta^{sd}, \Delta^{ds}). \quad (4.36)$$

Let $g_z(\lambda^{sd}) = \max(\Delta^{sd}, \Delta^{ds})$, then

$$\tilde{P^{(2)}} = \left(\frac{p_t + p_p}{B}\right)\left[\sum_{k}\sum_{\substack{(s,d)\in H_k \\ d<s}}(k-1)r g_z(\lambda^{sd}) + 2\sum_{s\in\mathcal{N}}\sum_{\substack{d\in\mathcal{N} \\ d<s}} g_z(\lambda^{sd})\right]. \tag{4.37}$$

The value of $\tilde{P^{(2)}}$ depends on the given topology (reflected in H_k) and the given traffic volume distribution $g_z(\lambda^{sd})$. This produces three lower bounds , one by setting all hop counts to the minimum, another by setting the traffic to a value that minimises the total power, and a third by setting the hop count and the traffic components to their minimum values. The same applies for the three upper bounds.

The bounds for the total power $\tilde{P}$ are as follows: For a given topology, the minimum value is when $g_z(\lambda^{sd}) = \max(\Delta^{sd}, \Delta^{ds}) = 0$ when $\Delta^{sd} = \Delta^{ds} = 0$. These values are attained when demands are equal. This gives the following expression of $\tilde{P}$ as

$$\tilde{P} \geq P_\lambda N(N-1)\left(1 + r\frac{h-1}{2}\right), \tag{4.38}$$

reducing the case to the previous case of the equal average demands.

For the optimal topology and generic traffic demands, we attain the following minimum value, when all demands have a single hop route ($i.e. h = 1$) when the network is connected in full mesh:

$$\tilde{P} \geq P_\lambda N(N-1). \tag{4.39}$$

This means, the higher the variation, the higher the power consumption. Also, when given a set of traffic demands with a given variation, the lowest power consumption will be when bidirectional demands with the highest variance happen to be allocated the route with the minimum hop count.

Likewise, We can also find the maximum value of $\tilde{P^{(2)}}$ by considering the topology

and traffic dimensions. Considering the traffic dimension, starting from equation (4.29) and by using the fact that $max(P_{\lambda}^{sd}, P_{\lambda}^{ds}) \leq \frac{p_t+p_p}{B}\lambda_{max}$ where λ_{max} is the upper limit to the traffic value, assuming uniform traffic distribution

$$\tilde{P} \leq 2\frac{p_t + p_p}{B}\lambda_{max} \sum_{s\in\mathcal{N}} \sum_{\substack{d\in\mathcal{N} \\ d<s}} \left[1 + r\frac{h^{sd} - 1}{2}\right], \tag{4.40}$$

this gives

$$\tilde{P} \leq \frac{p_t + p_p}{B}\lambda_{max} N(N-1)\left[1 + r\frac{h - 1}{2}\right]. \tag{4.41}$$

An upper bound considering the maximum hop count and the exact traffic is given by setting the hop count for each demand to the maximum in the network, i.e. $h^{s,d} = h_{max}$ in equation (4.35), which gives

$$\tilde{P^{(2)}} \leq 2\left(\frac{p_t + p_p}{B}\right)\left[1 + r\frac{h_{max} - 1}{2}\right] \sum_{s\in\mathcal{N}} \sum_{\substack{d\in\mathcal{N} \\ d<s}} g_z(\lambda^{sd}). \tag{4.42}$$

Therefore this bound for the total power consumption becomes

$$\tilde{P} \leq P_{\lambda}N(N-1)\left(1 + r\frac{h - 1}{2}\right) + 2\left(\frac{p_t + p_p}{B}\right)\left[1 + r\frac{h_{max} - 1}{2}\right] \sum_{s\in\mathcal{N}} \sum_{\substack{d\in\mathcal{N} \\ d<s}} g_z(\lambda^{sd}). \tag{4.43}$$

Considering both the maximum traffic and hop count, we have the following upper bound:

$$\tilde{P} \leq \frac{p_t + p_p}{B}\lambda_{max} N(N-1)\left[1 + r\frac{h_{max} - 1}{2}\right]. \tag{4.44}$$

The upper bound given by considering the maximum hop count is tighter than the one considering the maximum possible traffic demand, due to the lower variance the hop count has compared to the traffic demands variance. For the partitioning

approach, we develop closed form expression the same way we did with the zero padding approach. The number of NC ports X in the network for the partitioning case is given by

$$X = \frac{1}{B} \sum_{s \in \mathcal{N}} \sum_{\substack{d \in \mathcal{N} \\ d<s}} \min(\lambda^{sd}, \lambda^{ds})(h^{sd} - 1). \tag{4.45}$$

The number of conventional ports will be covering the traffic at source and destination nodes and the remaining traffic of the partitioning process at intermediate nodes.

$$Y = \frac{1}{B} \left(\sum_{s \in \mathcal{N}} \sum_{\substack{d \in \mathcal{N} \\ d \neq s}} \lambda^{sd} + \sum_{s \in N} \sum_{\substack{d \in \mathcal{N} \\ d<s}} (h^{sd} - 1)|\lambda^{sd} - \lambda^{ds}|) \right). \tag{4.46}$$

So the total power consumption will be

$$P_t = \frac{p_x + p_t}{B} \sum_{s \in \mathcal{N}} \sum_{\substack{d \in \mathcal{N} \\ d<s}} \min(\lambda^{sd}, \lambda^{ds})(h^{sd} - 1) + \frac{p_p + p_t}{B} \sum_{s \in \mathcal{N}} \sum_{\substack{d \in \mathcal{N} \\ d \neq s}} \lambda^{sd} + \frac{p_p + p_t}{B} \sum_{s \in \mathcal{N}} \sum_{\substack{d \in \mathcal{N} \\ s<d}} (h^{sd} - 1)|\lambda^{sd} - \lambda^{ds}|. \tag{4.47}$$

Terms can be combined together to give

$$P_t = \frac{p_p + p_t}{B} \sum_{s \in \mathcal{N}} \sum_{\substack{d \in \mathcal{N} \\ d \neq s}} \lambda^{sd} + \sum_{s \in \mathcal{N}} \sum_{\substack{d \in \mathcal{N} \\ d<s}} (h^{sd} - 1) \left(\frac{p_x + p_t}{B} \min(\lambda^{sd}, \lambda^{ds}) + \frac{p_p + p_t}{B} |\lambda^{sd} - \lambda^{ds}| \right). \tag{4.48}$$

By arranging terms we get

$$P_t = \frac{p_p + p_t}{B} N(N-1)\lambda + \frac{p_p + p_t}{B} \sum_{s \in \mathcal{N}} \sum_{\substack{d \in \mathcal{N} \\ d<s}} (h^{sd} - 1) \left(r \min(\lambda^{sd}, \lambda^{ds}) + |\lambda^{sd} - \lambda^{ds}| \right). \tag{4.49}$$

$$P_t = \frac{p_p + p_t}{B} N(N-1)\lambda + \frac{p_p + p_t}{B} \sum_{s \in \mathcal{N}} \sum_{\substack{d \in \mathcal{N} \\ d<s}} (h^{sd} - 1) \Big[\Delta + r \min(\lambda^{sd}, \lambda^{ds}) \Big]. \tag{4.50}$$

where $\Delta = |\lambda^{sd} - \lambda^{ds}| = \max(\lambda^{sd}, \lambda^{ds}) - \min(\lambda^{sd}, \lambda^{ds})$. When this is substituted in equation (4.50) it gives

$$P_t = \frac{p_p + p_t}{B} N(N-1)\lambda + \frac{p_p + p_t}{B} \sum_{s \in \mathcal{N}} \sum_{\substack{d \in \mathcal{N} \\ d<s}} (h^{sd} - 1) \Big[\max(\lambda^{sd}, \lambda^{ds}) - \min(\lambda^{sd}, \lambda^{ds}) + r \min(\lambda^{sd}, \lambda^{ds}) \Big]. \quad (4.51)$$

Grouping similar terms gives

$$P_t = \frac{p_p + p_t}{B} N(N-1)\lambda + \frac{p_p + p_t}{B} \sum_{s \in \mathcal{N}} \sum_{\substack{d \in \mathcal{N} \\ d<s}} (h^{sd} - 1) \Big[\max(\lambda^{sd}, \lambda^{ds}) + (r-1) \min(\lambda^{sd}, \lambda^{ds}) \Big]. \quad (4.52)$$

Let the function $g_p(\lambda^{sd})$ be defined as

$$g_p(\lambda^{sd}) = \max(\lambda^{sd}, \lambda^{ds}) + (r-1) \min(\lambda^{sd}, \lambda^{ds}). \quad (4.53)$$

The function $g_p(\lambda^{sd})$ represents the maximum traffic imbalance in a network where the network coding ports and the conventional ports consume the same power.

The total power becomes

$$P_t = \frac{p_p + p_t}{B} N(N-1)\lambda + \frac{p_p + p_t}{B} \sum_{s \in \mathcal{N}} \sum_{\substack{d \in \mathcal{N} \\ s<d}} (h^{sd} - 1) g_p(\lambda^{sd}). \quad (4.54)$$

The lower bound considering the traffic dimension is found from minimising equation (4.53)

$$g_{p_{min}}(\lambda^{sd}) = \bar{\lambda}^{sd} + (r-1)\bar{\lambda}^{sd} = r\bar{\lambda}^{sd}, \quad (4.55)$$

where $\bar{\lambda}^{sd}$ is the traffic volume between (s, d) when the maximum value equals the

minimum value and the average. The total power then becomes

$$P_t = \frac{p_p + p_t}{B} N(N-1)\lambda + \frac{p_p + p_t}{B} \sum_{s \in \mathcal{N}} \sum_{\substack{d \in \mathcal{N} \\ s<d}} (h^{sd} - 1)\bar{\lambda}^{sd} r. \tag{4.56}$$

By using Chebyshev's inequality shown in (4.57) where a lower bound on the average of the inner product of two vectors of size n is

$$\frac{1}{n} \sum_{k=1}^{n} a_k b_k \geq \left(\frac{1}{n} \sum_{k=1}^{n} a_k \right) \left(\frac{1}{n} \sum_{k=1}^{n} b_k \right), \tag{4.57}$$

then equation 4.56 becomes

$$P_t \geq \frac{p_p + p_t}{B} N(N-1)\lambda + \frac{p_p + p_t}{B} \sum_{k=1}^{\frac{N(N-1)}{2}} \frac{1}{\frac{N(N-1)}{2}} (h^k - 1) \sum_{k=1}^{\frac{N(N-1)}{2}} r\bar{\lambda}^k. \tag{4.58}$$

By further reducing the second term of the inequality (4.58) we get

$$P_t \geq \frac{p_p + p_t}{B} N(N-1)\lambda + \frac{p_p + p_t}{B} \left[\frac{1}{\frac{N(N-1)}{2}} \left(h \frac{N(N-1)}{2} - \frac{N(N-1)}{2} \right) r\lambda \frac{N(N-1)}{2} \right]. \tag{4.59}$$

This is reduced to

$$P_t \geq \frac{p_p + p_t}{B} N(N-1)\lambda \left[1 + (h-1)\frac{r}{2} \right]. \tag{4.60}$$

When we consider the topology dimension

$$P_t \geq P_\lambda N(N-1) + \frac{p_p + p_t}{B} (h_{min} - 1) \sum_{s \in \mathcal{N}} \sum_{\substack{d \in \mathcal{N} \\ s<d}} g_p(\lambda^{sd}), \tag{4.61}$$

since $h_{min} = 1$

$$P_t \geq P_\lambda N(N-1). \tag{4.62}$$

For the upper bound, considering the topology dimension

$$P_t \leq P_\lambda N(N-1) + \frac{p_p + p_t}{2B}(h_{max} - 1) \sum_{s \in \mathcal{N}} \sum_{\substack{d \in \mathcal{N} \\ s<d}} g_p(\lambda^{sd}), \tag{4.63}$$

and considering the traffic dimension, using the fact that the maximum power consumption of the network under network coding occurs when network coding is not used. Under the partitioning approach, network coding is not used when the bidirectional traffic is fully asymmetric, i.e. in one direction $\lambda^{sd} = \lambda_{max}$ and in the other $\lambda^{sd} = 0$. Then equation (4.54) becomes:

$$P_t \leq P_\lambda N(N-1) + \frac{p_p + p_t}{B} \lambda_{max} \sum_{s \in \mathcal{N}} \sum_{\substack{d \in \mathcal{N} \\ s<d}} (h^{sd} - 1), \tag{4.64}$$

which gives:

$$P_t \leq N(N-1) \frac{p_p + p_t}{B} \left[\lambda + \lambda_{max} \frac{h-1}{2} \right]. \tag{4.65}$$

When we consider both the largest hop count and the maximum traffic in the network we get the following upper bound in (4.67). This upper bound is important as the previous two special upper bounds (considering the topology and considering the traffic separately) can have a varying performance. The bound with the max traffic volume is generally higher than the one with the maximum hop count, but in the case of a network with a flat traffic and a very large hop count the opposite occurs.

$$P_t \leq P_\lambda N(N-1) + \frac{p_p + p_t}{B} (h_{max} - 1).\lambda_{max} \frac{N(N-1)}{2} \tag{4.66}$$

$$P_t \leq N(N-1)\frac{p_p + p_t}{B}\left[\lambda + \lambda_{max}\frac{h_{max}-1}{2}\right]. \tag{4.67}$$

We notice that the power consumption given by network coding with traffic partitioning approach under equal traffic demands between all node pairs given by equation (4.61) is the same as the one given by the zero padding case with equal traffic demands given by equation (4.61). Also the lower bounds are the same in both cases, when optimising the topology, giving the full mesh which produces no contribution from network coding, or the minimal traffic case when both bidirectional flows are equal to the average.

As mentioned above, the upper bound given by considering the maximum hop count is tighter than the one considering the maximum possible traffic demand.

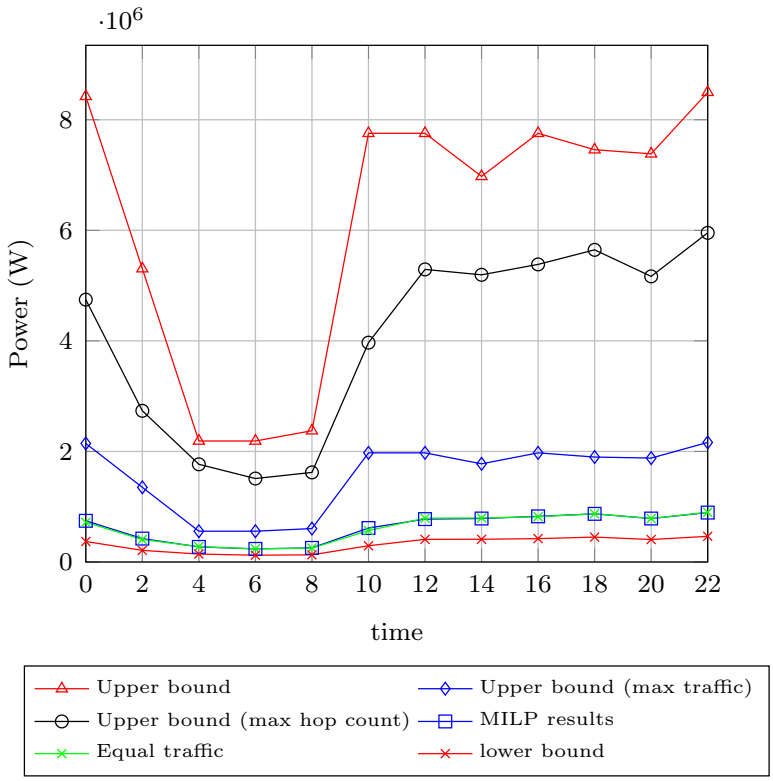

Figure 4.3: MILP results, the upper and lower bounds of the zero padding network coding approach

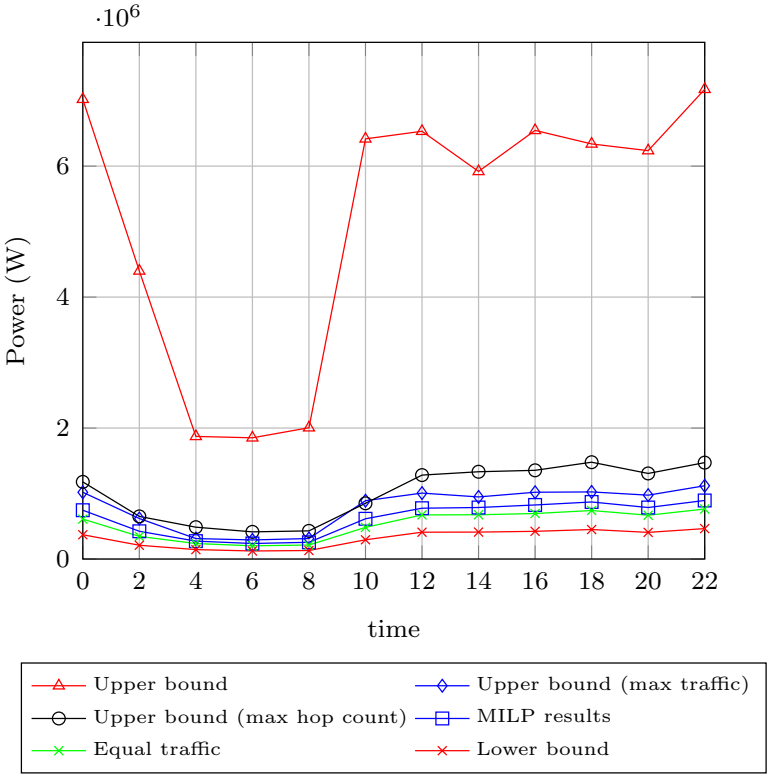

Figure 4.4: MILP results, the upper and lower bounds of the partitioning network coding approach

Figures (4.3) and (4.4) show the upper and lower bounds along side the MILP results of the power consumption of network coding under the zero padding and partitioning approaches respectively. The MILP results lie between these bounds. The power consumption under equal traffic demands which are equal to the average traffic demand is shown to be an approximate representation of the case of random traffic demands. This is due to the fact that multiple demands end up having comparable volumes in most cases, and also because the aggregate bidirectional flows passing through a node, from multiple demands reduce traffic variation and thus the traffic approaches the equal demand case, making the equal traffic formulas of significant value. However, if the MILP was used in a case where one data centre dominates for example, the MILP and the analytical case with equal average traffic volumes

may not agree.

4.4 Summary

In this chapter, analytical closed form expressions and bounds are derived and the MILP results are verified. The formulas are developed for the zero padding and partitioning network coding approaches for the cases of equal traffic volumes as well as the uniformly distributed traffic demands. These formulas were used to study regular networks as their size grows.

Chapter 5

Energy Efficient Survivable IP over WDM Networks with Network Coding

5.1 Introduction

In this chapter, we present a novel design of survivable opaque IP over WDM networks with network coding enabled at various network nodes for multiple unicast connections. We present an evaluation of this design using a Mixed Integer Linear Programming model and a heuristic. We present an evaluation of the scheme on multiple networks and traffic scenarios.

5.2 Background

Providing resilience against failures has become an integral part of the network planning process, and efficient schemes to do so, that also reduce capital and operational cost, have therefore been constantly sought out. The central issue in designing protection schemes is the compromise between redundant capacity and recovery speed [105].

In practice, dedicated protection (1+1) is widely implemented in backbone networks to provide instantaneous recovery against single link failures with remarkable simplicity. This simplicity is due to the fact that there are two live connections between the source and destination, and the destination is simply equipped with decision circuitry to select the stronger of the two paths. This approach, nevertheless, has inherent limitations as a large amount of spare capacity is required, typically doubling the resources [105]. Typical protection schemes that provide high network availability in addition to the 1+1 include 1:N and M:N protection. To reduce the resource requirement of the 1+1, the 1:N protection scheme has been proposed where N connections share a single dedicated protection path to be used by any path that suffers link failure. Assuming that only one of the N paths fails at a time, and under normal circumstances, the single shared protection path carries low priority traffic that is preempted when failure happens. For example, a 1:2 scheme enables two paths to share a single protection path, where the protection link is set to idle state or carries low priority traffic until a failure occurs. The 1:1 protection scheme is a special case of the 1:N scheme where N=1. The main difference between the 1+1 and the 1:1 protection schemes, is that the traffic in the 1+1 is continuously routed through both paths, while in the 1:1 the traffic is bridged only when a failure occurs, and therefore 1+1 does not allow the protection paths to carry any extra

traffic. Another difference is that the 1:1 scheme is a revertive protection scheme where the traffic reverts back to the working path after recovering from failure, while the 1+1 is a non revertive protection scheme, where the traffic does not switch back when the network is restored.

In recent years, the application of network coding to failure recovery in optical network has been noted and increasingly studied, collectively known as network coding based protection [106]. Indeed, this marks a major departure from traditional research in optical protection as it can potentially achieve both rapid recovery and capacity improvement, challenging the well-known trade-off of trading speed of recovery for capacity, efficiency or vice versa.

Protection and network coding appear to be a good match as the multiple paths to the same destination requirement of protection acts as a ripe environment for network coding to improve network efficiency. In [107] the authors provided a $1+N$ network coding protection scheme, and through integer linear programmes and simulation they showed that significant cost savings can be achieved over the $1+1$ approach can be achieved. Network coding was proposed in [108] and [109] as a technique to improve protection in $1+N$ protection schemes that employ p-cycles. The p-cycle are used to protect multiple bidirectional link-disjoint connections, which are also link disjoint from the p-cycle links. In [82], network coding is used to provide protection against node failures by reducing the problem to a problem of multiple link failures as a consequence of the node failure. In [110] it is shown that for networks with multiple subdomains, network coding can be used to enable the network to survive any node or link failure in each subdomain. The study of $1+1$ protection schemes with network coding was carried out by [111], through an integer non linear programme. This study is limited however, to equal traffic demands between different sources, provides results that are considerably lower than those

achievable through network coding, and constrains the network coding to only nodes with degree greater than or equals to 3.

This chapter attempts to address energy efficient network coding based protection for nonbypass IP over WDM networks, by presenting an in depth study. Numerical results based on MILP models and heuristics are presented to demonstrate the energy efficiency improvements.

5.3 $1+1$ Protection with Network Coding

Figure 5.1 shows a comparison between the conventional and the network coded $1+1$ protection scheme in an arbitrary topology. Consider two connections representing two demands a and b having the source destination pairs $(2, 11)$ and $(3, 11)$, respectively. This setting represents the case where two sources (i.e. 2 and 3) have different flows transmitted to the same destination (i.e. 11). With traditional dedicated protection, the cost is two distinct wavelengths for the whole network (e.g. $\lambda 1$ and $\lambda 2$) and a total of sixteen wavelength-links. With the utilisation of an XOR coder at node 1, new opportunities arise. The protection path of demand $(2, 11)$ and demand $(3, 11)$ on the same wavelength $\lambda 1$ are combined at node (1) such that one signal represented by $a \oplus b$ is transmitted on wavelength $\lambda 1$ from node (1) to node (11) passing through nodes $(8), (9)$ and (10). Only a coding operation is needed at node 1 and a single decoding operation is needed at the destination (i.e. node (11)), leaving the remaining intermediate nodes of the shared protection path to route the encoded flows. It is noted that under any single link failure on primary paths, the destination still receives the two remaining signals which allow it to reconstruct the lost signal by performing an all-optical XOR operation (e.g., a $\oplus$ (a $\oplus$ b) = b). This

NC-based solution simply requires one wavelength for the whole network and 12 wavelength-links. This corresponds to a 50% saving in the total number of distinct wavelengths, 25% saving in the total number of wavelength-links in the network and 40% saving of the protection resources. This additional throughput comes with the same survivability benefits of the $1 + 1$ protection scheme. The drawback is the coding delay at encoding nodes (i.e. coding at node (1) and decoding at node (11)).

The savings in the aforementioned example depend on the underlying topology, the nature of demands and routes, and the location of network coding points. Our solution to the problem determines the routes, and network coding points for demands in the network given a certain topology and traffic demands.

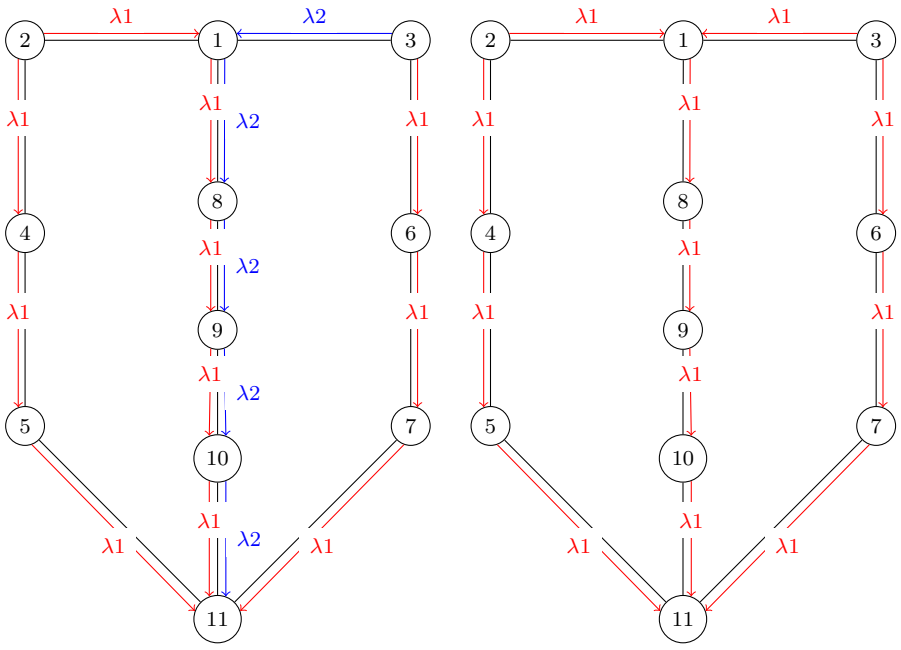

Figure 5.1: Example of using network coding for protection

This example highlights the promise of NC-based protection in optical networks and it is clear that by properly performing a coding operation among appropriate demands, better resource utilisation can be achieved.

5.4 MILP model

In this section we develop an MILP model to minimise the total power consumption of survivable IP over WDM network with 1+1 protection employing network coding. The model optimises the routes each demand takes, and the number and location of coding operations, for a given network topology and demands matrix. Below are the lists of sets, parameters and variables defined in the MILP model:

Table 5.1: List of the sets used in the MILP model

Set	description
$\mathcal{N}$	Set of the network nodes
$\mathcal{N}_m$	Set of the neighbouring nodes to node m

Table 5.2: List of the parameters used in the MILP model

parameter	description
V^d	The volume of demand d in Gbps
$src(d)$	The source node of demand d
$dst(d)$	The destination node of demand d
p_p	The power consumption of a router port
p_t	The power consumption of a transponder
p_e	The power consumption of an EDFA
B	The capacity of a wavelength in Gbps
W	Number of wavelengths per fibre
p_{xor}	The power used by a network coding/decoding operation

Table 5.3: List of the variables used in the MILP model

variable	description
x_{mn}^{d}	Binary variable, $x_{mn}^{d} = 1$ if the working path of demand d is routed over link (m, n), and $x_{mn}^{d} = 0$ otherwise.
y_{mn}^{d}	Binary variable, $y_{mn}^{d} = 1$ if the protection path of demand d is routed over link (m, n), and $y_{mn}^{d} = 0$ otherwise.
$b_{d_2}^{d_1}$	Binary variable, $b_{d_2}^{d_1} = 1$ if demand d_1 is encoded with demand d_2, and $b_{d_2}^{d_1} = 0$ otherwise
$h_{d_2}^{d_1}$	The number of shared links between the demand d_1 and d_2
$\beta_{mn}^{d_1 d_2}$	Binary variable, $\beta_{mn}^{d_1 d_2} = 1$ if demand d_1 is encoded with demand d_2 on link (m, n), and $\beta_{mn}^{d_1 d_2} = 0$ otherwise
A_{mn}	The number of EDFAs in a physical link (m, n). Typically $A_{mn} = \lfloor L_{mn}/S - 1 \rfloor$, where S is the distance between two neighbouring EDFAs.
f_{mn}	The number of fibres on physical link (m, n)

The MILP model is defined as follows:

Objective: minimise the total power of the network:

$$P_T = \frac{p_p + p_t}{B} \sum_{m \in \mathcal{N}} \sum_{n \in \mathcal{N}_m} \left(\sum_{d \in D} V^d \left(x_{mn}^d + y_{mn}^d \right) - \sum_{d_1, d_2 \in D} \min(V^{d_1}, V^{d_2}) \frac{\beta_{mn}^{d_1 d_2}}{2} \right) + 2p_{xor} \sum_{d_1, d_2 \in D} \frac{b_{d_2}^{d_1}}{2} + p_e \sum_{m \in N} \sum_{n \in \mathcal{N}_m} F_{mn} A_{mn} \quad (5.1)$$

The total power of the network is composed of the power consumption of the following components:

- $\frac{p_p+p_t}{B}\sum_{m\in\mathcal{N}}\sum_{n\in\mathcal{N}_m}\sum_{d\in D}V^d(x^d_{mn}+y^d_{mn})$ represents the total power consumption of router ports and transponders without network coding.
- $\frac{p_p+p_t}{B}\sum_{m\in\mathcal{N}}\sum_{n\in\mathcal{N}_m}\left(\sum_{d_1,d_2\in D}\min(V^{d_1},V^{d_2})\frac{\beta^{d_1d_2}_{mn}}{2}\right)$ represents the reduction in router ports and transponders resulting from sharing links facilitated by network coding. In the case of two unequal demand volumes, the larger volume is partitioned into two parts, the first has the size of the other demand and hence gets encoded with it, and the second is routed using conventional (non network coding) ports.
- $p_e\sum_{m\in\mathcal{N}}\sum_{n\in\mathcal{N}_m}F_{mn}A_{mn}$ represents the total power consumption of EDFAs
- $2p_{xor}\sum_{d_1,d_2\in D}\frac{b^{d_1}_{d_2}}{2}$ represents the total power consumption of the xor operations at encoding and decoding nodes. The sum calculates the total number of encoded demands (division by 2 so a demand pair is not counted twice). The Multiplication by a factor of 2 is because an encoding and a decoding operation are needed for each encoded demand pair.

Subject to:

$$\sum_{n\in\mathcal{N}_m}x^d_{mn}-\sum_{n\in\mathcal{N}_m}x^d_{n,m}=\begin{cases}1 & m=src(d)\\ -1 & m=dst(d)\\ 0 & otherwise\end{cases} \tag{5.2}$$

$$\forall d\in D, m\in N$$

$$\sum_{n \in \mathcal{N}_m} y^d_{mn} - \sum_{n \in \mathcal{N}_m} y^d_{n,m} = \begin{cases} 1 & m = src(d) \\ -1 & m = dst(d) \\ 0 & otherwise \end{cases} \tag{5.3}$$

$$\forall d \in D, m \in \mathcal{N}$$

$$x^d_{mn} + y^d_{mn} \leq 1 \tag{5.4}$$

$$\forall d \in D, m \in \mathcal{N}, n \in \mathcal{N}_m$$

Constraints (5.2) and (5.3) represent the flow conservation constraints for the working and the protection paths, respectively, where the total incoming traffic equals the outgoing traffic for all nodes except the source and destination. They also impose single path routing behaviour for the working and protection paths. Constraint (5.4) ensures that the working and protection paths of each demand are link disjoint.

$$\sum_{d \in D} V_d(x^d_{mn} + y^d_{mn}) - \sum_{d_1, d_2 \in D} \min(V_{d_1}, V_{d_2}) \frac{\beta^{d_1 d_2}_{mn}}{2} \leq WBf_{mn} \tag{5.5}$$

$$\forall m \in \mathcal{N}, n \in \mathcal{N}_m$$

Constraint (5.5) represents the capacity conservation constraint. It ensures that the sum of all the flows (in working or protection paths) minus the network coding reduction in a certain link is below the capacity of that link, given by the number of fibres and the capacity of each fibre. Note that here we consider partitioning which selects the minimum of the two flows if they differ in volume:

$$\beta^{d_1 d_2}_{mn} \leq y^{d_1}_{mn} \tag{5.6}$$

$$\forall d_1, d_2 \in D : d_1 \neq d_2, \forall m \in \mathcal{N}, n \in \mathcal{N}_m$$

Constraint (5.6) ensures that only the protection path of a demand gets encoded. The model sees the variables $y_{mn}^{d_1}$ and $x_{mn}^{d_1}$ as binary variables over a link (m, n) and hence does not distinguish between protection and working paths. This allows working and protection paths to be encoded, if the model finds it useful power wise, in four combinations, i.e. w-w (working-working), w-p (working-protection), p-w (protection-working) and p-p (protection-protection).

$$\beta_{mn}^{d_1 d_2} = \beta_{mn}^{d_2 d_1} \tag{5.7}$$

$$\forall d_1, d_2 \in D : d_1 \neq d_2, \forall m \in \mathcal{N}, n \in \mathcal{N}_m$$

Constraint (5.7) ensures that if demand d_1 is encoded with demand d_2, demand d_2 is also encoded with d_1.

$$h_{d_2}^{d_1} = \sum_{m \in N} \sum_{n \in N_m} \beta_{mn}^{d_1 d_2} \tag{5.8}$$

$$\forall d_1, d_2 \in D : d_1 \neq d_2$$

Constraint (5.8) calculates the number of shared hops between two demands.

$$b_{d_2}^{d_1} \leq h_{d_2}^{d_1} \tag{5.9}$$

$$\forall d_1, d_2 \in D : d_1 \neq d_2$$

$$h_{d_2}^{d_1} \leq M b_{d_2}^{d_1} \tag{5.10}$$

$$\forall d_1, d_2 \in D : d_1 \neq d_2$$

Constraints (5.9) and (5.10) convert the shared hops variable $h_{d_2}^{d_1}$ into binary, and hence determine if demand d_1 is encoded with d_2. When there are no shared hops between the two demands, they do not get encoded (i.e. $b_{d_2}^{d_1} = 0$), and if at least

there exists a shared hop, then potentially encoding can take place. As a demand can share hops with multiple demands, there is a potential for the variable $b_{d_2}^{d_1}$ to be set to 1 for each of the multiple potential demands. However, to ensure that only a single demand out of the multiple potential demands gets encoded, constraint (5.11) is used.

$$\sum_{d_2 \in D} b_{d_2}^{d} \leq 1. \tag{5.11}$$

$$\forall d \in D$$

Constraint (5.11) ensures that each demand $d \in D$ is not encoded with more than a single demand.

$$\beta_{mn}^{d_1 d_2} = 0 \tag{5.12}$$

$$\forall d_1, d_2 \in D : dst(d_1) \neq dst(d_2)$$

Constraint (5.12) ensures that only demands that share a single destination can be encoded. The mixed integer linear programme for the conventional $1+1$ protection is provided as follows:

Objective: minimise the total power of the network:

$$P_T = (p_r + p_t) \sum_{m \in \mathcal{N}} \sum_{n \in \mathcal{N}_m} \sum_{d \in D} V^d \left(x_{mn}^d + y_{mn}^d \right) + \sum_{m \in N} \sum_{n \in N_m} p_e F_{mn} A_{mn} \tag{5.13}$$

Subject to:

$$\sum_{n \in \mathcal{N}_m} x_{mn}^d - \sum_{n \in \mathcal{N}_m} x_{nm}^d = \begin{cases} 1 & m = src(d) \\ -1 & m = dst(d) \\ 0 & otherwise \end{cases} \tag{5.14}$$

$$\forall d \in D, m \in N$$

$$\sum_{n \in \mathcal{N}_m} y^d_{mn} - \sum_{n \in \mathcal{N}_m} y^d_{nm} = \begin{cases} 1 & m = src(d) \\ -1 & m = dst(d) \\ 0 & otherwise \end{cases} \tag{5.15}$$

$$\forall d \in D, m \in \mathcal{N}$$

$$x^d_{mn} + y^d_{mn} \leq 1 \tag{5.16}$$

$$\forall d \in D, m \in \mathcal{N}, n \in \mathcal{N}_m$$

$$\sum_{d \in D} V^d (x^d_{mn} + y^d_{mn}) \leq W B f_{mn} \tag{5.17}$$

$$\forall m \in \mathcal{N}, n \in \mathcal{N}_m$$

Constraints (5.14) and (5.15) represent the flow conservation constraints for the working and protection paths respectively, where the total incoming traffic equals the outgoing traffic for all nodes except the source and destination nodes. While constraint (5.16) ensures that the working path and protection paths are link disjoint. Constraint (5.17) represents the capacity conservation constraint.

5.5 Heuristic

In this section we develop a heuristic and use it to evaluate the performance of large networks that proved complex for the MILP. We provide a general case of the heuristic, named Optimal Search Heuristic (OSH), and then we provide four special cases, where in each case the encoding of paths is unified across encodable demand

pairs, and covers the possibilities of encoding the working and protection paths of the two demands, and is hence given the tags w-w, w-p, p-w, and p-p, respectively where the (w) refers to the working path and (p) to the protection path.

The central approach of the heuristic is to implement the search on a much reduced search space. The heuristic is hence divided into four steps: The first is forming the encodable graph where demands are classified into clusters. The second step calculates the two link disjoint paths by using the Suurballe algorithm [112] which produces two link disjoint paths for each demand. In the third step the number of shared hops between each demand pair is calculated and the weighted encodable graph is formed. Finally, on the encodable graph, a stable matching solution is found that produces the encoded demand pairs and from that the total power consumption of the network is calculated. The details of each step is discussed in further detail.

5.5.1 Encodable Graph Formation

The demands graph (complete graph) is reduced to the set of encodable demands, satisfying the condition that limits encoding to be only between demands sharing the same destination and having different sources. This reduces the complete graph by dividing it into a set of complete $N-1$ smaller graphs each of size N nodes rather than a complete graph of the size N^2. The encodable graph for the example of a six node network (Figure 5.2) is shown in Figure 5.3.

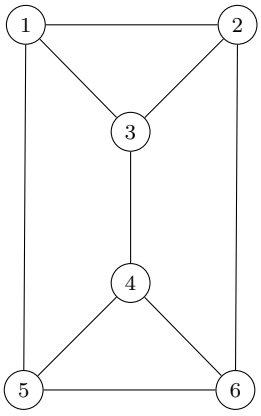

Figure 5.2: Six node topology under consideration

In this six node example, each node has 5 possible destinations, and each node receives traffic from 5 possible sources. Therefore, if demands are clustered such that each cluster contains demands that share the same destination, then each cluster will have 5 demands as shown in Figure 5.3 (a)-(f). Each of the 5 demands in the cluster shares its destination with 4 other demands, hence Figure 5.3 (a)-(f) shows that each demand is linked (encodable) with 4 other demands.

For 6 nodes, the 6x6 traffic matrix has 36 entries, which is reduced to 30 after removing demands from a node to itself (i.e. demands 1, 8, 15, 22, 29 and 36 in the traffic matrix), the remaining 30 demands, their clusters, and encodable graph links are as shown in Figure 5.3.

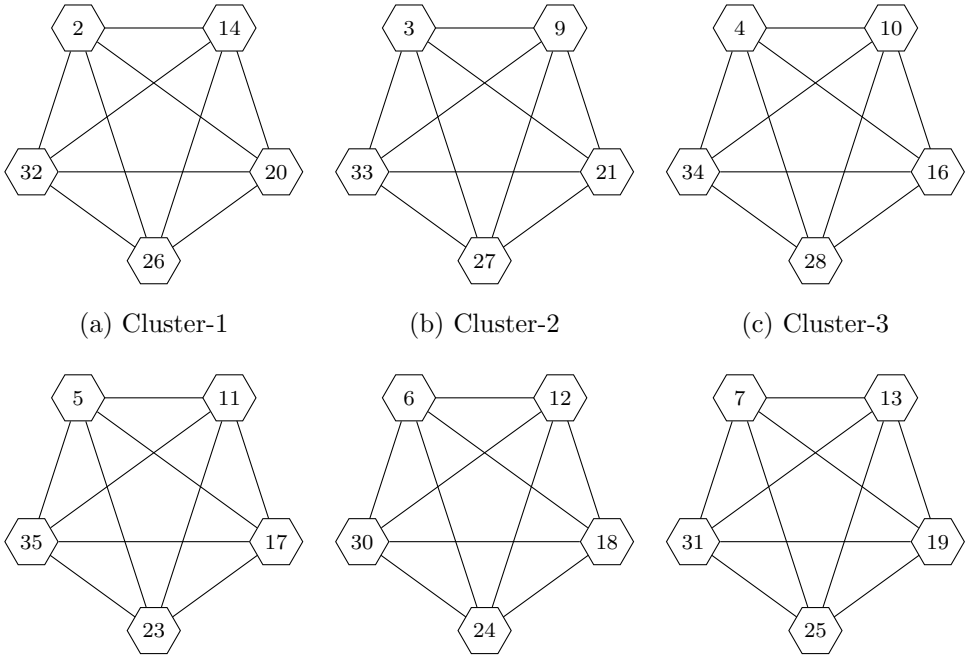

(a) Cluster-1 (b) Cluster-2 (c) Cluster-3

(d) Cluster-4 (e) Cluster-5 (f) Cluster-6

Figure 5.3: The encodable graph where each node represents a demand for a six node topology

5.5.2 Paths Calculation

For each source-destination demand, the working and protection paths are determined using Suurballe's algorithm which finds two disjoint paths connecting the source and destination nodes of a demand that also have the minimum total number of hops [112]. The algorithm uses Dijkstra algorithm to find the first minimum hops path, and uses it again after changing the weights of the graph. A detailed example on how the algorithm operates is shown in Appendix A. As the result of the Suurbelle algorithm are two disjoint paths for each demand, where the shorter route is labelled as the working path and the longer as the protection path, hence there exists different combinations for encoding. There exist a general algorithm that finds the best path selection for encoding between the 4 combinations (working-

working (w-w), working-protection (w-p), protection-working (p-w) and protection-protection(p-p)) for each demand. We label this the Optimum Search Heuristic. We also create a more restricted version of the heuristic where the decision of which of the 4 combinations is used is unified for all encoded pairs. This means for the choice of encoding protection paths together, all encoded demands will have their protection paths encoded together pairwise. This makes the total number of heuristics equal to five.

5.5.3 Weighted Encodable Graph

The next step is forming the weighted encodable graph by assigning weights to the encodable graph. The weights represent the number of common links shared by the two encodable demands. This weight is a positive integer, that can take a value of zero, which represents no shared links. The total number of links in the graph is reduced by removing any link with a zero weight. This is shown for the six nodes network, in Figure 5.4.

Each link in the weighted encodable graph represents the number of shared hops between demands, and because there exists 4 possible path combinations between each pair of demands (i.e. w-w, w-p, p-w and p-p), therefore 4 links can exist between each demand in the weighted encodable graph. Four versions of the heuristic are generated by limiting all the links in the graph to a given path combination, therefore producing 4 weighted encodable graphs, each represents a heuristic. For example, in the NC heuristic p-p, each demand pair in the weighted encodable graph is connected by a link with a weight that represents the number of shared hops between the protection paths of the two demands. The optimal search heuristic searches over all 4 parallel links between demands.

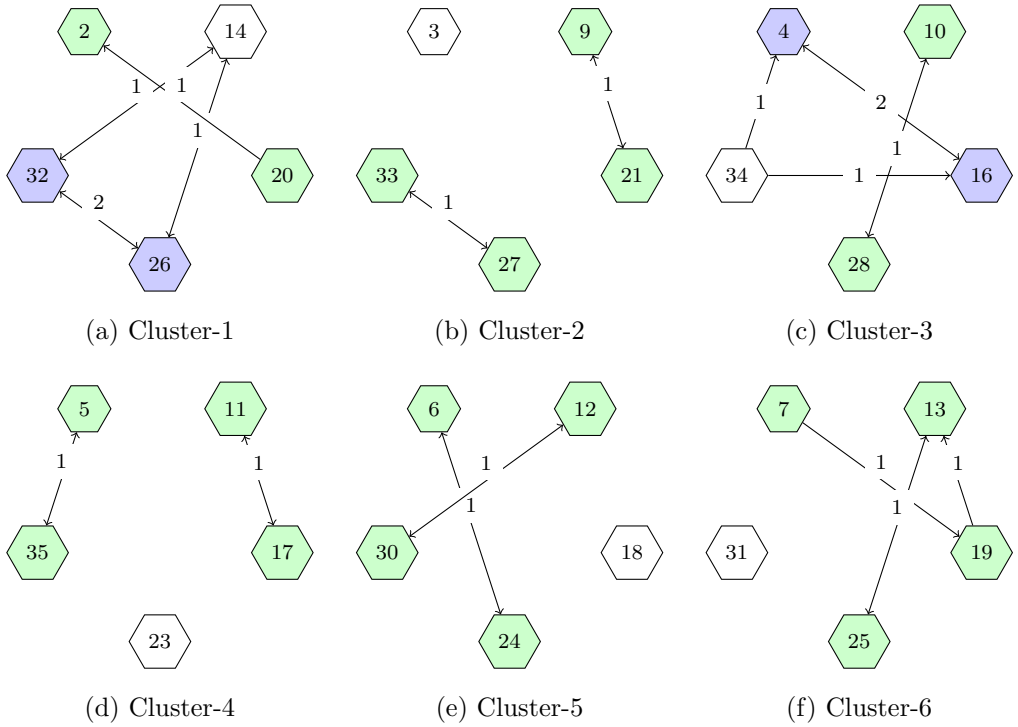

(a) Cluster-1 (b) Cluster-2 (c) Cluster-3

(d) Cluster-4 (e) Cluster-5 (f) Cluster-6

Figure 5.4: The Weighted encodable graph

5.5.4 The Stable Matching Problem

Not all demands favour the demands that favour them in the encoding pair selection. For example, demand d_1 may be best encoded with demand d_2 which in turn prefers demand d_3. Ensuring fair pair selection given the preference criteria is essential to maximising the performance of the algorithm.

To select which demands to encode together, in each cluster, the links with the highest weights in the weighted encodable graph are selected first. If there exist multiple links with the same weight, the selection is done randomly which is implemented by progressing sequentially through the list of demands (demands in numeric order). The selected link is removed from the weighted encodable graph, since each demand should be encoded with one demand only. Encoded nodes (demands) and their as-

sociated links to all other nodes (demands) are also removed from the graph. This process is repeated until all links in the cluster are exhausted, and this process is repeated for all clusters. Then the total power is calculated.

Figure 5.4 shows the different steps (as colors) in selecting the encoding pairs for the six node topology under consideration. The blue nodes are those selected (and deleted from the graph) first, which have the highest mutual preference (link weight=2). The green nodes come second, and so on. The graph weight search stops here for this example as the possible encodable node set is not large given the small network size. The remaining demands are not selected either because their possible encodable demands are already selected or because they do not have a link with another demand.

5.6 Results

Due to the huge complexity of evaluating the MILP model for networks of large sizes (e.g. NSFNET with 14 nodes), we performed an evaluation for a 5 node topology (Figure 5.5) and benchmark the heuristic results against the MILP model results, then the heuristic is used to study the behaviour of larger network sizes.

5.6.1 Five Node Topology

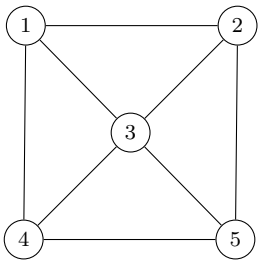

Figure 5.5: Five node topology under consideration

We show the results of the MILP model and the various heuristics for the 5 node topology. We compare the results to the MILP model of the conventional protection approach under equal traffic demands and uniformly distributed random traffic demands evaluated in steps of 20Gbps starting from 20Gbps up to 200Gbps. The power consumption values used in Chapter 3 are used here, and we use $p_{xor} = 20W$ at 40Gbps.

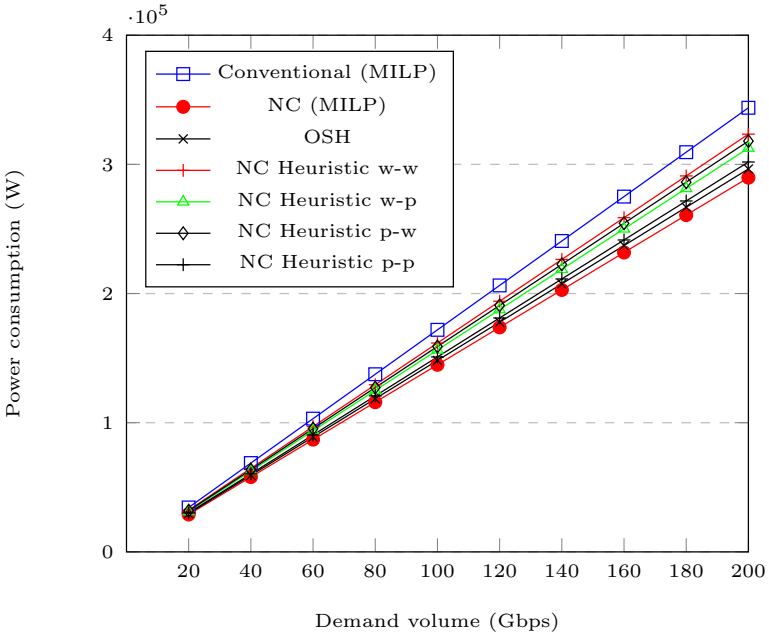

Figure 5.6: Power consumption of the 5 node topology with equal demands

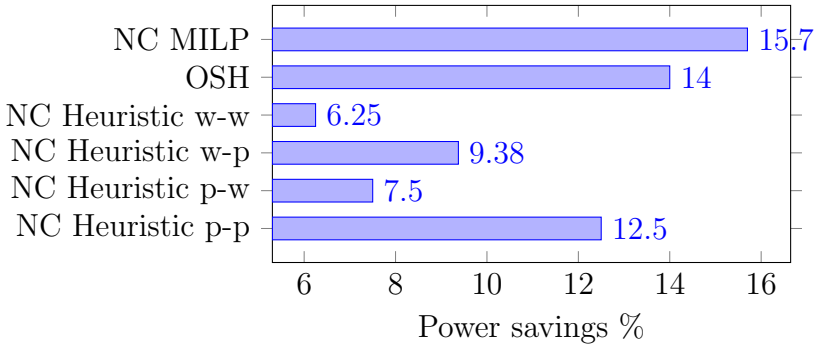

Figure 5.7: Power savings of the various approaches with equal traffic for 5 nodes topology

For the Equal demands case, the results in Figure 5.6 show a linear relationship between the power consumption and the demand volume, and this relationship applies to all of the heuristics and the MILP. The corresponding savings are shown in Figure 5.7. The optimum search heuristic is comparable to the MILP model with savings reaching 14%, while the heuristic version that encodes protection paths together approaches the MILP with savings of 12.5%.

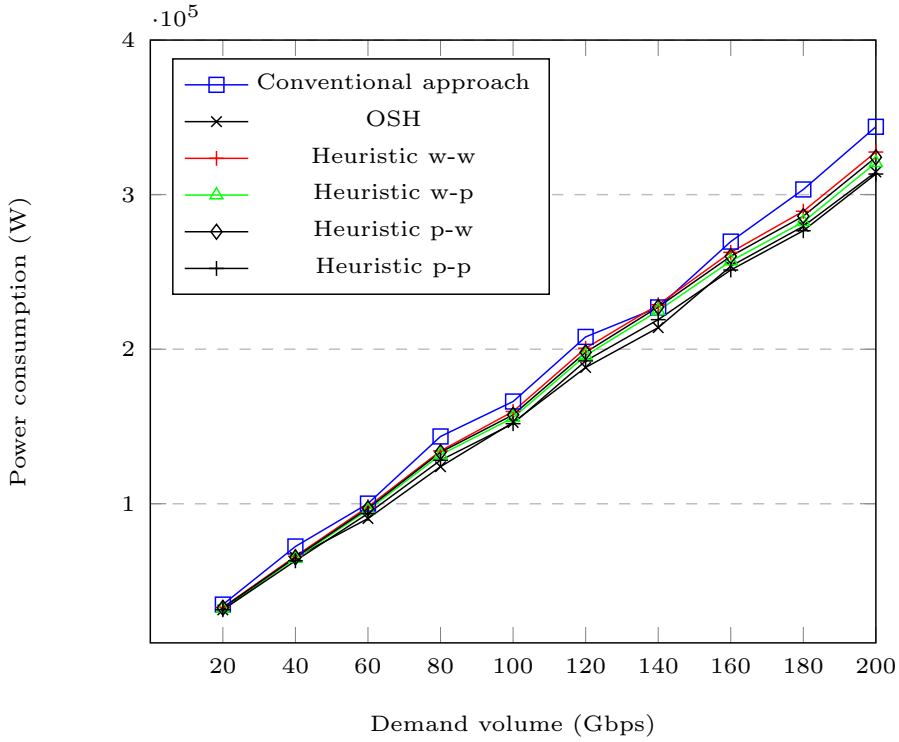

Figure 5.8: Power consumption of the 5 node topology for random demands

Figures 5.8 and 5.9 show the power consumption and the corresponding power savings for the case of uniformly distributed random demands in the 5 nodes topology. The savings achieved by the different heuristics follow the same order as the case of equal demands, and the power savings are lower than those achieved under the equal demands case (8.8% compared to 15.7% when using OSH). The power consumption overall follows a linear function when the model is evaluated for a very high number of runs (current number of runs is 40). The reason behind this reduction in savings for the case of random demands as compared to equal demands is that demand partitioning is used and hence the minimum value between the 2 flows is encoded. The power saving added by network coding are maximised the closer the demands volumes get to each other, ultimately at equal demand values, the savings are maximum.

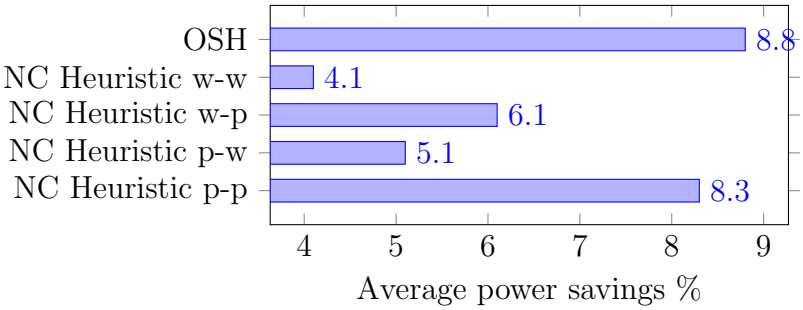

Figure 5.9: Power savings of the various approaches with random demands for the 5 nodes topology

5.6.2 Common Topologies

We evaluated the performance of the heuristic on the NSFNET and the USNET topologies. The results are shown in Figure 5.10 and 5.11. We followed the same approach when evaluating the results considering the demand variation as with the 5 nodes topology case. The figures show the same linear trend in power consumption as the average demand in the network grows, and show that the two networks provide comparable power savings of 23% and 21% for the NSFNET and the USNET respectively, using OSH. Although the USNET has a higher average hop count than the NSFNET, the savings are slightly less. This is due to the topology as not every time a longer path is found a corresponding larger hop count is found. However, if the topology is optimised to maximise network coding performance, the USNET will have a higher chance of producing more savings than the NSFNET. The figures also shows that the fourth network coding approach (Heuristic p-p) is the most energy efficient of the four cases after OSH.

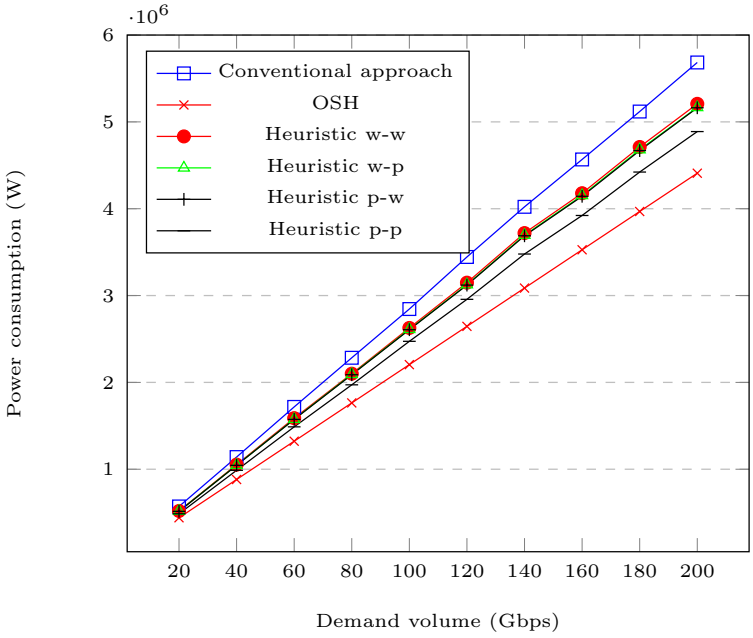

Figure 5.10: Power consumption of the NSFNET

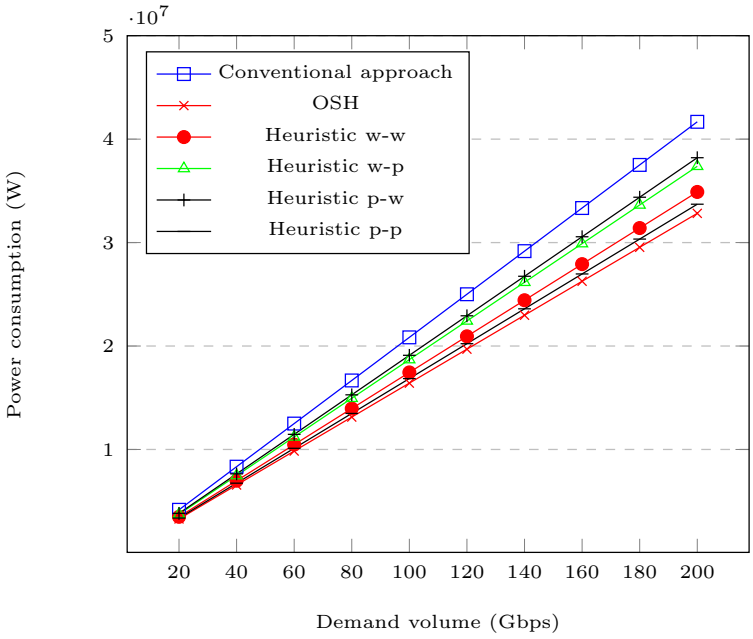

Figure 5.11: Power consumption of the USNET

5.7 Regular Topologies

In this section we study the behaviour of the proposed approach on regular topologies, namely the star, line, full mesh and the ring topologies.

The star topology does not show any savings with network coding due to the fact that the protection concept itself is not satisfied. Since each node is connected by a single link to the center of the star, no link disjoint paths for protection can be established. The line topology also is irrelevant as no protection path can be formed.

The power consumption values of the full mesh topology are shown in Figure 5.12 and the power savings in Figure 5.13. The savings can reach 15% considering the optimum search heuristic, and 10% when using the heuristic with encoding limited to protection paths. Encoding working flows together provides no improvements over the conventional approach (0% savings) because encoding is not possible in this case as all working paths have a single link from the source to the destination. The other two approaches where the protection path of one demand is encoded with the working path of the other, produce savings of 2%.

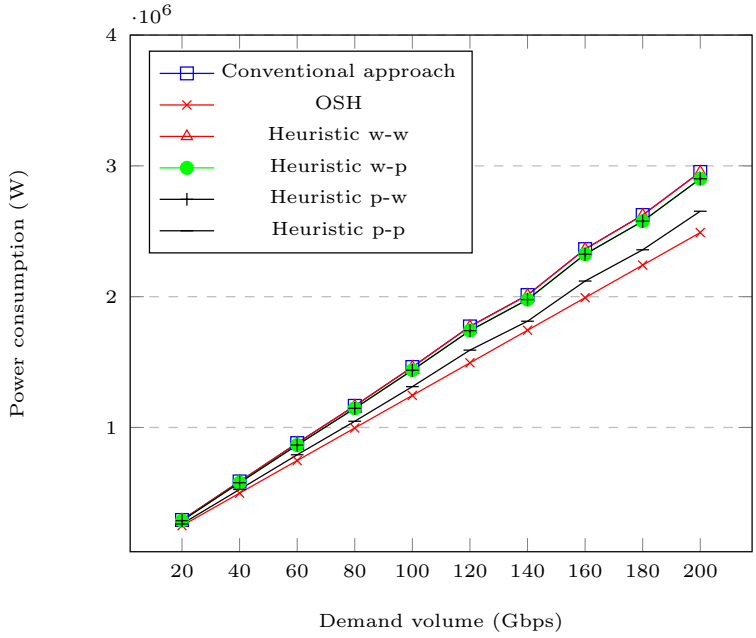

Figure 5.12: Power consumption of the various approaches for a 14 node fullmesh topology

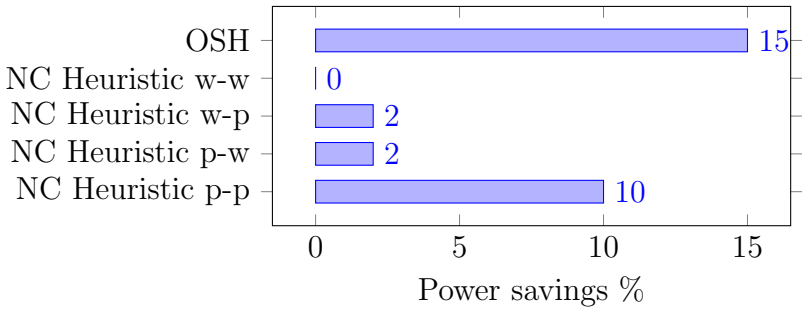

Figure 5.13: Power savings of the various approaches with equal traffic for 14 node full mesh topology

For the ring topology, the results are shown in Figure 5.14 for a ring of 14 nodes. Encoding protection paths together produces savings of up to 33% while encoding working paths together produces 11% savings. This large difference is due to the fact that protection paths in the ring are considerably longer than working paths, and this difference increases as the ring size increases. The other two approaches of encoding the working path with protection paths produce savings of 14% and 15%.

Savings of 33% can be achieved when the optimum search heuristic is used.

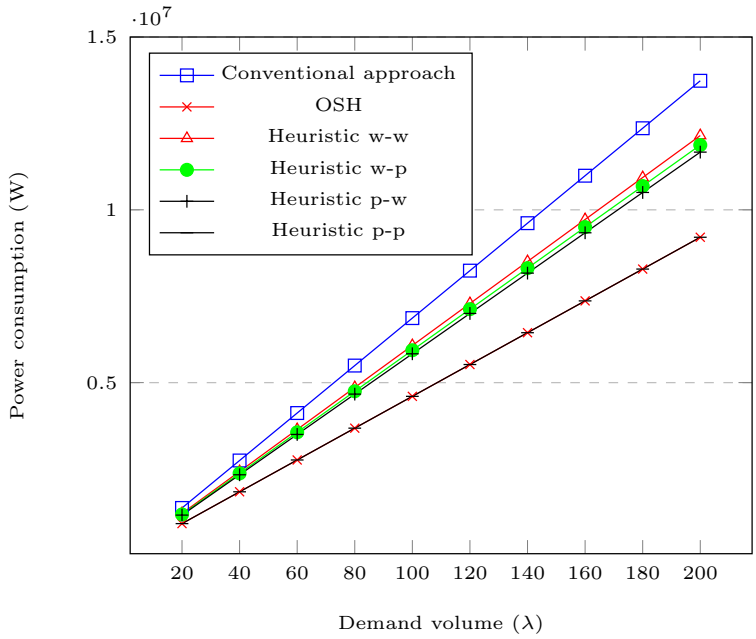

Figure 5.14: Power consumption of the various approaches for a 14 node ring topology

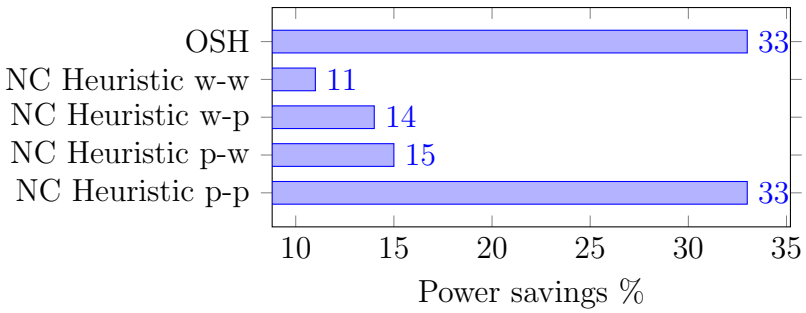

Figure 5.15: Power savings of the various approaches with equal traffic for 14 node ring topology

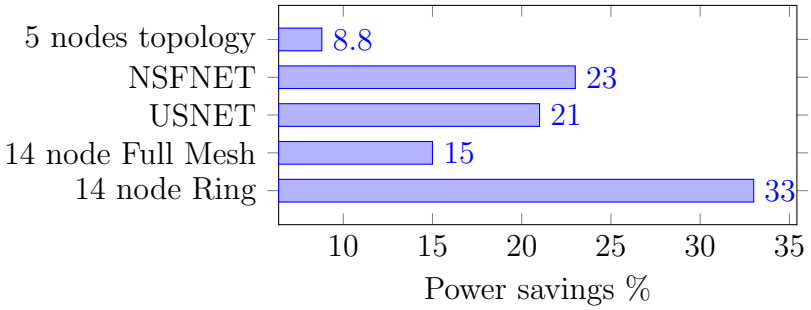

Figure 5.16: Comparison of the power consumption for different topologies

In Figure 5.16 we show a comparison of the power savings obtained in different topologies. The ring topology has the highest power savings followed by the NSFNET and the USNET topologies which are comparable. Smaller topologies produce low savings as the chance of finding multiple shared links is reduced.

5.8 Impact of Traffic Variation

In this section, we study the impact of traffic variation. Assuming the demands have an average value of V, we want to study the impact of the variation of individual demands around the average on the total power consumption of the network when network coding is implemented.

We study the impact of the volume of the traffic by varying the range of the uniform distribution. We study traffic demands with average values of 80 Gbps. The range is increased, starting from 0, representing equal demands volumes, increasing in steps of 10Gbps until 160Gbps which represents the largest range possible. The larger the range, the larger the probable difference between the volumes of the encoded demands, which due to partitioning, reduces the power saving potential compared to the equal demand case represented by the zero range.

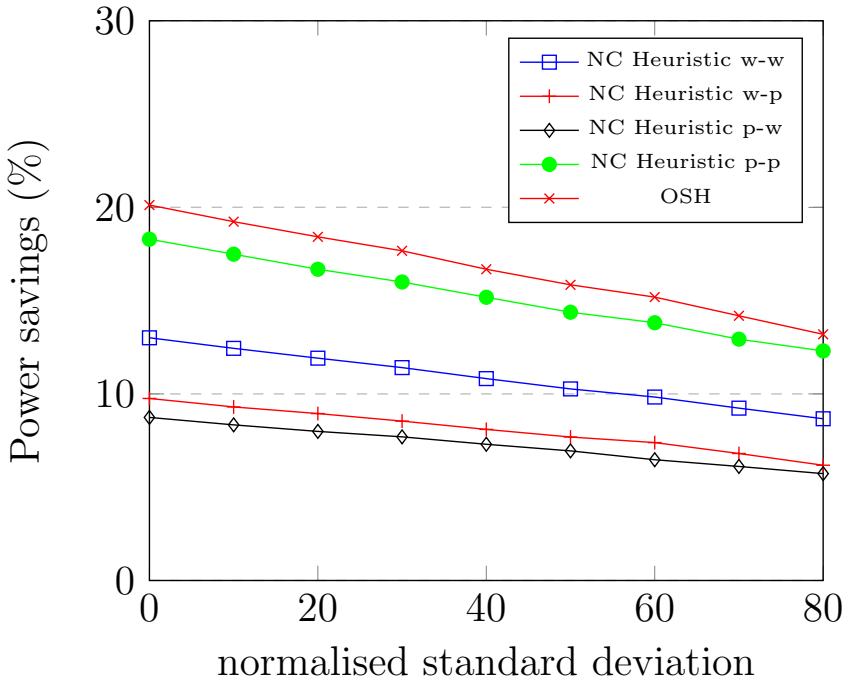

Figure 5.17: Power consumption of the various approaches for equal demands vs demand volume

Figure 5.17 shows the power consumption of the network using the various heuristics vs the normalised traffic standard deviation (i.e. the range of the distribution) in the NSFNET. Note that in the uniform distribution where samples are selected between two values (a, b), the range is $(b-a)$ and the standard deviation is $(\frac{1}{\sqrt{(12)}}b-a)$ which when normalized gives $(b-a)$. The figure clearly shows the linear relationship of the power savings to the standard deviation for all heuristic forms, having a maximum saving of 20% and a minimum saving of 13% for the OSH.

5.9 Summary

In this chapter we presented an approach where network coding can be used in 1+1 protection scheme to provide instantaneous recovery with resources less than those

used by the conventional 1+1 scheme by up to 33%. We evaluated the system using a MILP model and a heuristic considering common networks and traffic scenarios as well as regular topologies focusing on the ring and the full mesh.

Chapter 6

Bounds on Energy Efficient Survivable Optical Networks with and Without Network Coding

6.1 Introduction

In this chapter we derive analytical bounds for the power consumption and savings of the survivable optical networks enhanced by network coding presented in the previous chapter.

6.2 Analytical Formulas

The total power consumption of the survivable optical networks with network coding as presented in the previous chapter is given by

$$P = (\frac{p_p + p_t}{B}) \left(\sum_{d \in D} \sum_{m,n} V^d (x^d_{mn} + y^d_{mn}) - \sum_{d1,d2} \sum_{m,n} \min(V^{d_1}, V^{d_2}) \frac{\beta^{d_1 d_2}_{mn}}{2} \right), \quad (6.1)$$

where the contribution of the xor operations, and of the EDFAs have not been included as their associated power consumption is low and to simplify the expressions.

Let the expression given in (6.1) be divided into its two summable components, which we refer to as P_1 and P_2 (i.e. $P = P_1 - P_2$), such that

$$P_1 = (\frac{p_p + p_t}{B}) \left(\sum_{d \in D} \sum_{m,n} V^d (x^d_{mn} + y^d_{mn}) \right), \quad (6.2)$$

$$P_2 = (\frac{p_p + p_t}{B}) \left(\sum_{d1,d2} \sum_{m,n} \min(V^{d_1}, V^{d_2}) \frac{\beta^{d_1 d_2}_{mn}}{2} \right). \quad (6.3)$$

Expression (6.2) can be rewritten as

$$P_1 = (\frac{p_p + p_t}{B}) \left(\sum_{d \in D} V^d \sum_{m,n} (x^d_{mn} + y^d_{mn}) \right). \quad (6.4)$$

Given the fact that the sum of the hop count of the working and protection paths of a given demand is always greater than or equal to twice the minimum hop count h^d_{min} of the path serving it, that is

$$\sum_{m,n} (x^d_{mn} + y^d_{mn}) \geq 2h^d_{min}, \quad (6.5)$$

therefore P_1 can be written as

$$P_1 \geq (\frac{p_p + p_t}{B}) \left(\sum_{d \in D} 2V^d h^d_{min} \right). \tag{6.6}$$

Assuming that all demands are routed through the minimum hop count path of the network, i.e. $h^d_{min} = h_{min}, \forall d \in D$, we then have

$$P_1 \geq (\frac{p_p + p_t}{B}) h_{min} \left(\sum_{d \in D} 2V^d \right), \tag{6.7}$$

which gives

$$P_1 \geq 2(\frac{p_p + p_t}{B}) N(N-1) V h_{min}. \tag{6.8}$$

Expression (6.8) represents a lower bound on the power consumption of the first component of the total power consumption of the network coded case as a result of routing traffic flows in the working and the protection paths, without the network coding component. It also represents the lower bound on the power consumption of the conventional case, which we refer to as P_0, where

$$P_0 \geq 2(\frac{p_p + p_t}{B}) N(N-1) V h_{min}. \tag{6.9}$$

The upper bound of P_2 is found by starting from the fact that the minimum volume of two demands is never greater than their average, that is

$$\min(V^{d_1}, V^{d_2}) \leq \frac{V^{d_1} + V^{d_2}}{2}, \tag{6.10}$$

then (6.3) becomes

$$P_2 \leq (\frac{p_p + p_t}{B}) \left(\sum_{d1,d2} \sum_{m,n} \frac{V_{d_1} + V_{d_2}}{2} \frac{\beta^{d_1 d_2}_{mn}}{2} \right). \tag{6.11}$$

The expression $\min(V^{d_1}, V^{d_2})$ has its highest value when the maximum traffic is equal to the minimum traffic, therefore the equality in (6.10) is met when $V^{d_1} = V^{d_2} = V^{d_1,d_2}$. In this case (6.12) becomes

$$P_2 \leq \frac{p_p + p_t}{2B} \left(\sum_{d_1,d_2} \sum_{m,n} V^{d_1,d_2} \beta_{mn}^{d_1 d_2} \right). \tag{6.12}$$

This can be rearranged as

$$P_2 \leq \frac{p_p + p_t}{2B} \left(\sum_{d_1,d_2} V^{d_1,d_2} \sum_{m,n} \beta_{mn}^{d_1 d_2} \right). \tag{6.13}$$

The expression $\sum_{m,n} \beta_{mn}^{d_1 d_2}$ represents the number of shared links between the demand pair (d_1, d_2). We refer to this value as $h_{d_2}^{d_1}$, where

$$h_{d_2}^{d_1} = \sum_{m,n} \beta_{mn}^{d_1 d_2}. \tag{6.14}$$

Therefore equation (6.13) becomes:

$$P_2 \leq \frac{p_p + p_t}{2B} \left(\sum_{d_1,d_2} V^{d_1,d_2} h_{d_2}^{d_1} \right). \tag{6.15}$$

Considering the lower bound of the component P_1 in (6.6) and the upper bound of the component P_2 in (6.15), we can get a lower bound on the total power consumption by combining the two, since $P = P_1 - P_2$, minimising P is achieved by minimising P_1 and maximising P_2. The total power is then lower bounded by the following

$$P \geq (\frac{p_p + p_t}{B}) \left(2 \sum_{d \in D} V^d h_{min}^d - \frac{1}{2} \sum_{d_1,d_2} V^{d_1,d_2} h_{d_2}^{d_1} \right). \tag{6.16}$$

The result in (6.16) shows that there exist a heuristic that can provide close to

optimal solution, if it employs the following principles

- Select the minimum number of hops for the working and protection paths (minimising the first term of (6.16))
- Encode a demand with another demand that has the highest number of shared hops and closest demand volume (maximising the second term of (6.16))
- More weight is given to finding minimal hop paths than searching for better encoding pair (from the equation, the weight ratio of the first to second terms is 4:1)
- Three heuristics can be conceived. The first finds encodable pairs by searching only for the highest link sharing, the second searches for the demand with the closest traffic volume, and a better heuristic searches for the highest sharing and closest traffic volume, at the expense of increased complexity. The first heuristic approaches the performance of the third the smaller the traffic variation becomes.

The bound (6.16) can be reduced by setting $V^d = V^{d,d_2}$, which gives

$$P \geq (\frac{p_p + p_t}{B}) \sum_{d \in D} V^d \left(2h^d_{min} - \frac{1}{2} \sum_{d_2} h^d_{d_2} \right). \tag{6.17}$$

Since each demand is constrained to be encoded with a maximum of a single other demand only, which is expressed as

$$\sum_{d2 \in D} b^{d_1}_{d_2} \leq 1. \tag{6.18}$$

Therefore we let the value $\hat{h}^d = \sum_{d_2} h^d_{d_2}$ represent the amount of shared links (hops) between demand d and the demand it is encoded with. Equation (6.17) can then be

reduced to

$$P \geq (\frac{p_p + p_t}{B}) \left(\sum_{d \in D} V^d (2h^d_{min} - \frac{\hat{h}^d}{2}) \right), \tag{6.19}$$

which is equal to

$$P \geq 2(\frac{p_p + p_t}{B}) \left(\sum_{d \in D} V^d (h^d_{min} - \frac{\hat{h}^d}{4}) \right). \tag{6.20}$$

If we define the variable $\tilde{h}^d$ as the characteristic hop count for demand d, such that

$$\tilde{h}^d = h^d_{min} - \frac{\hat{h}^d}{4}, \tag{6.21}$$

therefore the lower bound of the total power becomes

$$P \geq 2(\frac{p_p + p_t}{B}) \left(\sum_{d \in D} V^d \tilde{h}^d \right). \tag{6.22}$$

Using Chebyshev Sum Inequality, i.e.

$$\frac{1}{n} \sum_{k=1}^{n} a_k b_k \geq \left(\frac{1}{n} \sum_{k=1}^{n} a_k \right) \left(\frac{1}{n} \sum_{k=1}^{n} b_k \right), \tag{6.23}$$

then, (6.22) can be written as

$$P \geq 2(\frac{p_p + p_t}{B}) \left(\frac{1}{N(N-1)} \sum_{d \in D} V^d \sum_{d \in D} \tilde{h}^d \right), \tag{6.24}$$

which gives

$$P \geq 2(\frac{p_p + p_t}{B}) V \sum_{d \in D} \tilde{h}^d, \tag{6.25}$$

where $V = \sum_{d \in D} V^d$ is the average demand volume. Defining $\tilde{h} = \sum_{d \in D} \tilde{h}^d$ as the average characteristic hop count, then

$$P \geq 2(\frac{p_p + p_t}{B}) N(N-1) V \tilde{h} \tag{6.26}$$

The lower bound given in (6.26) bears resemblance to the lower bound of the conventional case in (6.9), where the minimum hop count of the conventional case h_{min} is replaced by the characteristic minimum hop count of the network coding case $\tilde{h}$.

6.3 Regular Topologies

In the previous chapter we established that the star and the line topologies exhibits no network coding benefits as the concept of protection does not apply. Here we develop formulas and bounds for the full mesh and ring topologies for the case where protection paths are encoded together, and study the impact of the network size on the performance of network coding.

6.3.1 Full Mesh Topology

The total power consumption under conventional protection is given by

$$P_0 = (\frac{p_p + p_t}{B}) \left(\sum_{d \in D} \sum_{m,n} V^d (x^d_{mn} + y^d_{mn}) \right) \tag{6.27}$$

For the full mesh topology, the optimal paths are the direct path (a single hop) for the working path, and a path with an intermediate node for the protection path (2 hops). This means $(\sum_{m,n} x^d_{mn} = 1)$ and $(\sum_{m,n} y^d_{mn} = 2)$, $\forall d \in D$. Therefore

$$P_0 = (\frac{p_p + p_t}{B}) \left(\sum_{d \in D} 3V^d \right), \tag{6.28}$$

which can be written as

$$P_0 = 3(\frac{p_p + p_t}{B})VN(N-1). \tag{6.29}$$

For the network coded approach the network power consumption is given by

$$P = P_0 - (\frac{p_p + p_t}{B}) \sum_{d_1,d_2} \sum_{m,n} \min(V_{d_1}, V_{d_2}) \frac{\beta_{mn}^{d_1 d_2}}{2}, \tag{6.30}$$

which can be reduced to the following, given that equal traffic demands that produces the highest savings

$$P = P_o - (\frac{p_p + p_t}{B}) \frac{V}{2} \sum_{d1,d2} \sum_{m,n} \beta_{mn}^{d_1 d_2}. \tag{6.31}$$

$$P = P_o - (\frac{p_p + p_t}{B}) \frac{V}{2} \sum_{d1,d2} \sum_{m,n} \beta_{mn}^{d_1 d_2}. \tag{6.32}$$

Since the number of encodable pairs in each cluster in the encodable graph depends on the total number of nodes in the network, therefore the total number of encoded nodes depends on the network size. This is illustrated in Figure 6.1 for full mesh topologies of size 4 (clusters of size 3), 5 and 6 nodes respectively. If the network has an even number of nodes, then each cluster in the encodable graph will have an odd number of demands (i.e. each receiving node in the network will have demands from $N-1$ nodes, N is even and hence each cluster has an odd number of demands). With an odd number of demands, one demand cannot be paired and hence cannot be network coded and is therefore transmitted using conventional router ports and transponders. This leads to a higher power consumption compared to a network with an odd number of nodes. In the latter case (network with an odd number of nodes) each cluster has an even number of demands, therefore all demands can be

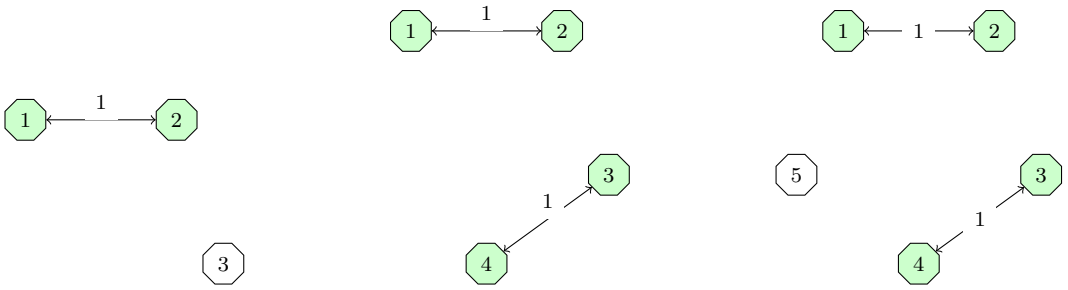

Figure 6.1: The weighted encodable graph for a full mesh of size 4, 5 and 6 respectively

encoded leading to higher power savings. As such the odd and even cases have to be treated separately. For the full mesh topology with an odd number of nodes (e.g. 5 nodes network, 4 cluster nodes), any two encodable demands have a single hop shared between them (recall the working path for the full mesh is a single hop, and the protection path is 2 hops), therefore

$$\sum_{d1,d2} \sum_{m,n} \beta_{mn}^{d_1 d_2} = N(N-1). \tag{6.33}$$

Therefore the total power consumption for the network coded case is

$$P = (\frac{p_p + p_t}{B}) N(N-1) \frac{5V}{2}. \tag{6.34}$$

Therefore the total savings is given by

$$\phi_{odd} = 1 - \frac{(\frac{p_p+p_t}{B}) N(N-1) \frac{5V}{2}}{3(\frac{p_p+p_t}{B}) VN(N-1)} = 0.166 \tag{6.35}$$

which means the savings are upper bounded by a value of 16.67%.

For the full mesh topology that has an even number of nodes, each cluster will have an odd number of encodable demands, which means a single encodable node (demand) will not be encoded due to the pairing of all other demands, making the

number of encodable demands $N-2$, in each of the N clusters. This fact makes the power savings for the even case less than the power savings of the odd case in (6.35). With N clusters, and $N-2$ encodable demands in each cluster, the total number of shared hops is given by

$$\sum_{d_1,d_2}\sum_{m,n}\beta_{mn}^{d_1 d_2} = N(N-2). \tag{6.36}$$

The total power consumption of the even case of the full mesh topology under network coding becomes

$$P = 3(\frac{p_p+p_t}{B})VN(N-1) - (\frac{p_p+p_t}{B})V\frac{N(N-2)}{2}, \tag{6.37}$$

which gives

$$P = (\frac{p_p+p_t}{B})VN\left(\frac{5N-4}{2}\right). \tag{6.38}$$

Therefore, the power saving is given by

$$\phi_{even} = 1 - \frac{(\frac{p_p+p_t}{B})VN\left(\frac{5N-4}{2}\right)}{3(\frac{p_p+p_t}{B})VN(N-1)}, \tag{6.39}$$

which leads to

$$\phi_{even} = \frac{N-2}{6(N-1)}. \tag{6.40}$$

From equation (6.40) and (6.35), we can see that the power consumption fluctuates between the upper value (i.e. 16.67%) when the number of nodes is odd, and the value given by equation (6.40) with an even number of nodes. These fluctuations, however, decrease as the number of nodes grows making the network power consumption converge to 16.67% for any number of nodes. This decrease in fluctu-

ations follows the inverse of the number of nodes and is given by

$$\epsilon(N) = \frac{1}{6} - \frac{N-2}{6(N-1)} = \frac{1}{6(N-1)}, \tag{6.41}$$

and for a very large number of nodes

$$\lim_{N\to\infty} \epsilon(N) = \lim_{N\to\infty} \frac{1}{6(N-1)} = 0. \tag{6.42}$$

We show in Figure 6.2 the power savings of full mesh topologies with a number of nodes ranging from 3 nodes up to 15 nodes. It is obvious that encoding both working flows together produces no savings as both working flows use the direct link between each node in the network which is not shared with the direct link of a working path of another demand. It also shows that the OSH heuristic is superior, while the form of the heuristic that encodes protection paths together produces optimal savings at even network sizes. The savings of the optimal heuristic jumps increasing and decreasing as the network size changes between odd and even number of nodes, agreeing with the analytical formulas, but overall converges to the maximum possible savings value (i.e. 16.67%).

6.3.2 Ring Topology

The power consumption of the conventional 1+1 protection of the ring is given as:

$$P_0 = (\frac{p_p + p_t}{B}) \left(\sum_{d\in D} \sum_{m,n} V^d (x^d_{mn} + y^d_{mn}) \right). \tag{6.43}$$

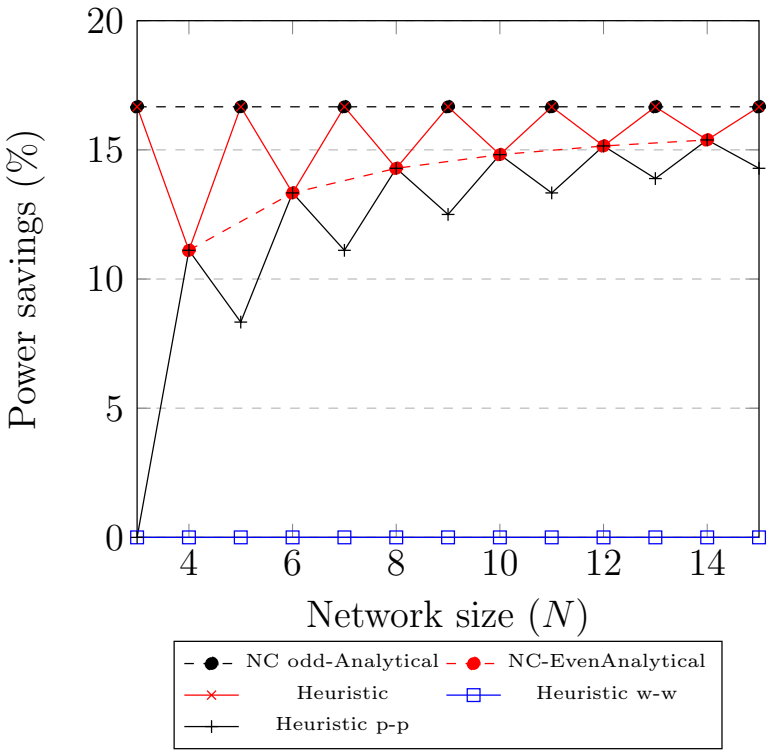

Figure 6.2: The power savings of the full mesh topology with multiple sizes

The total count of working hops for the odd number of nodes is given as

$$h_w = \sum_{d \in D} \sum_{m,n} x_{mn}^d = 2N \left(1 + 2 + ... + (\frac{N-1}{2}) \right) = \frac{(N-1)N(N+1)}{4}. \quad (6.44)$$

Since each working path of length k has a protection path of length $N-k$ in the other direction, this makes the total number of protection hops for the case of odd number of nodes

$$h_p = \sum_{d \in D} \sum_{m,n} y_{mn}^d = 2N \left(N-1+N-2+...+N-\frac{N-1}{2} \right) = N(N-1)(\frac{3N-1}{4}), \quad (6.45)$$

and the total number of hops of both working and protection paths for the odd

number of nodes is given as

$$\sum_{d\in D}\sum_{m,n}(x_{mn}^{d}+y_{mn}^{d})=\frac{(N-1)N(N+1)}{4}+N(N-1)(\frac{3N-1}{4})=N^{3}-N^{2}. \quad (6.46)$$

For the case of even number of nodes, the number of working hops is

$$h_{w}=\sum_{d\in D}\sum_{m,n}x_{mn}^{d}=2N\left(1+2+...+(\frac{N-2}{2})\right)+N\frac{N}{2}=\frac{N^{3}}{4}, \quad (6.47)$$

and the number of protection hops is given by:

$$h_{p}=\sum_{d\in D}\sum_{m,n}y_{mn}^{d}=2N\left(N-1+N-2+...+N-\frac{N-2}{2}\right)+N\frac{N}{2} \quad (6.48)$$

$$h_{p}=2N\left(N(\frac{N-2}{2})-1-2-...-\frac{N-2}{2}\right)+\frac{N^{2}}{2}=\frac{N^{2}(3N-4)}{4} \quad (6.49)$$

and the total number of hops of both working and protection paths for the even number of nodes is given as

$$\sum_{d\in D}\sum_{m,n}(x_{mn}^{d}+y_{mn}^{d})=\frac{N^{3}}{4}+\frac{N^{2}(3N-4)}{4}=N^{3}-N^{2} \quad (6.50)$$

This expression is for the conventional case and is the same for rings of odd and even number of nodes (i.e. (6.46) is the same as (6.50)).

6.3.2.1 Rings with Odd Size

We start with the case of a ring with odd number of nodes, as shown in Figure (6.3). The figure shows a ring with 11 and 13 nodes where all nodes send to node 11 and 13, respectively. To maximise the number of shared links, protection paths are

encoded together so the longest protection path is encoded with the second longest protection path and so on, leading to a number of shared hops that is equal to the number of hops of the shorter protection path. This is shown in Figure (6.3), where we pair the source nodes of demands that can be encoded. Figure 6.3 shows that the demands $(1, 11)$ and $(2, 11)$ are encoded together, where demand $(1, 11)$ has a protection path with a length of 10 hops and demand $(2, 11)$ has a protection path of 9 hops, leading to 9 shared hops. The same principle applies between demands $(3, 11)$ and $(4, 11)$ leading to 7 shared hops, which is equal to the length of the protection path of demand $(4, 11)$. The same applies to demands $[(10, 11), (9, 11)]$ and $[(8, 11), (7, 11)]$. As node 5, and node 6 do not share a protection path because they send their protection signals in opposite directions, they do not get encoded together.

The second example of a 13 nodes ring, shows that all nodes can find another node to be paired with. Therefore, compared to the 11 nodes ring, better savings are achieved. As a result, the power savings obtained under network coding go up and down as the number of nodes in the odd ring changes between the odd number where $\frac{N-1}{2} \mod 2 = 1$, classified as odd-1, and the odd number where $\frac{N-1}{2} \mod 2 = 0$, which is classified as odd-2. For example, when $N = 11$, we have $\frac{11-1}{2} \mod 2 = 1$ meaning 11 nodes belong to group 1 (i.e. odd-1), and when $N = 13$, we have $\frac{13-1}{2} \mod 2 = 0$ meaning a ring with 13 nodes belongs to group 2 (i.e. odd-2).

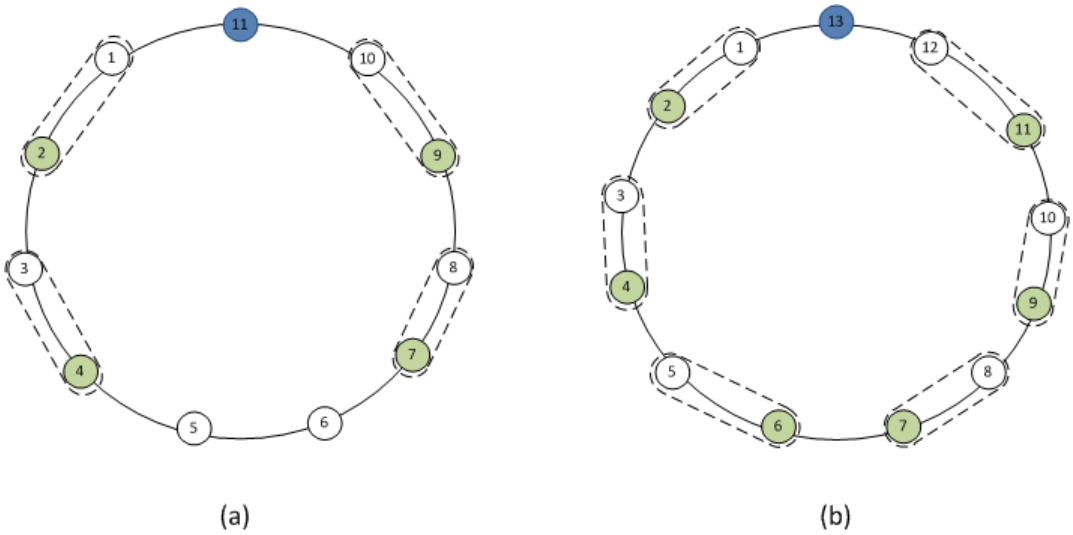

Figure 6.3: Encoding pairs for two rings with different odd number of nodes

We start with the first odd group (i.e. odd-1), of which Figure 6.3 (a) is an example, with 11 nodes. To calculate the total number of shared hops between all encoded demands (i.e. the hop count of green nodes as explained earlier), we first determine the total number of shared hops between encoded demands destined to one destination (i.e. to destination node 11 in the example in Fig. 6.3a), and then multiply it by the total number of destinations (i.e. N). For demands going to the same destination, it can be seen that for each demand on one side of the destination node there exists another demand with the same length of the protection path on the other side of the ring. Therefore we derive an expression for one side of the ring and then multiply the result by two. To determine the number of shared hops on one side of the ring, we calculate the number of pairs on that side, which is given as $\frac{N-3}{4}$, deduced by removing three nodes (i.e. the destination node (node 11), and the other two non-encodable nodes (5) and (6)), then dividing by two to account for one side, and dividing again by two to count the pairs on that side.

Therefore, the total number of shared hops for the odd-1 ring group is

$$h_t(odd1) = 2N\Bigg[(N-2) + (N-4) + ... + (N - \frac{N-3}{2})\Bigg], \tag{6.51}$$

Equation 6.51 can be described with the aid of Fig. 6.3a, where on one side, the encoded pair (node 1 and node 2) have a shared hop count of $(N-2)$, which is added to $(N-4)$ that represents the shared hop count between the encoded pair (node 3 and node 4). For larger rings, the number of shared hops continues to decrease by two, and the final term is given by $(N - \frac{N-3}{2})$. After adding similar terms, we have

$$h_t(odd1) = 2N\Bigg[N(\frac{N-3}{4}) - 2 - 4 - ... - \frac{N-3}{2}\Bigg], \tag{6.52}$$

and that gives

$$h_t(odd1) = 2N\Bigg[N(\frac{N-3}{4}) - 2\sum_{k=1}^{\frac{N-3}{4}} k\Bigg] = \frac{N(N-3)(3N-1)}{8}. \tag{6.53}$$

The total power saving for this case is represented by

$$\phi_{odd1} = \frac{N(N-3)(3N-1)}{8(N^3-N^2)}. \tag{6.54}$$

$$\lim_{N\to\infty} \phi_{odd1} = \lim_{N\to\infty} \frac{N(N-3)(3N-1)}{8(N^3-N^2)} = \frac{3}{8} = 37.5\%. \tag{6.55}$$

For the second odd group, represented by Figure (6.3b), the total number of encodable demands in each half is given by $\frac{N-1}{4}$ as only the destination node is not selected. This gives

$$h_t(odd2) = 2N\Bigg[(N-2) + (N-4) + ... + (N - \frac{N-1}{2})\Bigg], \tag{6.56}$$

which gives

$$h_t(odd2) = 2N\left[N\frac{N-1}{4} - 2 - 4 - \frac{N-1}{2}\right], \tag{6.57}$$

which can be written as

$$h_t(odd2) = 2N\left[N\frac{N-1}{4} - 2\sum_{k=1}^{\frac{N-1}{4}} k\right] = \frac{3}{8}N(N-1)^2. \tag{6.58}$$

This makes the total power saving

$$\phi_{odd2} = \frac{\frac{3}{8}N(N-1)^2}{N^3 - N^2}, \tag{6.59}$$

$$\lim_{n\to\infty} \phi_{odd2} = \lim_{n\to\infty} \frac{\frac{3}{8}N(N-1)^2}{N^3 - N^2} = \frac{3}{8} = 37.5\%. \tag{6.60}$$

6.3.2.2 Rings with Even Sizes

Here we also face the same distinction between two sets of even ring sizes, where rings of size $(4, 8, 12, ...)$ will be in a different group (i.e. even-1) and have a different expression compared to the group (i.e. even-2) containing the other ring sizes $(6, 10, 14, ...)$. This is illustrated in Figure (6.4). In both cases, the destination node and another demand source node (i.e. node 5 in Figure 6.4a and node 7 in Figure 6.4b) are not paired. A ring with an even size N is classified into its appropriate group, and hence its bound, by checking if $\frac{N-2}{2} \mod 2 = 1$, if so it belongs to the even-1 group, and it belongs to even-2 when $\frac{N-2}{2} \mod 2 = 0$. For example, when $N = 12$, $\frac{12-2}{2} \mod 2 = 1$ meaning 12 nodes belong to group 1, and when $N = 14$, $\frac{14-2}{2} \mod 2 = 0$ meaning a ring with 14 nodes belong to group 2.

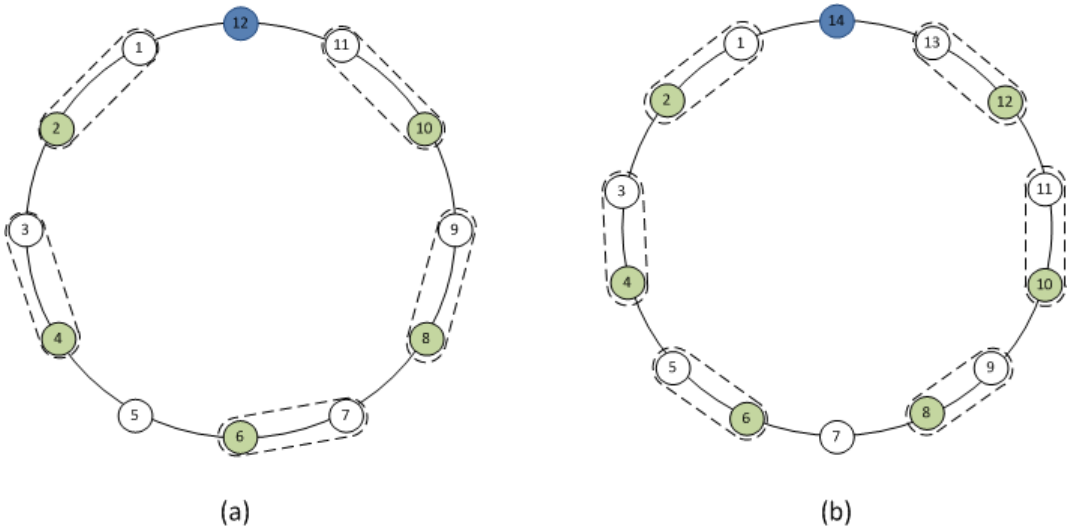

Figure 6.4: Encoding pairs for two rings with different even number of nodes

We start by the even-1 group represented by Figure 6.4a. The total number of encoded pairs in the ring is given by $N(2\frac{N-4}{4} + \frac{N}{2})$, where the number of encoded pairs on one side is $\frac{N-4}{4}$ which is deduced by removing four nodes (i.e. 12, 5, 6 and 7) to maintain the symmetry needed for the whole expression, while the $\frac{N}{2}$ accounts for the shared hop count of the encoded pair (node 6 and node 7). Therefore the total number of shared hops is given by

$$h_t(even1) = N\left(2\left[N\frac{N-4}{4} - 2 - 4 - ... - \frac{N-4}{2}\right] + \frac{N}{2}\right), \tag{6.61}$$

The additional $\frac{N}{2}$ term inside the brackets is the shared hop count as a result of encoding between node 6 and node 7) in Fig. 6.4a.

which equals

$$h_t(even1) = N\left(2\big[N\frac{N-4}{4} - 2\sum_{k=1}^{\frac{N-4}{4}} k\big] + \frac{N}{2}\right) \tag{6.62}$$

which gives

$$h_t(even1) = \frac{N^2}{2}\big[1 + \frac{3(N-4)}{4}\big]. \tag{6.63}$$

The savings for the even-1 ring is

$$\phi_{even1} = \frac{\frac{1}{2}N^2(\frac{3N}{4} - 2)}{N^3 - N^2}, \tag{6.64}$$

therefore

$$\lim_{N\to\infty} \phi_{even_1} = \lim_{N\to\infty} \frac{\frac{1}{2}N^2(\frac{3N}{4} - 2)}{N^3 - N^2} = \frac{3}{8} = 37.5\%. \tag{6.65}$$

For the even-2 ring, the same approach applies, just by removing two nodes (destination node and central node), and it becomes completely symmetrical, having a number of encodable demands on each side of the destination node given by $\frac{N-2}{4}$. Therefore giving the following total number of shared hops

$$h_t(even2) = N\left(2\left[N\frac{N-2}{4} - 2 - 4 - ... - \frac{N-2}{2}\right]\right), \tag{6.66}$$

which gives

$$h_t(even2) = N\left(2\left[N\frac{N-2}{4} - 2\sum_{k=1}^{\frac{N-2}{4}} k\right]\right), \tag{6.67}$$

which can be written as

$$h_t(even2) = \frac{N(N-2)(3N-2)}{8}. \tag{6.68}$$

so the savings of the even-2 ring is

$$\phi_{even2} = \frac{\frac{1}{8}N(N-2)(3N-2)}{N^3 - N^2}, \tag{6.69}$$

therefore

$$\lim_{N\to\infty} \phi_{even_2} = \lim_{N\to\infty} \frac{\frac{1}{8}N(N-2)(3N-2)}{N^3 - N^2} = \frac{3}{8} = 37.5\%. \tag{6.70}$$

We evaluate the impact of the ring size by showing the power savings of ring topologies ranging from 3 nodes up to 15 nodes as shown in Figure 6.5. The figure shows that the analytical formulas developed for the 2 cases of the even number of nodes and the other two cases of the odd number of nodes matches exactly the results of the heuristic, all together converging to the highest possible savings of 37.5% as the number of nodes grows. The figure also shows that the other heuristics (i.e. w-w, w-p, and p-w), have comparable savings around 15% that are far inferior to the OSH heuristic and the p-p heuristic.

The figure also shows that the the difference between the values of the analytical formulas for the odd-1 and odd-2 case are higher than the difference of the analytical value between even-1 and even-2 cases. This can be explained with the aid of Figure (6.3) and Figure (6.4), where in the case of an even number of nodes, 2 nodes get left out each time for both even cases, while for the odd case, one node gets left out in one case and three at the other. This also explains why the first odd group has the highest savings where only 1 node gets left out (all nodes are encoded). It also shows that the power savings of the OSH heuristic are higher than the heuristic p-p in the odd-2 case (e.g. size 7, 11 and 15), because in this case not all nodes are encodable and the heuristic tries all possible combinations while the heuristic p-p chooses only protection paths.

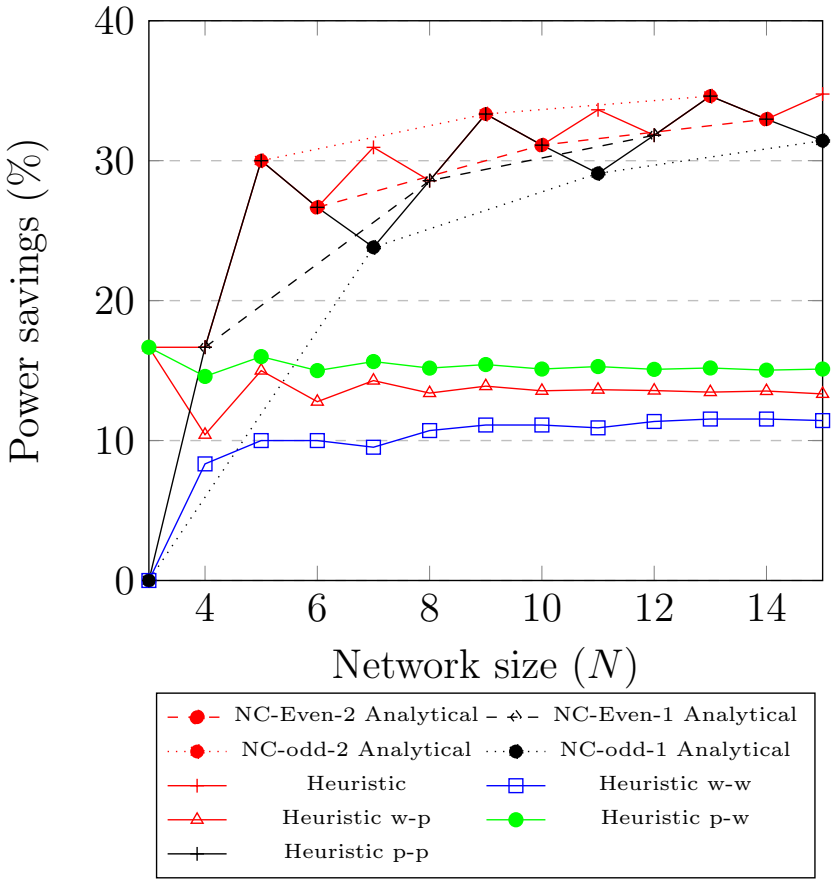

Figure 6.5: The power savings of the ring topology with multiple sizes

6.4 Summary

In this chapter we provided analytical bounds to the power consumption and power savings of the survivable 1+1 optical networks with and without network coding with an emphasis on the full mesh and ring topologies.

Chapter 7

Conclusions and Future Directions

In this chapter,the thesis is concluded by providing a summary of the contributions, listing several remaining challenges, and proposing directions for future work.

7.1 Summary of Thesis Contributions

In this work, an energy efficient technique for IP over WDM networks using network coding was introduced. The idea presented here proposes a departure from the conventional router ports, and offers a new architecture that encodes bidirectional flows using a simple XOR operation. In order to evaluate the potential power savings, we formulated a MILP model, with the objective of minimising the operational power. A minimum hop count routing heuristic and a closed form expression for the power savings as a function of the average hop count were derived. The results suggest that network coding can improve energy efficiency, as daily average savings of 27.3% and 33% are obtained when the networks under use were NSFNET an USNET respectively.

We investigated the impact of topology on the savings by first replacing the NSFNET by line, ring, star and full mesh topologies. The highest savings are of the line topology (33%), a result of the high average hop count. Network coding offers no energy saving contribution to the full mesh topology with an average hop count of 1 due to the unavailability of intermediate nodes. The minimal contribution of network coding for the star topology is due to its low average hop count (1.85). It is also shown that energy efficient routing protocols in the conventional approach are portable to the network coded approach as the minimum hop routing heuristic is used to route traffic flows in network coding enabled IP over WDM networks where network coding is performed in all intermediate nodes traversed by bidirectional traffic flows. The power savings gained by the heuristic approach match those obtained by the MILP model.

We also presented a sensitivity analysis showing the impact on savings as a result of varying the amount of power the network coded ports consume to account for the uncertainty in our estimation. The highest efficiency is when the network coded port consumes the same power as the conventional port. While losses can be encountered if the NC ports power consumption exceeds twice the power of the conventional port under typical parameters. We analysed two approaches for coding imbalanced bidirectional traffic; the first pads the smaller flow with zeros and the second partitions the larger flow into two components one of them the size of the smaller packet that gets coded and the other routed in a conventional manner. We show that the packet partitioning approach is superior to the zero padding approach especially under asymmetric traffic. We also studied the implementation of network coding when the network employs bypass routing. In this case, network coding is performed in the optical layer. Rather than saving resources at IP layer resources are saved in the transponders of the intermediate nodes. We have shown that implementing

network coding in the optical layer (bypass case) offers less energy savings when compared to the IP layer implementation (nonbypass case) as the IP routers are the highest power consuming devices in the network. In contrast, when considering the expected improvement in router ports power consumption efficiency suggested by Greentouch and the rise in power consumption of transponders, the savings of the bypass approach become more significant.

Furthermore, the analytically calculated power savings based on a derived closed form expressions confirm those of the MILP model and heuristic. Using the derived expressions, the power savings for regular topologies such as for the ring (and line), and star topology are found to asymptotically approach 45% and 22.5%, respectively as the number of nodes grows. We provided analytical upper and lower bounds showing that the expected results under any topology or demand volume distribution lies between these bounds.

An additional proposed implementation of network coding was devised to improve energy efficiency for survivable optical core networks employing $1 + 1$ protection. The idea is to provide the same reliability and instantaneous recovery provided by the $1 + 1$ protection but with a considerable reduction in the amount of protection resources by performing an XOR operation on routes for demands sharing the same destination and hence approaching the resource utilisation of the 1:2 protection scheme. The analysis is done using three techniques: a MILP model, a heuristic and analytical bounds. The work considered the impact of topology on the energy efficiency of the approach, including small or common core networks, and regular topologies. The traffic impact is also studied, covering the demand size and demand size distribution. The Heuristic is evaluated first considering the optimal selection of paths between each encoded pair and another 4 schemes covering the possibilities of encoding the two link disjoint paths of each demand with its pair, but unified for

all demands. We showed that depending on the underlying topology, the decision of the encodable paths between demands has an impact on the savings. We also provided analytical bounds and expressions to verify the MILP and heuristic results and provided a study for large network sizes, as well as a detailed study on the special ring and full mesh topology, which saturates to 37.7% and 16.67% power savings respectively.

7.2 Future Directions

7.2.1 Extension to the Network Coded Ports

The system requirements assumed perfect in this thesis require realistic evaluation as a valid extension of this work. The studies can include buffering requirements, synchronisation of bidirectional flows and their energy efficiency impact, and the introduced latency as a result of performing coding on a number of intermediate nodes as well as the impact of packet sizes. Control and management of where the coding is performed and between which flows and through which paths should be addressed in detail. Software defined networking is an attractive technique to aid in the control and management of network coding by decoupling the control plane from the data plane. Network coding functionality implementation in OpenFlow will enable remote communication with the network plane elements for the purpose of determining the path of packets across network nodes.

7.2.2 Network Coded PON Based Data Centre Architectures

PON technology has been recently suggested as a potential optical replacement for the data centre networks to provide energy efficiency [113], [114]. Servers are connected through an ONU to an OLT that serves the server to server traffic nature. Applying network coding has been considered in the PON access network to provide potential reduction in the number of transmissions and hence the overall energy of the system. Network coding under this situation is expected to produce a considerable power efficiency as the PON technology and the asymmetry in the traffic demands between servers in the data centre constitute a ripe environment for network coding as compared to the access network.

7.2.3 High Order Codes for Survivable Network Coded Optical Networks

The work presented in this thesis regarding network coding for normal and survivable optical networks considered only using xor codes between two flows that share the same destination. By generalising and removing such constraints, more interesting insights can be achieved and a probable increase in energy efficiency can be achieved. Performing coding on multiple flows, using codes other than the simple XOR operation, and having the destination as part of the other flows path rather than their same destination are possible directions in this regards.

7.2.4 Routing, Wavelength and Network Coding Assignment in All Optical Networks

The use of network coding for survivable optical networks has demonstrated not only the potential to save running power consumption costs but also reducing the overall number of wavelengths in the network. This sets the stage to a new problem as a generalization to the Routing and Wavelength Assignment (RWA) problem [115], i.e. the Routing, Wavelength and Network Coding Assignment (RWNCA). The problem involves deciding the optimal routes for demands, selected wavelengths and the location of network coding nodes and the encoding of pairs of demands. As much of the research is done on opaque optical network, there is a huge gap on whether network coding can be useful in transparent all optical networks especially under the maturing of all optical processing capabilities. This makes the RWNCA problem in all optical networks interesting to solve.

7.2.5 Network Coding for Flexible WDM Grid

The WDM flexible grid approach is the likely implementation of the WDM grid of the future due to the benefits it provides to operators in terms of efficiency. Rather than the fixed division of bandwidth into fixed sized blocks, it gives finer control of the spectrum. As the performance of network coding deteriorates the more the difference between the two encoded flows appears. Having a flexible spectrum allocation that matches the correct rate improves network coding benefits as it minimises the waste attributed to the mismatch of the two encoded packet flows. This can also aid in the practical implementation of the partitioning approach where a flow is divided between network coding ports and conventional ports. By correctly

assigning encoded flows to the correct spectrum block size, the probability of finding an exact port match increases.

7.2.6 Industrial implementation

To make the network coding approaches presented in this work a practical reality, for example in terms of cards fitted into router ports, the work has to go through three main steps. The first step is preparing a hardware demonstration on a smaller scale core network that demonstrates routing the traffic successfully with reduced power consumption, and present the work in international industrial conferences. The second step is to complete an IEEE standard, and the third step is to collaborate with equipment manufacturers to build the card and with operators to implement it and analyse the performance on a network level.

Appendices

Appendix A

Suurbelle algorithm

The Suurbelle algorithm was published in 1974 by J.W. Suurballe to find multiple link disjoint paths, where the total cost of all the paths is minimised.

The following example describing how the algorithm works is found in

http://www.macfreek.nl/memory/Disjoint_Path_Finding.

Problem: find the two shortest node-disjoints paths between A and H in this graph:

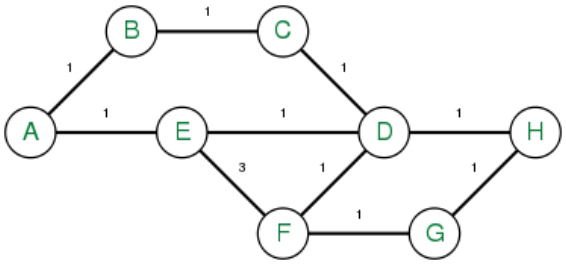

Step 1 Find the first shortest path using Dijkstra's algorithm

Step 2: Change the graph into a directed graph, and then replace all the edges contained in the shortest path from Step 1 with inverse edges and negative costs.

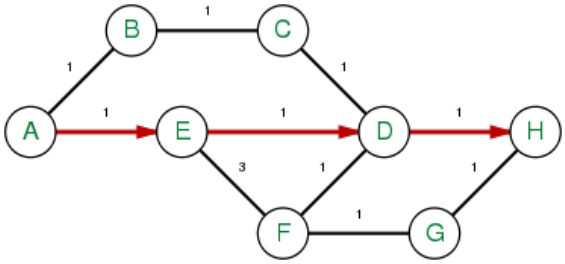

The graph will become

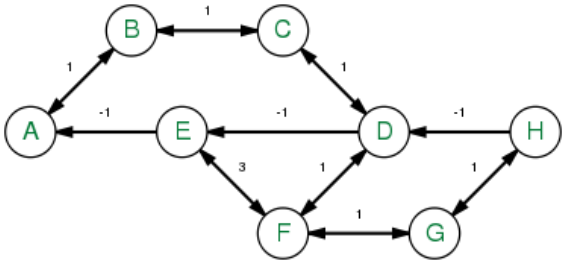

all intermediate nodes that are part of p1 are duplicated into incoming and outgoing nodes. This makes a constraint on the routing of trees coming into one of these nodes to only inverse edges. These inverse edges terminate at the outgoing nodes and start at the incoming nodes. leaving regular links to either start at source nodes or end at destination nodes.

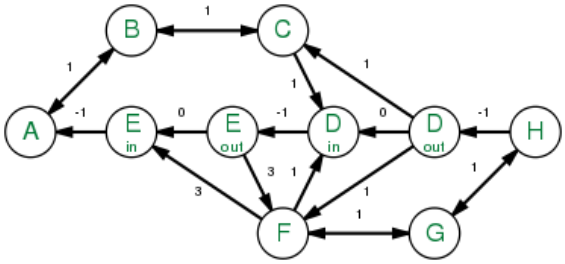

Step 3: Use Bellman-Ford algorithm to find the shortest path in the new graph. Bellman-Form algorithm performs shortest path routing on a graph that contains links with negative weights.

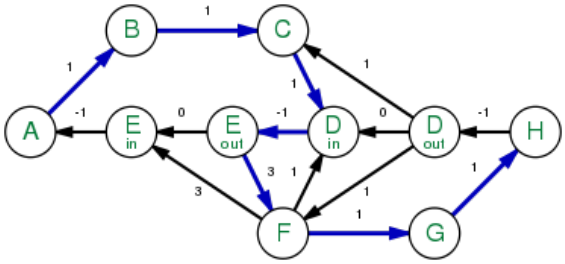

Steps 2 and 3 are repeated. to get k-shortest paths, they are repeated until all paths are found.

Step 4: All found shortest paths are add on top of each other on the original graph.

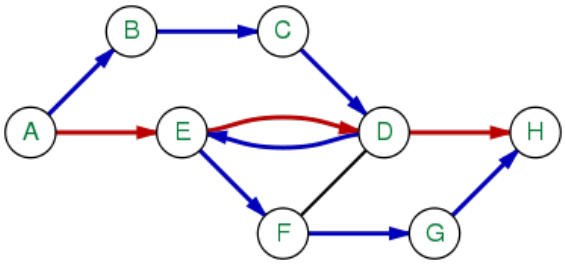

Step 5: All the edges with inverse weights are removed from the graph. Original edges are also removed. (Edge E-D in this example).

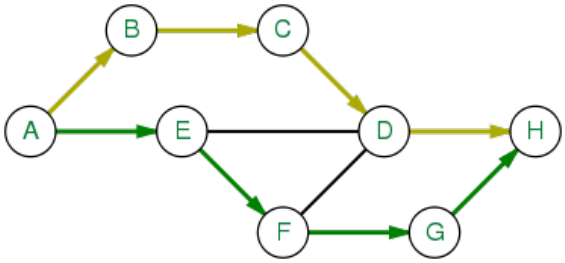

The algorithm now produces 2 (k) link disjoint shortest paths.

Bibliography

[1] Cisco, "Cisco Visual Network Index Global IP Traffic Forecast, 2015–2020."

[2] "Greentouch final results from green meter research study." http://www.ourenergypolicy.org/wp-content/uploads/2015/06/ GreenTouch_Green_Meter_Final_Results_18_June_2015.pdf. Accessed: 30-09-2016.

[3] J. A. Laitner and M. Berners-Lee, "Gesi smarter 2020: The role of ict in driving a sustainable future," tech. rep., Technical report, Global e-Sustainability Initiative, 2012., 2012.

[4] D. C. Kilper, G. Atkinson, S. K. Korotky, S. Goyal, P. Vetter, D. Suvakovic, and O. Blume, "Power trends in communication networks," *IEEE Journal of Selected Topics in Quantum Electronics*, vol. 2, no. 17, pp. 275–284, 2011.

[5] R. Ahlswede, C. Ning, S. Y. R. Li, and R. W. Yeung, "Network information flow," *Information Theory, IEEE Transactions on*, vol. 46, no. 4, pp. 1204–1216, 2000.

[6] K. Kao and G. A. Hockham, "Dielectric-fibre surface waveguides for optical frequencies," *Electrical Engineers, Proceedings of the Institution of*, vol. 113, no. 7, pp. 1151–1158, 1966.

[7] I. Jacobs, "Lightwave system development: looking back and ahead," *Optics and Photonics News*, vol. 6, no. 2, p. 19, 1995.

[8] R. C. Alferness, H. Kogelnik, and T. H. Wood, "The evolution of optical systems: Optics everywhere," *Bell Labs Technical Journal*, vol. 5, no. 1, pp. 188–202, 2000.

[9] A. Gnauck, S. Korotky, J. T. j. R. V. J. Kasper, BL Campbell, and A. Mccormick, "Information bandwidth limited transmission at 8 gbit/s over 68-3 km of single mode optical fiber'. digest of conf. on optical fiber comm," *Atlanta*, 1986.

[10] M. N. Zervas, R. I. Laming, and D. N. Payne, "Optical amplifier," Dec. 20 1994. US Patent 5,375,010.

[11] C. A. Brackett, "Dense wavelength division multiplexing networks: Principles and applications," *IEEE Journal on Selected Areas in Communications*, vol. 8, no. 6, pp. 948–964, 1990.

[12] A. Chraplyvy, A. Gnauck, R. Tkach, and R. Derosier, "8* 10 gb/s transmission through 280 km of dispersion-managed fiber," *IEEE photonics technology letters*, vol. 5, no. 10, pp. 1233–1235, 1993.

[13] A. Chraplyvy, A. Gnauck, R. Tkach, J. Zyskind, J. Sulhoff, A. Lucero, Y. Sun, R. Jopson, F. Forghieri, R. Derosier, *et al.*, "1-tb/s transmission experiment," *IEEE Photonics Technology Letters*, vol. 8, no. 9, pp. 1264–1266, 1996.

[14] A. Sano, T. Kobayashi, S. Yamanaka, A. Matsuura, H. Kawakami, Y. Miyamoto, K. Ishihara, and H. Masuda, "102.3-tb/s (224 x 548-gb/s) c- and extended l-band all-raman transmission over 240 km using pdm-64qam

single carrier fdm with digital pilot tone," in *National Fiber Optic Engineers Conference*, pp. PDP5C–3, Optical Society of America, 2012.

[15] D. Hillerkuss, R. Schmogrow, T. Schellinger, M. Jordan, M. Winter, G. Huber, T. Vallaitis, R. Bonk, P. Kleinow, F. Frey, *et al.*, "26 tbit s-1 line-rate super-channel transmission utilizing all-optical fast fourier transform processing," *Nature Photonics*, vol. 5, no. 6, pp. 364–371, 2011.

[16] D. Qian, M.-F. Huang, E. Ip, Y.-K. Huang, Y. Shao, J. Hu, and T. Wang, "101.7-tb/s (370× 294-gb/s) pdm-128qam-ofdm transmission over 3× 55-km ssmf using pilot-based phase noise mitigation," in *National Fiber Optic Engineers Conference*, p. PDPB5, Optical Society of America, 2011.

[17] M. Peach, "Nec and corning achieve petabit optical transmission (2013)," *http://optics.org/news/4/1/29*. Accessed: 2016-08-04.

[18] F. Poletti, N. Wheeler, M. Petrovich, N. Baddela, E. N. Fokoua, J. Hayes, D. Gray, Z. Li, R. Slavík, and D. Richardson, "Towards high-capacity fibre-optic communications at the speed of light in vacuum," *Nature Photonics*, vol. 7, no. 4, pp. 279–284, 2013.

[19] R. Ramaswami, K. Sivarajan, and G. Sasaki, *Optical networks: a practical perspective*. Morgan Kaufmann, 2009.

[20] I.T.U, "Spectral grids for wdm applications: CWDM frequency grid." http://www.itu.int/rec/T-REC-G.694.2-200312-I/en, 2003. Accessed: 30-09-2016.

[21] I.T.U, "Spectral grids for wdm applications: DWDM frequency grid." https://www.itu.int/rec/T-REC-G.694.1-201202-I/en, 2012. Accessed: 30-09-2016.

[22] B. Mukherjee, "Wdm optical communication networks: progress and challenges," *IEEE Journal on Selected Areas in communications*, vol. 18, no. 10, pp. 1810–1824, 2000.

[23] K. H. Liu, *IP over wdm*. John Wiley & Sons, 2003.

[24] S. Dixit, *IP over WDM: building the next-generation optical internet*. John Wiley & Sons, 2004.

[25] E. Rosen, A. Viswanathan, and R. Callon, "Multiprotocol label switching architecture," tech. rep., 2000.

[26] N. Ghani, S. Dixit, and T.-S. Wang, "On ip-over-wdm integration," *IEEE Communications Magazine*, vol. 38, no. 3, pp. 72–84, 2000.

[27] Cisco, "Cisco crs 16-slot single-shelf system data sheet." http://www.cisco.com/c/en/us/products/collateral/routers/carrier-routing-system/CRS-3_16-Slot_DS.html. Accessed: 30-09-2016.

[28] G. P. Agrawal, *Fiber-Optic Communication Systems*. John Wiley & Sons, 2002.

[29] B. Mukherjee, *Optical WDM networks*. Springer Science & Business Media, 2006.

[30] A. Tzanakaki, I. Zacharopoulos, and I. Tomkos, "Broadband building blocks [optical networks]," *IEEE Circuits and Devices Magazine*, vol. 20, no. 2, pp. 32–37, 2004.

[31] W.-D. Zhong, "Optical cross connects," *Handbook of Computer Networks: Key Concepts, Data Transmission, and Digital and Optical Networks, Volume 1*, pp. 783–794.

[32] E. Desurvire, *Erbium-doped fiber amplifiers: principles and applications*. Wiley-Interscience, 2002.

[33] E. Desurvire, C. R. Giles, J. R. Simpson, and J. L. Zyskind, "Erbium-doped fiber amplifier," Apr. 2 1991. US Patent 5,005,175.

[34] M. Gupta and S. Singh, "Greening of the internet," in *Proceedings of the 2003 conference on Applications, technologies, architectures, and protocols for computer communications*, pp. 19–26, ACM, 2003.

[35] K. J. Christensen, C. Gunaratne, B. Nordman, and A. D. George, "The next frontier for communications networks: power management," *Computer Communications*, vol. 27, no. 18, pp. 1758–1770, 2004.

[36] GreenTouch, "Greentouch consortium." http://www.greentouch.org, 2010. Accessed: 30-09-2016.

[37] J. Elmirghani, T. Klein, K. Hinton, T. eh El-Gorashi, A. Lawey, and X. Dong, "Greentouch greenmeter core network power consumption models and results," in *Green Communications (OnlineGreencomm), 2014 IEEE Online Conference on*, pp. 1–8, IEEE, 2014.

[38] E. Bonetto, L. Chiaraviglio, D. Cuda, G. A. G. Castillo, and F. Neri, "Optical technologies can improve the energy efficiency of networks," *ECOC 2009*, 2009.

[39] J. Baliga, R. Ayre, K. Hinton, and R. Tucker, "Photonic switching and the energy bottleneck," in *Photonics in Switching*, vol. 2007, pp. 125–126, 2007.

[40] V. W. Chan, "Optical flow switching networks," *Proceedings of the IEEE*, vol. 100, no. 5, pp. 1079–1091, 2012.

[41] Cisco, "Converge IP and DWDM layers in the core network." http://www.webtorials.com/main/resource/papers/cisco/ paper114/ConvergeIPandDWDMLayersintheCoreNetwork.pdf, 2007. Accessed: 30-09-2016.

[42] J. Chabarek, J. Sommers, P. Barford, C. Estan, D. Tsiang, and S. Wright, "Power awareness in network design and routing," in *INFOCOM 2008. The 27th Conference on Computer Communications. IEEE*, IEEE, 2008.

[43] P. Chowdhury, M. Tornatore, and B. Mukherjee, "On the energy efficiency of mixed-line-rate networks," in *Optical Fiber Communication Conference*, p. OWY3, Optical Society of America, 2010.

[44] C. Lange and A. Gladisch, "Energy efficiency limits of load adaptive networks," in *Optical Fiber Communication Conference*, p. OWY2, Optical Society of America, 2010.

[45] Y. Zhang, M. Tornatore, P. Chowdhury, and B. Mukherjee, "Time-aware energy conservation in ip-over-wdm networks," in *Photonics in Switching*, p. PTuB2, Optical Society of America, 2010.

[46] F. Idzikowski, S. Orlowski, C. Raack, H. Woesner, and A. Wolisz, "Saving energy in ip-over-wdm networks by switching off line cards in low-demand scenarios," in *Optical Network Design and Modeling (ONDM), 2010 14th Conference on*, pp. 1–6, IEEE, 2010.

[47] R. Bolla, R. Bruschi, A. Cianfrani, and M. Listanti, "Enabling backbone networks to sleep," *IEEE Network*, vol. 25, no. 2, pp. 26–31, 2011.

[48] K. J. Christensen, C. Gunaratne, B. Nordman, and A. D. George, "The next frontier for communications networks: power management," *Computer Communications*, vol. 27, no. 18, pp. 1758–1770, 2004.

[49] J. Chabarek, J. Sommers, P. Barford, C. Estan, D. Tsiang, and S. Wright, "Power Awareness in Network Design and Routing," in *INFOCOM 2008. The 27th Conference on Computer Communications. IEEE*, pp. 457–465, 2008.

[50] D. Kilper *et al.*, "Insights on coding and transmission energy in optical networks," *E-energy 2011*, 2011.

[51] X. Dong, A. Lawey, T. E. El-Gorashi, and J. M. Elmirghani, "Energy-efficient core networks," in *Optical Network Design and Modeling (ONDM), 2012 16th International Conference on*, pp. 1–9, IEEE, 2012.

[52] W. Van Heddeghem, M. De Groote, W. Vereecken, D. Colle, M. Pickavet, and P. Demeester, "Energy-efficiency in telecommunications networks: link-by-link versus end-to-end grooming," in *14th Conference on Optical Network Design and Modeling (ONDM 2010)*, IEEE, 2010.

[53] X. Dong, T. El-Gorashi, and J. M. H. Elmirghani, "Green IP Over WDM Networks With Data Centers," *Journal of Lightwave Technology*, vol. 29, pp. 1861–1880, June 2011.

[54] N. I. Osman, T. El-Gorashi, and J. M. Elmirghani, "Caching in green ip over wdm networks," *Journal of High Speed Networks*, vol. 19, no. 1, pp. 33–53, 2013.

[55] K. Guan, D. C. Kilper, and G. Atkinson, "Evaluating the energy benefit of dynamic optical bypass for content delivery," in *Computer Communications*

Workshops (INFOCOM WKSHPS), 2011 IEEE Conference on, pp. 313–318, IEEE, 2011.

[56] K. Guan, G. Atkinson, D. C. Kilper, and E. Gulsen, "On the energy efficiency of content delivery architectures," in *2011 IEEE International Conference on Communications Workshops (ICC)*, pp. 1–6, IEEE, 2011.

[57] A. Q. Lawey, T. El-Gorashi, and J. M. Elmirghani, "Energy-efficient peer selection mechanism for bittorrent content distribution," in *Global Communications Conference (GLOBECOM), 2012 IEEE*, pp. 1562–1567, IEEE, 2012.

[58] N. Wang, K. H. Ho, G. Pavlou, and M. Howarth, "An overview of routing optimization for internet traffic engineering," *IEEE Communications Surveys & Tutorials*, vol. 10, no. 1, pp. 36–56, 2008.

[59] G. Shen and R. S. Tucker, "Energy-minimized design for ip over wdm networks," *Journal of Optical Communications and Networking*, vol. 1, no. 1, pp. 176–186, 2009.

[60] N. Amaya, G. S. Zervas, and D. Simeonidou, "Architecture on demand for transparent optical networks," in *2011 13th International Conference on Transparent Optical Networks*, pp. 1–4, IEEE, 2011.

[61] L. Nonde, T. El-Gorashi, and J. Elmirghani, "Energy efficient virtual network embedding for cloud networks," *Lightwave Technology, Journal of*, vol. 33, pp. 1828–1849, May 2015.

[62] X. Dong, T. El-Gorashi, and J. M. Elmirghani, "Ip over wdm networks employing renewable energy sources," *Lightwave Technology, Journal of*, vol. 29, no. 1, pp. 3–14, 2011.

[63] L. R. Ford and D. R. Fulkerson, "Maximal flow through a network," *Canadian journal of Mathematics*, vol. 8, no. 3, pp. 399–404, 1956.

[64] P. Elias, A. Feinstein, and C. E. Shannon, "A note on the maximum flow through a network," *Information Theory, IRE Transactions on*, vol. 2, no. 4, pp. 117–119, 1956.

[65] S.-Y. Li, R. Yeung, and N. C. N. Cai, "Linear network coding," *IEEE Transactions on Information Theory*, vol. 49, 2003.

[66] R. Koetter and M. Medard, "An algebraic approach to network coding," *IEEE/ACM Transactions on Networking*, vol. 11, 2003.

[67] T. Ho, M. Médard, R. Koetter, D. R. Karger, M. Effros, J. Shi, and B. Leong, "A random linear network coding approach to multicast," *Information Theory, IEEE Transactions on*, vol. 52, no. 10, pp. 4413–4430, 2006.

[68] P. A. Chou, Y. Wu, and K. Jain, "Practical network coding," 2003.

[69] R. W. Yeung, *Information theory and network coding*. Springer Science & Business Media, 2008.

[70] R. W. Yeung, S.-Y. R. Li, N. Cai, and Z. Zhang, "Network coding theory: single sources," *Communications and Information Theory*, vol. 2, no. 4, pp. 241–329, 2005.

[71] R. W. Yeung and N. Cai, *Network coding theory*. Now Publishers Inc, 2006.

[72] Z. Li and B. Li, "Network coding in undirected networks," CISS, 2004.

[73] S.-Y. R. Li and Q. T. Sun, "Network coding theory via commutative algebra," *Information Theory, IEEE Transactions on*, vol. 57, no. 1, pp. 403–415, 2011.

[74] R. W. Yeung, N. Cai, *et al.*, "Network error correction, i: Basic concepts and upper bounds," *Communications in Information & Systems*, vol. 6, no. 1, pp. 19–35, 2006.

[75] N. Cai, R. W. Yeung, *et al.*, "Network error correction, ii: Lower bounds," *Communications in Information & Systems*, vol. 6, no. 1, pp. 37–54, 2006.

[76] C. Chekuri, C. Fragouli, and E. Soljanin, "On average throughput and alphabet size in network coding," *IEEE/ACM Transactions on Networking (TON)*, vol. 14, no. SI, pp. 2410–2424, 2006.

[77] S. Jaggi, P. Sanders, P. A. Chou, M. Effros, S. Egner, K. Jain, and L. M. Tolhuizen, "Polynomial time algorithms for multicast network code construction," *Information Theory, IEEE Transactions on*, vol. 51, no. 6, pp. 1973–1982, 2005.

[78] S. Jaggi, P. A. Chou, and K. Jain, "Low complexity algebraic multicast network codes," in *In IEEE International Symposium on Information Theory (ISIT*, Citeseer, 2003.

[79] P. Sanders, S. Egner, and L. Tolhuizen, "Polynomial time algorithms for network information flow," in *Proceedings of the fifteenth annual ACM symposium on Parallel algorithms and architectures*, pp. 286–294, ACM, 2003.

[80] S. Katti, H. Rahul, W. Hu, D. Katabi, M. Muriel, #233, Dard, and J. Crowcroft, "XORs in the air: practical wireless network coding," *SIGCOMM Comput. Commun. Rev.*, vol. 36, no. 4, pp. 243–254, 2006.

[81] A. E. Kamal, "OPN04-3: 1+N Protection in Mesh Networks Using Network Coding over p-Cycles," in *Global Telecommunications Conference, 2006. GLOBECOM '06. IEEE*, pp. 1–6, 2006.

[82] S. A. Aly and A. E. Kamal, "Network coding-based protection strategy against node failures," in *Communications, 2009. ICC'09. IEEE International Conference on*, pp. 1–5, IEEE, 2009.

[83] A. E. Kamal, A. Ramamoorthy, L. Long, and L. Shizheng, "Overlay Protection Against Link Failures Using Network Coding," *Networking, IEEE/ACM Transactions on*, vol. 19, no. 4, pp. 1071–1084, 2011.

[84] M. Belzner and H. Haunstein, "Network coding in passive optical networks," in *Optical Communication, 2009. ECOC '09. 35th European Conference on*, pp. 1–2, 2009.

[85] K. Fouli, M. Maier, and M. Medard, "Network coding in next-generation passive optical networks," *Communications Magazine, IEEE*, vol. 49, no. 9, pp. 38–46, 2011.

[86] X. Liu, K. Fouli, R. Kang, M. Maier, and S. Member, "Network-Coding-Based Energy Management for Next-Generation Passive Optical Networks," vol. 30, no. 6, pp. 864–875, 2012.

[87] E. D. Manley, J. S. Deogun, and X. Lisong, "Network coding for optical-layer multicast," in *Broadband Communications, Networks and Systems, 2008. BROADNETS 2008. 5th International Conference on*, pp. 452–459, 2008.

[88] E. D. Manley, J. S. Deogun, L. Xu, and D. R. Alexander, "All-Optical Network Coding," *Optical Communications and Networking, IEEE/OSA Journal of*, vol. 2, no. 4, pp. 175–191, 2010.

[89] Z. Liu, M. Li, L. Lu, C.-K. Chan, S.-C. Liew, and L.-K. Chen, "Optical Physical-Layer Network Coding," *IEEE Photonics Technology Letters*, vol. 24, pp. 1424–1427, Aug. 2012.

[90] G. B. Dantzig, *Linear programming and extensions*. Princeton university press, 1998.

[91] G. L. Nemhauser and L. A. Wolsey, "Integer programming and combinatorial optimization," *Wiley, Chichester. GL Nemhauser, MWP Savelsbergh, GS Sigismondi (1992). Constraint Classification for Mixed Integer Programming Formulations. COAL Bulletin*, vol. 20, pp. 8–12, 1988.

[92] E. L. Lawler and D. E. Wood, "Branch-and-bound methods: A survey," *Operations research*, vol. 14, no. 4, pp. 699–719, 1966.

[93] L. Davis, "Handbook of genetic algorithms," 1991.

[94] R. Fourer, D. Gay, and B. Kernighan, *Ampl*, vol. 117. Boyd & Fraser Danvers, MA, 1993.

[95] IBM, "12.2 User's Manual for CPLEX," 2010.

[96] A. Makhorin, "Glpk (gnu linear programming kit)," 2008.

[97] J. Forrest, "Cbc (coin-or branch and cut) open-source mixed integer programming solver, 2012," *URL https://projects. coin-or. org/Cbc*.

[98] M. Berkelaar, K. Eikland, P. Notebaert, *et al.*, "lpsolve: Open source (mixed-integer) linear programming system," *Eindhoven U. of Technology*, 2004.

[99] Cisco, "Cisco CRS-1 16-Slot Single-Shelf System." http://www.cisco.com/c/en/us/products/collateral/routers/carrier-routing-system/CRS-3_16-Slot_DS.html. Accessed: 30-09-2016.

[100] Cisco, "Cisco ONS 15454 10-Gbps Multirate Transponder Card." http://www.cisco.com/c/en/us/products/collateral/optical-

networking/ons-15454-m12-multiservice-transport-platform-mstp/product_data_sheet0900aecd80121bf7.html. Accessed: 30-09-2016.

[101] Cisco, "Data sheet of Glimmerglass Intelligent Optical System 500." http://www.glimmerglass.com/products/intelligent-optical-system-500. Accessed: 30-09-2016.

[102] Cisco, "Data sheet of Cisco ONS 15454 100-GHz 4-CH Multi/Demultiplexer." http://www.cisco.com/c/en/us/products/optical-networking/ons-15454-series-multiservice-provisioning-platforms/index.html. Accessed: 30-09-2016.

[103] Cisco, "Cisco ONS 15501 Erbium Doped Fiber Amplifier Data Sheet." http://www.cisco.com/en/US/products/hw/optical/ps2011 /products_data_sheet09186a008008870d.html. Accessed: 30-09-2016.

[104] X. Dong, T. E. H. El-gorashi, and J. M. H. Elmirghani, "On the Energy Ef fi ciency of Physical Topology Design for IP Over WDM Networks," vol. 30, no. 12, pp. 1931–1942, 2012.

[105] D. Zhou and S. Subramaniam, "Survivability in optical networks," *IEEE network*, vol. 14, no. 6, pp. 16–23, 2000.

[106] A. E. Kamal and M. Mohandespour, "Network coding-based protection," *Optical Switching and Networking*, vol. 11, pp. 189–201, 2014.

[107] A. E. Kamal and O. Al-Kofahi, "Efficient and agile 1+ n protection," *Communications, IEEE Transactions on*, vol. 59, no. 1, pp. 169–180, 2011.

[108] A. E. Kamal, "Network protection for mesh networks: network coding-based protection using p-cycles," *Networking, IEEE/ACM Transactions on*, vol. 18, no. 1, pp. 67–80, 2010.

[109] S. A. Aly and A. E. Kamal, "Network protection codes against link failures using network coding," in *Global Telecommunications Conference, 2008. IEEE GLOBECOM 2008. IEEE*, pp. 1–6, IEEE, 2008.

[110] I. B. Barla, F. Rambach, D. A. Schupke, and M. Thakur, "Network coding for protection against multiple link failures in multi-domain networks," in *Communications (ICC), 2010 IEEE International Conference on*, pp. 1–6, IEEE, 2010.

[111] A. Muktadir, A. A. Jose, and E. Oki, "An optimum mathematical programming model for network-coding based routing with 1+ 1 path protection," in *World Telecommunications Congress (WTC), 2012*, pp. 1–5, IEEE, 2012.

[112] J. W. Suurballe and R. E. Tarjan, "A quick method for finding shortest pairs of disjoint paths," *Networks*, vol. 14, no. 2, pp. 325–336, 1984.

[113] A. Hammadi and L. Mhamdi, "A survey on architectures and energy efficiency in data center networks," *Computer Communications*, vol. 40, pp. 1–21, 2014.

[114] J. Elmirghani, T. EL-GORASHI, and A. HAMMADI, "Passive optical-based data center networks," June 2 2016. WO Patent App. PCT/GB2015/053,604.

[115] H. Zang, J. P. Jue, B. Mukherjee, *et al.*, "A review of routing and wavelength assignment approaches for wavelength-routed optical wdm networks," *Optical Networks Magazine*, vol. 1, no. 1, pp. 47–60, 2000.